DISSERTATION

HELICAL PILE CAPACITY TO TORQUE RATIO:

A FUNCTIONAL PERSPECTIVE

Submitted by

Moncef Souissi

Department of Civil and Environmental Engineering

In partial fulfillment of the requirements

For the Degree of Doctor of Philosophy

Colorado State University

Fort Collins, Colorado

Fall 2019

Doctoral Committee:

Advisor: Thomas Siller

Wayne Charlie
Howard. A. Perko
Wade Troxell

ABSTRACT

HELICAL PILE CAPACITY TO TORQUE RATIO:

A FUNCTIONAL PERSPECTIVE

The capacity to installation torque ratio, K_t, has been used in the design of helical piles and anchors for over half a century. Numerous researches have been conducted to accurately predict this capacity-torque correlation factor. However, almost of all these K_t factors published or released by the manufacturers are based on shaft geometry alone, Hoyt and Clemence (1989). Recent full-scale tests (axial compression and tension) in clay, sand and bedrock have shown that the traditional K_t used, based on shaft size only, can be improved upon. The capacity to torque ratio seems to depend on the shaft size, shaft geometry, helix configuration, load direction and soil type, Lutenegger (2015).

Seven hundred ninety-nine (799) full scale load tests in compression and tension were conducted on helical piles of varying shaft sizes, shaft geometry, helix configurations and different soil type (sand clay, and bed rock). The objective of this research is to determine the effect of these variables on the capacity torque correlation factor, develop a new empirical relationship between pile capacity and installation torque, and determine its reliability in comparison to the published K_t values used in the pile industry.

ACKNOWLEDGMENTS

I would like to thank my advisor, Dr. Tom Siller, for his guidance, his support and his steady encouragement throughout this research over these years. Thanks also to my Co-Advisor, Dr. Wayne Charlie, for all his support and his contribution.

Thanks to Dr. Howard Perko, whom I consider my mentor, for all his advice and guidance throughout this process. Dr. Perko was the first one to introduce me to helical piles many years ago. His passion for the industry inspired me to pursue a career in this type of foundations.

Thanks to my outside committee advisor, Dr. Wade Troxel, for all his support and help.

I would like also to extend my deepest gratitude to CTL|Thompson for its full support and encouragement throughout my career at CTL, and for letting me use the test data that we have collected over the years. Without these data, this research would not have come to light.

Finally, I would like to thank my wife for her encouragement and never-ending support. Thanks to my parents, my brothers and my sister for their support. Thanks to my friend, James Cherry, who was my colleague at CTL, for all his contribution through guidance, input and support.

TABLE OF CONTENTS

1. CHAPTER 1: INTRODUCTION

1.1 Scope of research

Helical piles have been used in the construction industry for over a century. The first recorded use of helical piles was in 1836 by Alexander Mitchell when he used this type of foundation to support the Maplin Sands lighthouse in England, Perko (2009). Since the development of modern hydraulic torque motors, advances in manufacturing, and new galvanizing techniques, helical piles have gained in popularity to the extent that they are often recommended for deep foundations in some geographical areas.

Due to the increase of usage of helical piles, the International Code Council (ICC, 2009) has included the addition of helical plies in chapter 18 'Soils and Foundations' since the 2009 edition. The allowable axial design load of the pile was determined from the lower value of the soil and mechanical capacities of the pile. The mechanical capacity refers to the axial capacity of the pile shaft, pile coupling, and helical bearing plates welded to the pile. The soil capacity is determined based on the individual plate bearing method, cylindrical shear method, load testing, or a well-documented capacity-torque correlation.

The relationship between the installation torque and pile capacity has been probably the most used and widely accepted in the helical pile industry as a means of predicting the ultimate capacity, as well as a quality control and assurance tool. This torque correlation method is an empirical one that relates the ultimate pile soil capacity to the installation torque via an empirical constant K_t. This method has been used since the 1960's. It has gained popularity since the study performed by Hoyt and Clemence (1989). Upon analysis of the test data, they determined that there is indeed a correlation between

the installation torque and the soil pile capacity in compression and tension. Based on their study, the common denominator was a parameter referred to as the capacity-t-torque ratio, K_t, used in the following equation to predict the pile capacity based on the final installation torque:

$$Q = K_t T \quad (1.1)$$

Where:

Q : the ultimate capacity of the helical pile [lbs. (N)]

K_t : the empirical torque factor based on the pile shaft size [ft^{-1} (m^{-1})]

T : the final installation torque [ft-lb (m-N)]

It is important to mention that all the tests conducted by Hoyt and Clemence were all in tension, and in soils represented by sand, silt and clay. The K_t factor in the above equation has been equally applied for both tension and compression, although, it has been demonstrated that the K_t factor in compression is higher than the K_t factor in tension. In addition, the K_t factor from this study has been determined as a function of the shaft size only.

There have been numerous studies, based either on field or lab testing, that were conducted to evaluate the capacity-torque correlation factor, K_t. To the best of the author's knowledge, most of all these studies have reported a K_t value that is solely dependent on the helical pile shaft size, similar to the results published by Hoyt & Clemence. In other words, the ultimate soil pile capacity was related to the final installation torque via a K_t factor as presented in the equation above. In addition, in most of these studies, the K_t

value was determined from the traditional plot of the ratio of the measured capacity to the final installation torque (Q/T) versus pile shaft diameter (D).

In the current study, 799 load tests have been conducted at two different soil sites, characterized generally as sandy and clayey soils. These tests include different shaft sizes and different helix configurations. All the load test results were analyzed to determine the effect of the shaft size and shape, the final installation torque (T), helix configuration and axial load direction (compression, tension) on the capacity-torque relationship.

In this analysis, a new approach was used to determine the pile capacity-torque relationship. Instead of using the traditional plot of measured capacity over installation torque (Q/T) vs shaft diameter (D) to determine the empirical K_t factor, the measured soil capacity (Q) was plotted against the ratio of the effective pile diameter to the final installation torque (D/T), which shows a very good correlation as indicated by the coefficient of determination R^2, a statistical measure of how close the data are to the fitted regression line.

Based on this new relationship, the effect of helix configuration, axial load direction (compression, tension), and shaft geometry were analyzed, quantified and incorporated in the new capacity-torque relationship via factors evaluated from the analysis.

1.2 Organization

The work performed for this research is presented in as follows:

Chapter 1 provides general information about helical piles, mainly its basic feature components and its installation into the ground.

Chapter 2 presents review and historical development of helical piles.

Chapter 3 presents testing type and procedures as well as test result interpretation.

Chapter 4 provides detailed information about the testing agency, testing standards, testing samples, installation procedures and testing sites description.

Chapter 5 presents detailed analysis of the load test results and its findings.

Chapter 6 presents the reliability of the predicted capacity based on the empirical relationship determined from this study

Chapter 7 presents the summary and conclusion of the findings of this study.

1.3 Definition, features and installation

1.3.1 Definition and Terminology

The helical pile is a factory manufactured steel foundation consisting of a central shaft with one or more helical shaped bearing plates (helices) affixed to it. The term helical pile usually refers to compression applications. The term helical anchor is usually associated with tension applications. Helical piles have two main components, lead section and extensions connected through couplings. Figures 1.1 and 1.2 below show typical helical lead section, extension and helix.

(a) (b) (c)

Figure 1.1 (a) & (c) Typical extension. (b) Typical lead section (courtesy of CTL|Thompson)

Figure 1.2. Typical spiral helix (Courtesy of CTL|Thompson)

1.3.2 Basic Features of Helical Piles

The basic features of a typical helical pile are shown in Figure 1.3 below. The lead section is usually the one that has the helices affixed to it. If needed, helices can also be affixed to the extensions. The lead section is the first section that gets screwed into the ground. To advance the helical pile to the depth required, and depending on the length of

the lead section, extensions are added until the pile is installed to the minimum depth needed. The connection between the lead and extension sections is termed the coupling. There are many different types of coupling used in the helical pile industry. To just name few, there are threaded coupler, bolted coupler and welded coupler. Figure 1.4 shows typical threaded and bolted coupler.

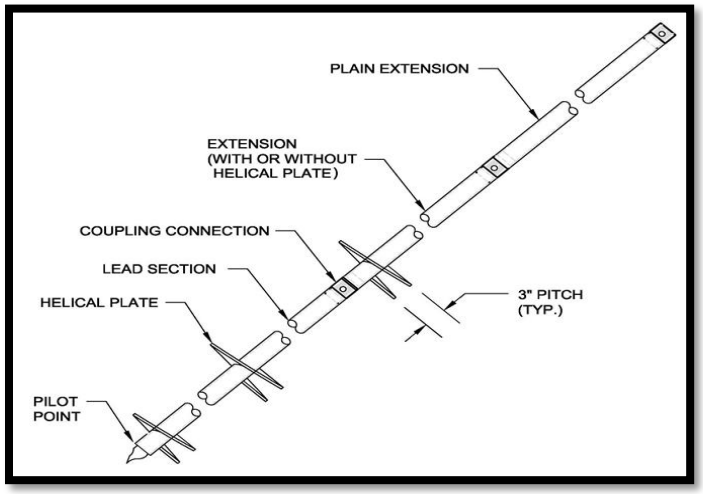

Figure 1.3. Basic components of helical pile. DFI (2012)

(a) (b)

Figure 1.4. (a) Bolted. (b) Threaded (Courtesy of CTL|Thompson)

The heliacal pile components in Figure 1.3 (lead and extension) are the ones that are screwed into the ground by application of torque and extended until a desired depth or suitable soil or bedrock stratum is reached. A pier cap or bracket is used to allow the attachment of the pile to the structure. Many different pier caps or brackets have been used throughout the helical pile industry, depending on the type of foundation it supports. Figures 1.5 through 1.8 show different type of brackets and their application in supporting different structures.

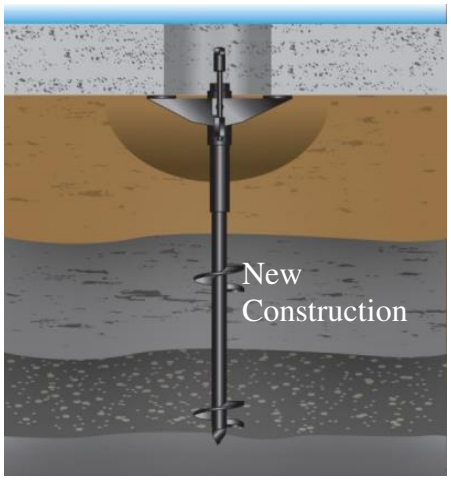

Figure 1.5 New Construction Bracket DFI (2012)

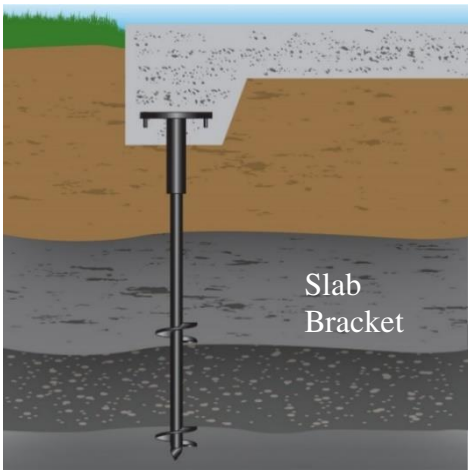

Figure 1.6 Slab Bracket DFI ((2012)

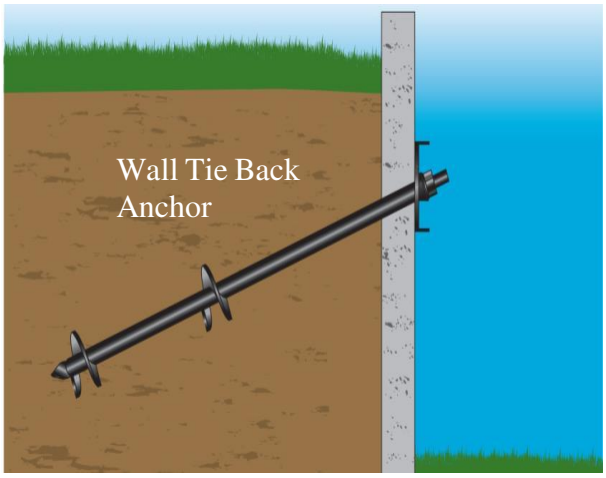

Figure 1.7. Tie Back Anchor DFI (2012)

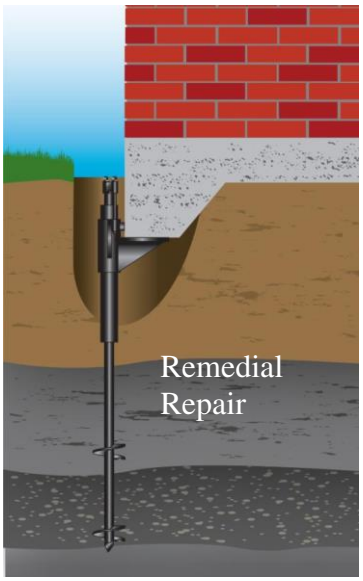

Figure 1.8. Remedial Bracket DFI (2012)

1.3.3 Helical Pile Installation

Helical piles or anchors are installed using a torque motor that is connected to a source of hydraulic pressure. Pressure gauges were first used to read the pressure differential (psi), which is then converted to torque (ft-lb) from calibration reports. This method was very common earlier in the installation of helical piles, but lately, it has been shown that, using pressure gauges to read the installation torque, is not as accurate as it was once thought. Nowadays, digital torque indicators are the most common used devices for

measuring installation torque. Usually, a drive tool (depending on the type of coupling and its size) is used to connect (via drive pins or bolts) the digital indicator to the pile that is being screwed into the ground.

The torque head or torque motor uses the hydraulics from the installation machine and is usually attached with quick release -disconnect hydraulic hoses. There are many different types of installation equipment used by helical pile manufacturers and contractors. The most common machines used for installation of helical piles include backhoes, skid steers, mini-excavators and mid-sized tire or track excavators, as shown in Figure 1.9. Smaller equipment is particularly used where accessibility is limited (such as crawl spaces and basements), and mobilization and operation of small equipment is more economical.

Typically, the installation proceeds quickly by rotating (screwing) the pile into the ground while applying a downward force to advance the pile to the desired depth. The shape of the helix facilitates the installation of the pile by rotation of the central shaft, with the pile ideally advancing into the soil at a rate of about one pitch for each full revolution. Figures 1.9 through 1.12 show the installation process and terminology of the installation components.

Figure 1.9 Typical Machines. (a) Backhoe; (b) Extend-boom. Lutenegger (2011)

Figure 1.10 Installation process. DFI (2015)

Figure 1.11 Installation equipment terminology (Courtesy of Hubbell Power Systems, Inc)

Figure 1.12 Installation of Helical Piles (Courtesy of Cantsink)

2. CHAPTER 2: BACKGROUND REVIEW AND HISTORICAL DEVELOPMENT

2.1 Early Effort at Helical Pile Application

Helical piles have been used as a deep foundation option since the early 1800's, Perko (2009). The first available literature is historically credited to Alexander Mitchel, an Irish engineer, who is considered to be the first to apply helical anchors in the geotechnical engineering field. Mitchell's early use of helical piles consisted of offshore marine structures on weak, soft marine soil, such as sand reefs, mudflats, and riverbanks. The early helical pile was similar to a screw, made of cast or wrought iron, hence the word screw pile. These types of piles were screwed into the ground, using human or animal power, via a large wood handle wheel called a capstan. The application of early helical piles was limited due to low bearing capacities, which in turn, is due to the limited installation power tools.

The Maplin Sands Lighthouse in England, built in 1836, is considered the first recorded structure on a helical pile foundation, used by Alexander Mitchell. A profile view of the Maplin sands Lighthouse is shown in Figure 2.1. The foundation consisted of nine wrought-iron screw piles arranged in a form similar to an octagon, with one screw pile in the center Perko (2009).

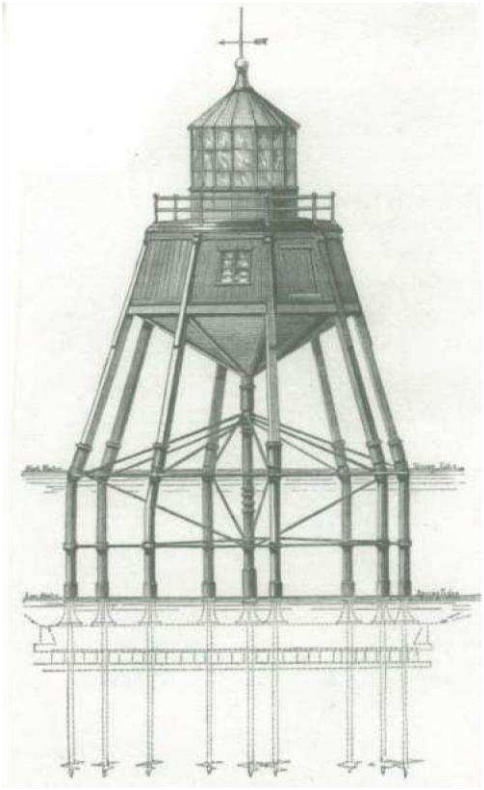

Figure 2.1 Maplin sands lighthouse. Lutenegger (2011)

2.2 Alexander Mitchell: The Origin of Helical (Screw) Pile

Historically, Alexander Mitchell is recognized as the inventor (Father) of the Screw pile foundation. He was the first to introduce the screw pile foundation as a practical foundation system in the early 1800's. He was born in Dublin, Ireland, on April 13th, 1780. He was a builder and brick manufacturer. Even though he had no formal training in engineering, Mitchell was considered as a civil engineer and was elected to Associate Membership of the Institution of Civil Engineers in 1837.

Mitchell's idea of screw piles was first associated with problems concerning the safety of mooring ships in harbors. He applied his invention to provide good, solid foundations

for lighthouses on weak soil. Figure 2.2 shows a few of the original screw piles devised by Mitchell.

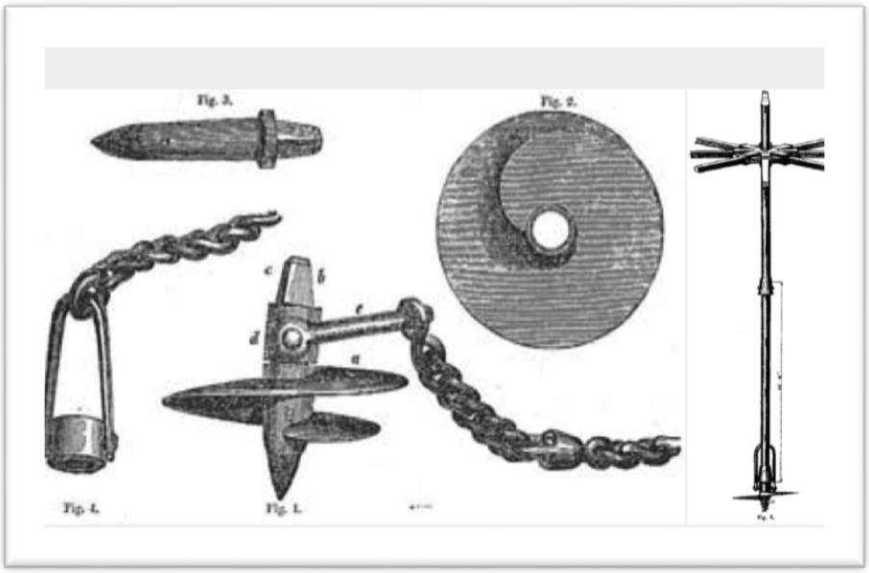

Figure 2.2 Mitchell's original piles. Lutenegger (2011)

Figure 2.3 shows the installation of the pile using manpower. The men use a capstan to apply the required torque to screw the pile into the soil. Mitchell authored several technical papers, one of which was published in the Civil Engineering and Architects journal, (1848). The below excerpt from this paper, shows that, in terms of geotechnical engineering practice, the work in applying screw piles in his era, is not that different from modern geotechnical approaches in the way that three basic design parameters are required for helical piles: minimum depth, soil strength, and bearing capacity.

"*whether this broad spiral flange, or "Ground Screw, "as it may be termed, be applied to support a superincumbent weight, or be employed… to resist an upward strain, its holding power entirely depends upon the area of its disc, the nature of the ground into which it is inserted, and the depth to which it is forced beneath the surface*." DFI (2015)

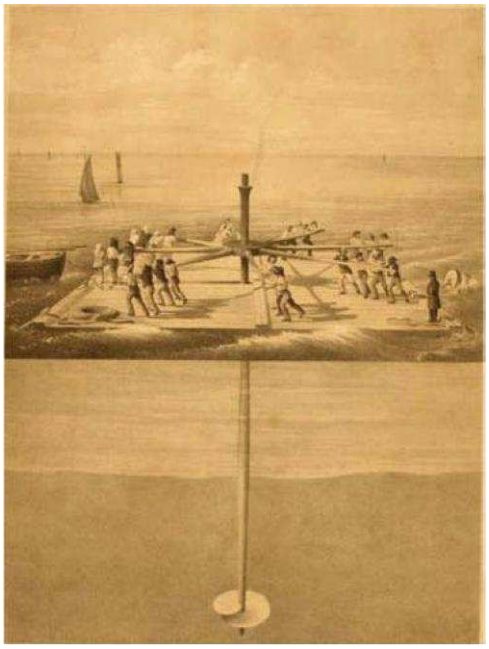

Figure 2.3. Early installation method. Lutenegger (2011)

Mitchell continued to develop screw piles in the 1800's, and used it successfully in building foundations for lighthouses, bridges, and piers as well as other engineering applications. Michell's invention of helical piles was so valuable to the construction of lighthouses, that Author Irwin Ross, as quoted by Hendrickson (1984, pp. 332-333) explained eloquently in the following excerpt:

"*The erection of lighthouses on this principle caused the technical world to wonder. This invention, which has been the means of saving thousands of lives and preventing the loss of millions of dollars' worth of shipping, has enabled lighthouses and beacons to be built on coasts where the nature of the foreshore and land formations forbade the erection of conventional structures. The screw pile has been used in the construction of lighthouses and beacons all over the world, and it earned for Mitchell and his family a large sum*". Perko (2009).

Lutenegger (2011), provides a great summary of the historical development of helical piles between the period 1836-1900. He wrote extensively about the life and work of Alexander Mitchell and his valuable contribution to the development and application of screw piles in the geotechnical engineering field.

2.3 Helical Piles in the Early to Mid-1900's

The period from the invention of screw piles to the late 1800's could be termed, as described by Perko (2009), the "Marine era", due to the fact that the use of these type of foundations was commonly built near marine shores, such as lighthouses, moorings, and ocean front piers. Few patents could be found during this period. Patent numbers 30,175 in 1860, 101,379 and 108,814 in 1870, which are referred to as improvement to prior art, indicate that earlier patents did exist (Perko, 2009).

The development of helical piles continues through the early 1900's and more patents were issued. During this period, helical piles saw a significant increase in use in regard to utility enclosures, tower legs and pipelines. This era was generally termed as the "utility era". However, from about 1920 to World War II, there was a "quiet" period that saw the rise of other types of foundations and a decrease in use of helical piles. This was primarily due to the development of other deep foundation methods and advances in pile driving/ installation equipment. With the advent of powerful hydraulic installation equipment and improved practical knowledge and advances in engineering design and geometry, helical pile usage increased substantially during the 1950's. They are used for foundation repair (underpinning in both residential and commercial), guy anchors, tie-down, new construction foundations, earth retention, seismic retrofit, and many other applications. Today, research continues in studying the behavior of helical piles as related to capacity

and serviceability and this type of foundation continues to provide cost effective deep foundation alternatives in the modern era.

2.4 Modern Approach to Helical pile Design

Helical piles, like all other foundations, are simply common means of transferring the weight of structures to the ground. For these structures to perform satisfactorily, the foundation must be properly designed, based on the soil engineering properties and its suitable application. Helical pile design uses traditional soil mechanics theories and analysis along with empirical correlations that were developed based on field test data. Design of helical piles, or any other foundation for that matter, requires a prior knowledge of the geotechnical engineering properties of the site along with structural design loads with a recommended factor of safety.

The field and laboratory investigations required to gather geotechnical information is termed soil or subsurface exploration. The degree of subsurface exploration depends heavily on the type of project and local building codes as well as local construction practices and standards. Basically, the elements of a site investigation should provide at least enough information to determine the type of foundation required (shallow or deep), help the geotechnical consultant to make a recommendation on the allowable load capacity of the foundation, to predict settlement, in addition to the water table location vis-à-vis the construction zone as well as identification of environmental problems and their solutions. During the design process of the project, subsurface exploration is often the one aspect that gets overlooked. Many clients obtain standard soil borings but are not willing to pay the extra money for a full laboratory analysis. This lack of geotechnical information on soil properties will lead the design engineer to estimate important

engineering properties of the soil based on in situ field tests. Very often the Standard Penetration Test (SPT: ASTM D3441; AS1289.6.3.1) blow counts and the Cone Penetration Test (CPT: ASTM D 3441: AS1289.6.5.1) are used to estimate the shear strength parameters of soil in helical pile foundation designs. Bowles (1988) and Das (2011) provide a summary on the use of the SPT and CPT. In the subsequent sections, the design methods for helical piles are described.

2.4.1 Theoretical axial capacity

Helical piles are designed to resist axial compression, axial tension, and/or lateral loads from residential or commercial structures. The torque capacity correlation factor is only used for predicting axial tension and compression capacities, and not applicable for lateral capacity prediction. Therefore, the pile lateral capacity will not be discussed herein. There are basically two design methods used to determine the theoretical soil capacity of a helical pile: individual bearing plate method and the cylindrical shear method. The other method, which is probably the most common one used to predict the ultimate pile capacity, termed “capacity to torque correlation”, is an empirical relationship between the final termination torque and ultimate pile capacity. These common design methods are discussed in detail below.

2.4.1.1 Compressive individual plate bearing method

It is generally considered that helical piles (with shaft diameter less than 3.5 inches), resist load mainly through the helix plates. The skin friction between the shaft and soil is usually ignored due to the small diameter of the helical pile. The soil capacity of a helical anchor/pile is dependent on the soil strength, the projected area of the helix plate, and the depth of the helix plates below grade. The soil strength can be evaluated

by various techniques and theories well described in the geotechnical engineering literature. The projected area of the helix plates can be controlled by the size and number of helices attached to the shaft. For a given pile depth, two modes of failure may occur, shallow and deep. The terms shallow and deep refers to the depth of the pile bearing plates with respect to the ground surface. Both failure modes are extensively described in geotechnical engineering books, (Perko, 2009).

In the helical pile design community, it is generally assumed that the soil failure mechanism will follow the theory of a general bearing capacity failure. In this case, the capacity of the helical pile/anchor can be determined as the sum of the capacities of the individual helix plates. The helix/plate capacity is evaluated by calculating the unit bearing capacity of the soil at each helix, and then multiplying the result by the individual helix's projected area (Figure 2.4a). For this method to be valid, the helices must be spaced far enough to avoid overlapping of their individual "pressure bulbs", i.e., the stressed soil zone. This will prevent the helix from significantly influencing the performance of another. Typically, the spacing between two adjacent helices is about 3 times or more the diameter of the lower helix.

Helical piles are deep foundations and Terzaghi's (1943) general bearing capacity equation is used to determine the helical pile capacity as follows:

$$Q_{ult} = \Sigma A_h(1.3c'N_c + q'N_q + 0.3\,\gamma DN_\gamma) \quad (2.1)$$

Where:

A_h = area of individual helix plate

c' = Effective cohesion

q' = Effective vertical overburden pressure

γ = Effective unit weight of soil

N_c, N_q & N_γ = Bearing capacity factors

D = Helix plate diameter

Note: in the helical pile industry, some engineers use Terzaghi's general bearing capacity equation in a form that is slightly different from equation (2.1). For example, Lutenegger (2015) uses the following equation to determine the pile capacity as:

$$Q_{ult} = \Sigma A_h(c'N_c + q'N_q + 0.5\gamma DN\gamma) \quad (2.2)$$

The helical pile ultimate capacity determined from the above equations assumes that the resistance due to the skin friction between the pile shaft and soil is negligible (valid for small diameter piles). The third term in the above equation is generally ignored as long as the ratio of the depth of the pile to diameter of the pile is very large, which is generally the case for helical piles. Based on these assumptions, the equation to calculate the ultimate bearing capacity of helical piles can be reduced to:

$$Q_{ult} = \Sigma A_h(c'N_c + q'N_q) \quad (2.3)$$

In the case of cohesive soil ($\varphi = 0$), the ultimate soil capacity can be determined as:

$$Qult = \Sigma A_h c'N_c \quad \text{for clay} \quad (2.4)$$

The Nc bearing capacity factor, when applied to helical anchors/piles is often taken equal to 9, as it is in other deep foundation applications. The design engineer has the option of changing the default clay bearing capacity factor of 9 as needed and applicable. For non-cohesive or granular soil (c = 0), the ultimate capacity can be determined as follows:

$$Qult = \Sigma A_h q'N_q \quad \text{for granular} \quad (2.5)$$

The bearing capacity factor Nq is dependent on the frictional angle (φ) of the cohesionless soil. A published graph that can be used to determine the factor Nq as a function of the friction angle φ was adapted from the work by Meyerhof (1976). It was based on the equation below, which is Meyerhof's Nq values divided by 2 for long term applications.

$$N_q = 0.5(12 \times \varphi)^{\varphi/54} \quad (2.6)$$

Where:

N_q = Bearing capacity factor for non-cohesive soil

Φ = Angle of internal friction

In the case that the angle of friction is not known, but the blow counts from the standard penetration test are available, the following relationship can be used to obtain the friction angle. This relationship was based on empirical data from Bowles (1968).

$$\Phi = 0.28N + 27.4 \quad (2.7)$$

Where:

N_{60} = Blow count per ASTM D 1586 Standard Penetration Test

Φ = Angle of internal friction

In the case of mixed soil or c – φ soil, Eq (2.1) can be used to determine the ultimate soil capacity by using the appropriate values for both the cohesion and friction terms in the equation.

2.4.1.2 Compressive Cylindrical Shear Method

As the spacing of the helices along the pile shaft decreases, it is more likely that the influence zones of the multiple helical plates will overlap, and the soil mass between the top and bottom helices will form into a cylindrical failure surface with diameter equal to

that of the helical plates, as shown in Figure 2.4.b The ultimate capacity is then equal to the sum of the shear strength along the cylinder of soil between the helix plates and the bearing capacity of the bottom helix blade. Figure 2.4.b shows how to determine the ultimate capacity using the cylindrical shear method with the following equation:

$$Q_{ult} = 2\pi RL\,(c' + K_o q' \tan\varphi) + A_h\,(c' N_c + q' N_q) \qquad (2.8)$$

Where:

Q_{ult} = Ultimate Capacity

R = Average helix radius

L = Total Spacing Between All Helix Plates

K_o = At-Rest Earth Pressure Coefficient

Φ = Soil friction Angle

A_h = Area of Bottom Helix Plate

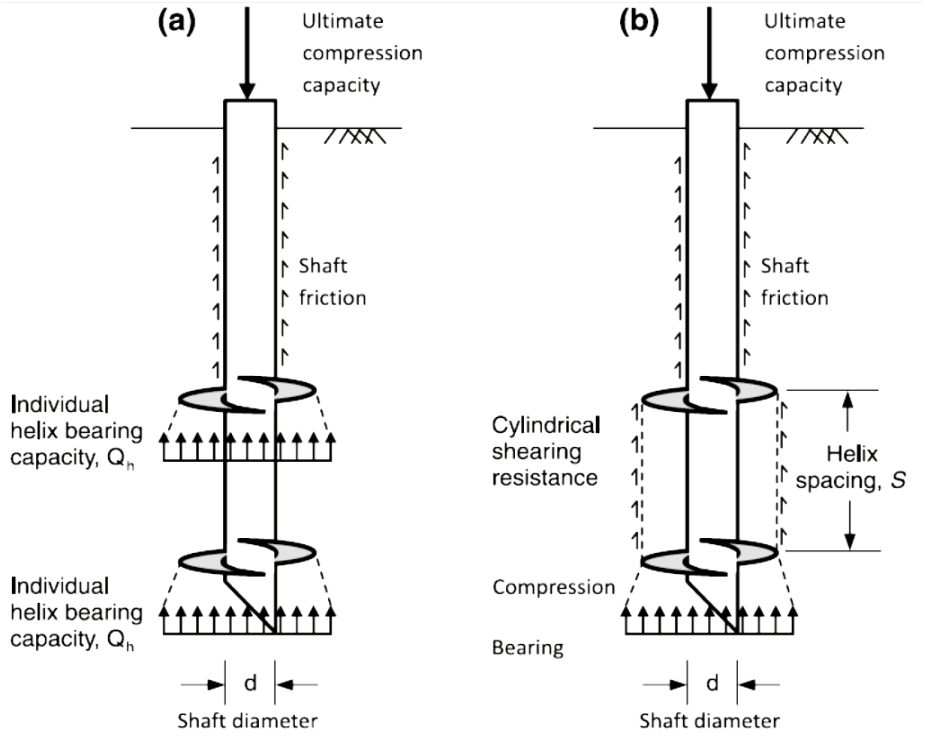

Figure 2.4. a) Individual bearing b) Cylindrical shear. Lutenegger (2011)

2.4.1.3 Uplift resistance

The total ultimate tension capacity of a helical pile can be determined using essentially the same procedure used for compression loading, provided that the pile is installed to a sufficient depth (not necessary required in compression loading) to ensure a deep mode of behavior. The embedment depth is a very important concept governing the performance of helical piles in tension. For a pile that is installed to a depth that is too shallow, the soil above the plates will be considered not sufficient enough to provide the needed pullout resistance, and the pile may fail in a shallow mode as depicted in Figure 2.5. To ensure a deep mode of failure, AC358 (2017) requires that the upper most helix needs to be installed at a depth equal to 12D below the ground surface, where is D is the largest diameter of the helix configuration.

Perko (2009) suggested that the required minimum depth of a helical pile should be equal to that depth where the weight of `cone of soil above the upper most helix is equal or higher than the theoretical ultimate capacity derived from basic soil mechanics, as shown in the next two sections. Figure 2.6 shows a 45-dgree influence cone used by Perko to compute the total weight of the cone of soil.

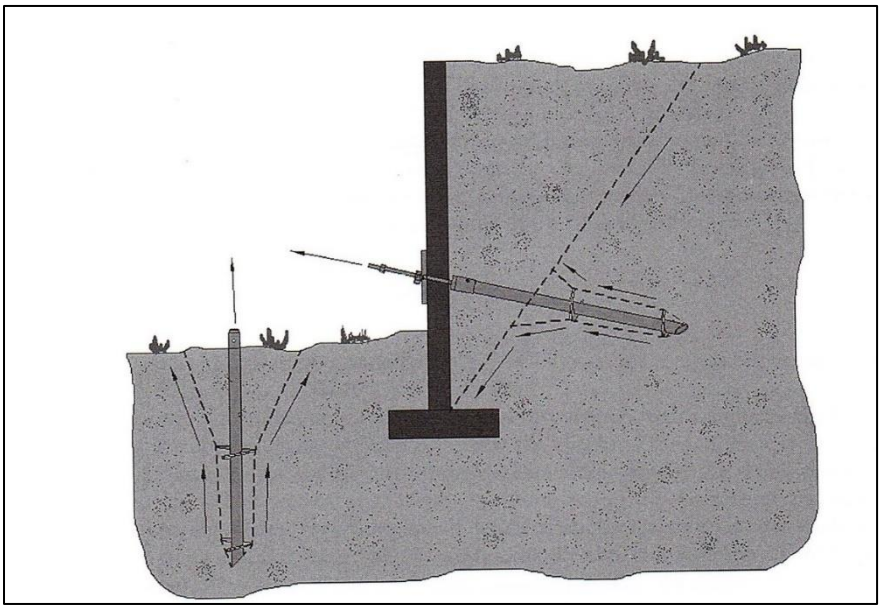

Figure 2.5 Insufficient embedment length. Perko (2009)

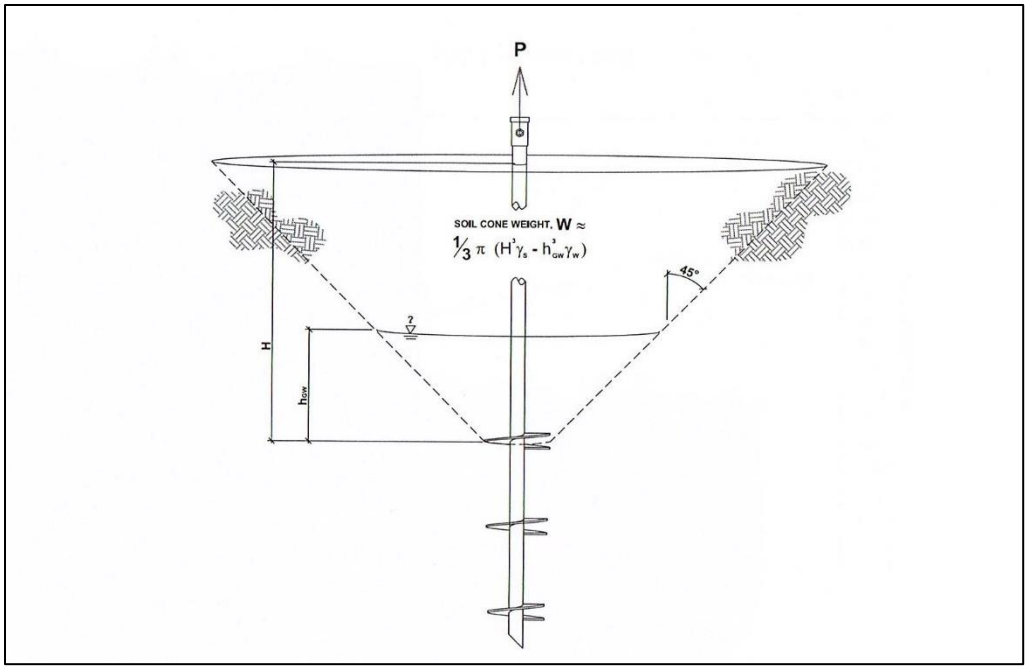

Figure 2.6 Influence cone. Perko (2009)

Depending on the helical bearing plates spacing, the helical pile can exhibit either an individual bearing or cylindrical shear mode of failure. In the following sections, both the individual bearing and cylindrical shear methods are discussed assuming a deep mode of failure.

2.4.1.4 Individual bearing method uplift

In this method, individual plates are assumed to develop full capacity with no interaction between the plates. Therefore, the total ultimate capacity of the pile could be determined as the sum of individual bearing plate capacities, obtained by calculating the bearing capacity above the helix as shown in Figure 2.7 below. In equation form:

$$Q_P = \Sigma Q_H \tag{2.9}$$

$$Q_H = \Sigma A_h(c'N_c + q'N_q) \tag{2.10}$$

Q_P : Total capacity of pile

Q_H : Capacity of an individual plate

All the other terms in the above equations are as discussed before.

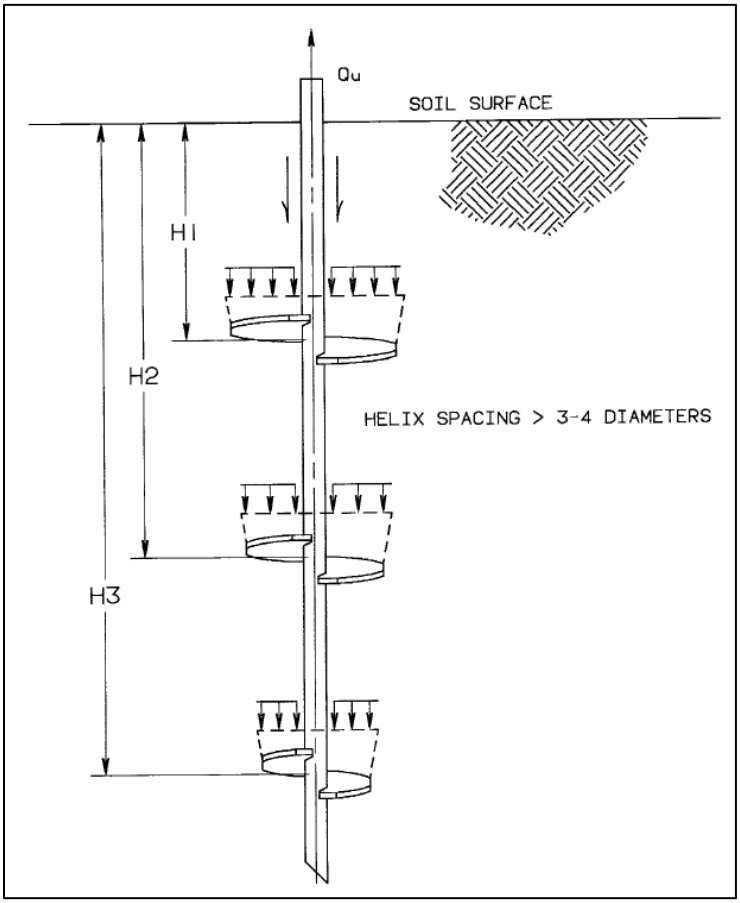

Figure 2.7 Individual Bearing Uplift. Lutenegger (2009)

2.4.1.5 Cylindrical shear method uplift

For the cylindrical shear method, the uplift capacity of the pile can be determined by considering the sum of the soil shear stresses mobilized along the surface of a presumed cylinder between the plates and bearing on the upper helix, as shown in Figure 2.8 below. The other plates are encased within the presumed cylinder envelope and therefore have no effect on the uplift capacity. In the case adhesion between the pile and

soil is considered in the computation of uplift capacity, it should be assumed to act along the shaft length above the upper most helix. In equation form, the total uplift capacity is given by:

$$Q_{ult} = 2\pi RL\,(c + K_o q'\tan\varphi) + A_u\,(cNc + q'Nq) \qquad (2.11)$$

Where A_u is the area of the upper most plate. All other terms are as defined before.

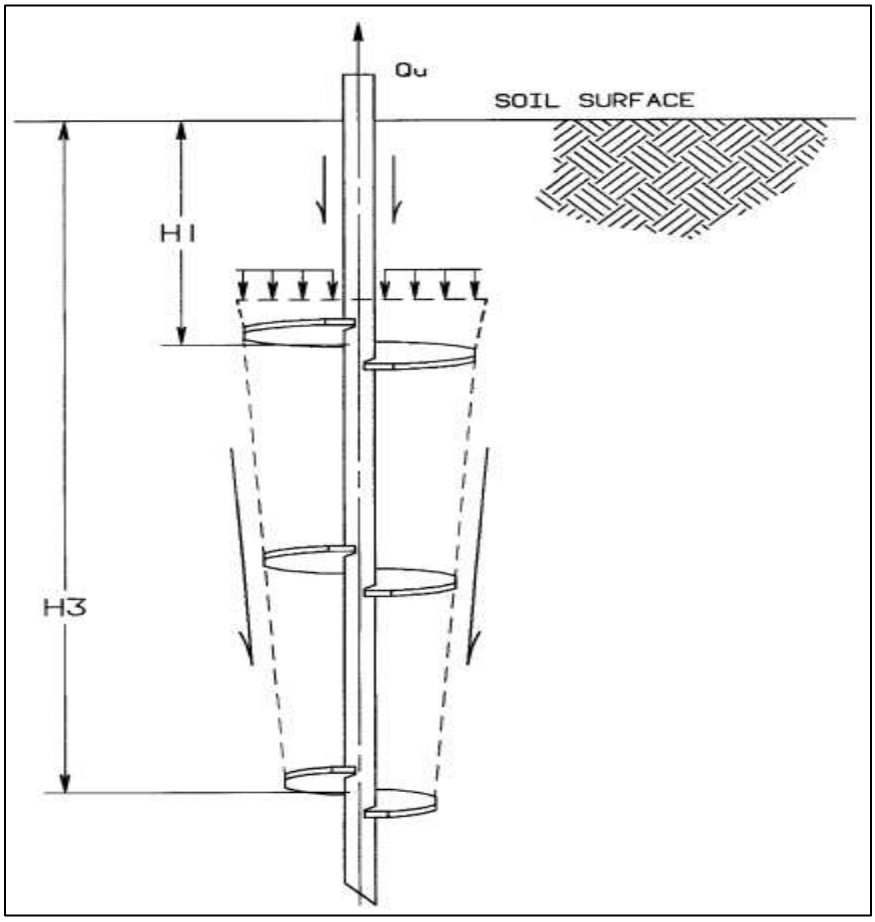

Figure 2.8 Cylindrical shear method uplift. Lutenegger (2009)

2.4.1.6 Shaft adhesion

In the previous sections, the shaft friction capacity was ignored based on the assumption that slender shaft contribution through frictional resistance is very small and negligible, Perko (2009), Lutenegger (2015). This assumption has been shown to be valid

for shafts sizes smaller than 3.5". however, for larger diameter piles, friction along the shaft has been shown to contribute a considerable portion of the total pile resistance.

Friction capacity of a helical pile can be determined by considering the unit frictional resistance between the pile material and the soil. Let P be the perimeter of the pile and f_s the sum of the friction and adhesion between the pile and soil, then the friction capacity of a small portion ΔL of the pile length can be calculated as:

$$\Delta Q_f = P\Delta L f_s \tag{2.12}$$

The friction capacity of the entire pile can then be determined by summation of equation (2.11) over the total length of the pile, which results into:

$$Q_f = \Sigma P\Delta L f_s \tag{2.13}$$

Where:

P: Perimeter of the pile

f_s: Sum of friction and adhesion between soil and pile

ΔL: Incremental pile length over which f_s and P are constant.

The terms ΔL and P are physical properties of the pile that can be calculated accurately. However, the unit frictional resistance will depend on several factors, mainly the soil type (cohesionless, cohesive) and the pile material (steel, concrete, timber). There are several methods available in the literature for estimating the unit friction resistance. For more on pile friction, the reader is referred to Das (2011), Fleming et.al. (2009) and Hu and Randolph (2002). Below is a simplified method used by the US Navy Design Manual DM-7 (1986) for either sand or clay. For clayey soil, f_s is taken as the adhesion

factor c_a that can be used in the above equation to determine the frictional shaft resistance. Table 2.1 below gives recommended value of c_a for steel piles.

Table 2.1 Recommended values of adhesion c_a, clay (from Navy Manual DM-7)

Soil Consistency	Cohesion, c (psf)	Adhesion, c_a (psf)
Very soft	0-250	0-250
Soft	250-500	250-460
Medium Stiff	500-1000	460-700
Stiff	1000-2000	700-720
Very Stiff	2000-4000	720-750

For sandy soil, the unit frictional resistance, f_s, is basically the horizontal normal soil pressure multiplied by tanφ. in equation form,

$$f_s = K\, q \tan\varphi \qquad (2.14)$$

Where:

f_s :Unit average frictional resistance (psf)

K : Coefficient of lateral earth pressure

q : Effective overburden pressure at increment ΔL (psf)

φ' : Effective angle of internal friction (degree)

Table 2.2 Recommended values of friction fs (psf), sand (from Navy Manual DM-7)

σ (psf)	***Friction angle φ (degree)***				
	20	25	30	35	40
500	*137*	*175*	*217*	*263*	*315*
1000	*273*	*350*	*433*	*525*	*629*
1500	*410*	*524*	*650*	*788*	*944*
2000	*546*	*700*	*866*	*1050*	*1259*
2500	*683*	*875*	*1080*	*1313*	*1574*
3000	*819*	*1050*	*1300*	*1575*	*1888*
3500	*956*	*1245*	*1520*	*1838*	*2203*
4000	*1092*	*1400*	*1732*	*2100*	*2517*

2.4.2 Capacity torque correlation

As mentioned in the previous sections and in literature, several analytical methods exist for the analysis and design of individual plate anchors and other foundations subjected to axial forces. For helical piles, the two most common analytical methods used in predicting the ultimate soil capacity are the individual bearing and cylindrical shear methods stated above. A third method, considered to be the greatest attribute (due to its simple application) of helical foundations, is based on the empirical relationship between the final installation torque and the predicted ultimate soil capacity of the pile. This is analogous to the relationship of pile driving effort to plie capacity. As a helical pile is installed into increasingly denser/harder and deeper soil, obviously, the resistance to installation (installation energy or torque) will increase.

The concept that there is a correlation between the installation torque and the ultimate pile capacity has been used as a rule of thumb as early as the 1950's, Wilson (1950). There was no precise definition of this relationship at the time, given the possible variables that were yet to be identified. In addition, the test data collected were kept proprietary and out of public use until the release of the first public reports in late 1970's, (Cole (1978), Gill and Udwari (1980) and Perko (2009)). However, simple empirical relationships did exist and were used successfully for many years.

Over the past 40 years, numerous studies have been conducted in an effort to determine and quantify the relationship between installation torque and ultimate pile capacity. Different authors have reported and asserted different variables and limits to the capacity-torque relationship. Yet, most of these studies did not conclude with capacity-torque relationship, similar to the one developed by Hoyt and Clemence (1989), that can

be useful for the helical pile industry. Ruberti (2015) conducted 63 tests and reported that the K_t value, defined in equation (1.1) is higher for tapered screw piles than circular ones, that K_t is higher in soft clay than in stiff clay, and that K_t depends on torque measurement precision as well as definition of final termination torque and failure criteria selected. Livneh and El Naggar (2008) suggested that the capacity-torque correlation is a useful tool for predicting pile capacity and that the final termination torque should be taken as the average over the last three readings. Sakr (2009) advocated that the correlations that exist with regards to the installation torque and capacity, were mostly based on the testing of small diameter helical piles, and therefore, should be used with caution with respect to large diameter helical piles.

In the following sections, studies relating pile capacity to installation torque are described. These studies reported very unique relationships between capacity and torque. These findings were either developed theoretically or based on test results.

2.4.2.1 Hoyt and Clemence, 1989

The empirical relationship between pile capacity and installation torque has been used for a long time. It has gained recognition and popularity in the past few decades, due to extensive research and testing, resulting in more rational capacity-torque correlation. To the best knowledge of the author, the capacity-torque correlation of helical piles has become widely accepted since the publication of a 1989 landmark paper by Hoyt & Clemence (1989). In this benchmark publication, the authors have proposed the following capacity-torque correlation:

$$Q_{ult} = K_t \times T \qquad (2.15)$$

Where:

Q_{ult} = Ultimate uplift Pile Capacity

K_t = Capacity to Torque Ratio (empirical factor)

T = Final installation (Termination) Torque

Hoyt and Clemence suggested that the parameter K_t is a constant that depends primarily on the shaft size, and it is independent of the number and size of the helical plates as well as the subsurface soil conditions and its engineering properties. The empirical relationship was based on the analysis of ninety-one (91) collected full scale field load tests. All these tests were performed in tension to measure the uplift capacity of the pile. The pile tests analyzed were performed at 24 different test sites with various soil types (sand, silt and clay). The full-scale load tests involve shaft sizes ranging from 1.5 inches (38 mm) square to 3.5 inches (89 mm) round shafts. The number of helices attached to each anchor varied from two to fourteen, with diameters ranging from 6 inches (152 mm) to 20 inches (508 mm). The spacing between the helices varied from 1.55 D to 4.50 D, which falls within the design limits of most commercially available multi-helix anchors.

For each pile configuration, the observed measured ultimate capacity, the recorded final torque measurement, and theoretically calculated expected ultimate capacity were considered in the analysis. The predicted ultimate capacity was evaluated using three methods: the cylindrical shear method, the individual plate bearing method, and the capacity torque correlation method. The third method was based upon a K_t factor of 33 m^{-1} (10 ft^{-1}) for all piles with shaft diameters less than 89 mm (3.5 inches), 23 m^{-1} (7 ft^{-1}) for helical piles with 89 mm (3.5 inch) shaft diameter, and 9.8 m^{-1} (3 ft^{-1}) for those with 219 mm (8.63 inch) shaft diameter.

Hoyt and Clemence suggested that the final installation torque should be taken as the average torque recorded over the final distance of penetration equal to three times the diameter of the largest helix. All the anchor tests were short term. Most of the tests used strain-controlled methodology, which included a final loading step of imposing continuous deflection at a rate of approximately four inches per minute and recoding the resulting load reaction as the ultimate pile capacity. In their study, Hoyt and Clemence compared the actual test results with the predicted capacity based on cylindrical shear, individual bearing and torque correlation methods. The results of these three comparisons are shown in Figures 2.9, 2.10 and 2.11. In each figure, the ratio of the actual measured capacity to the predicted capacity is plotted on the X-axis, while the number of occurrences is plotted on the y-axis. The statistical parameters (median, mean, standard deviation) are shown in the top right of each figure. As indicated by the representative histograms in Figures 2.9 through 2.11, the capacity-torque correlation predictions provided the least variance and all three methods showed equal potential for over predicting ultimate capacity.

Hoyt and Clemence explained that the major advantage for the capacity-torque correlation confirmation method is that it removes large source of errors and variances from the prediction process, mainly the soil testing errors, possible changes in soil properties between the time of anchor testing and boring drilling, engineering judgment, and soil strength parameters. The capacity-torque correlation has a drawback because it cannot be used until after the pile is installed, which makes this method more suitable for on-site production control than design.

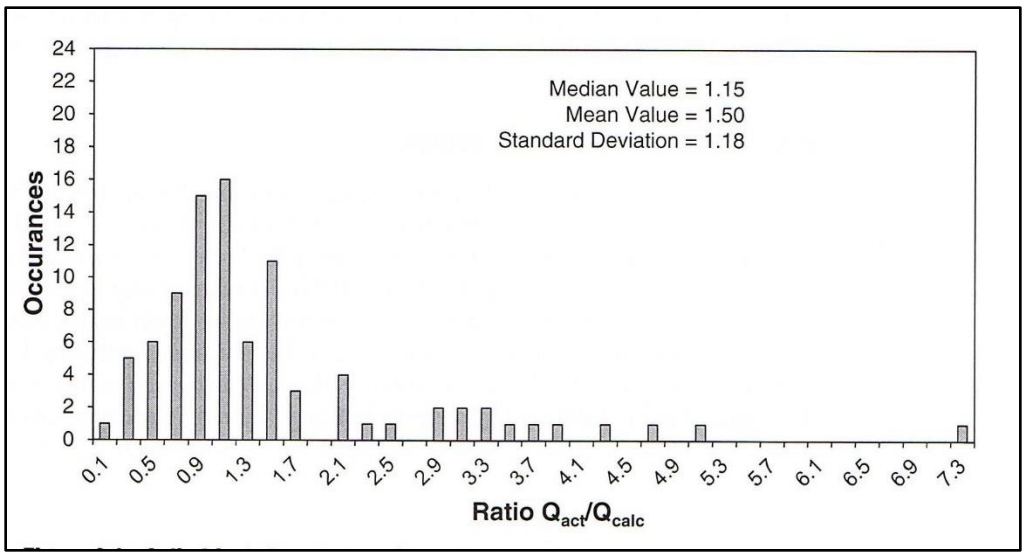

Figure 2.9 Cylindrical shear comparison (Hoyt and Clemence, 1989)

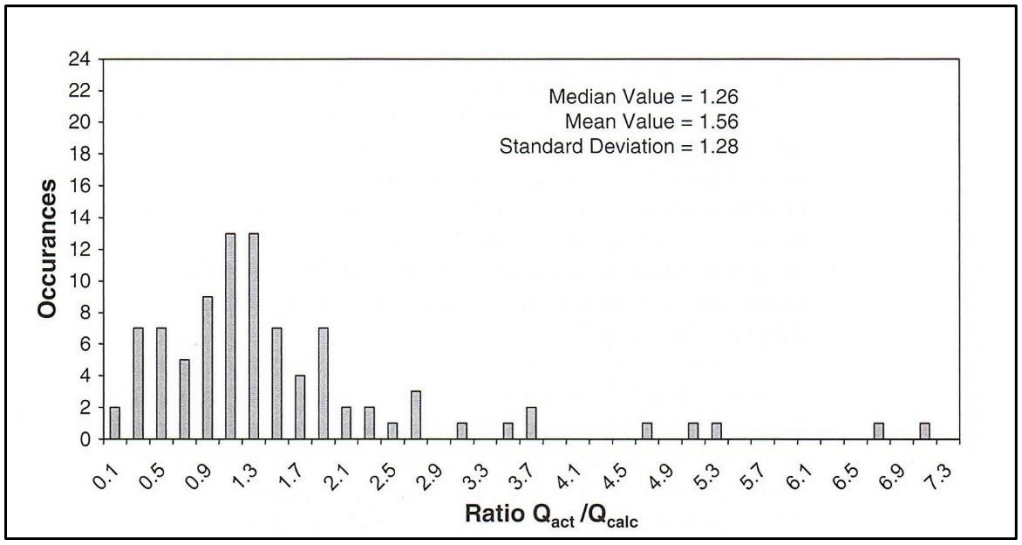

Figure 2.10 Individual bearing comparison (Hoyt and Clemence, 1989)

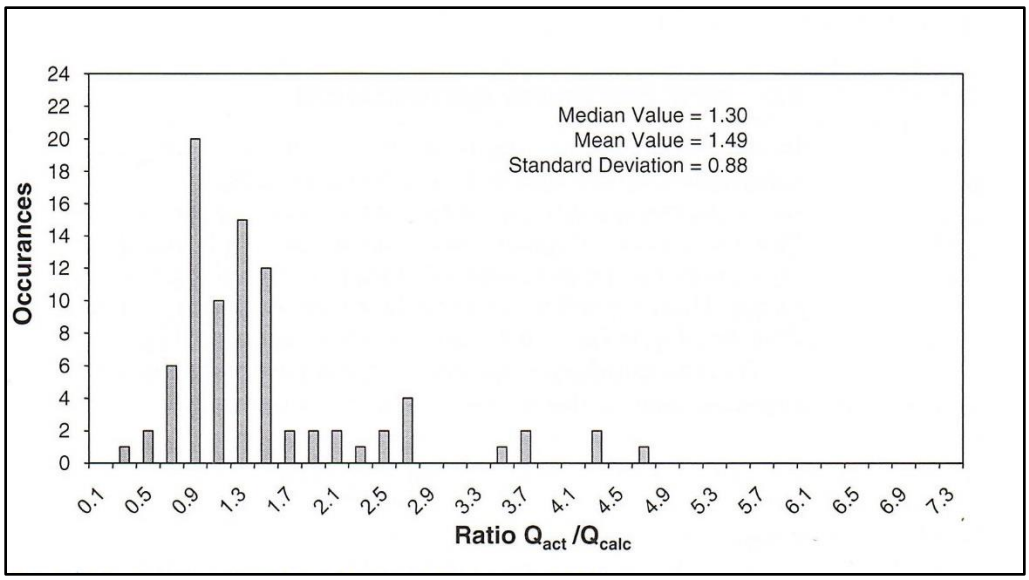

Figure 2.11 Torque correlation comparison (Hoyt and Clemence, 1989)

2.4.2.2 Ghaly and Hanna,1991

Ghaly and Hanna (1991) presented experimental and theoretical studies on the required torque needed to install helical anchors. The tests were conducted at the Lab using five model helical piles installed in sandy soil (dense medium and loose). The tests were set up in a way that allows direct measurements of installation torque, uplift capacity, pile displacement, stress development in the sand layer and sand surface deflection throughout the testing procedure. From the test results, a theoretical model was developed, taking into account the factors affecting the installation torque. This particular relationship between capacity and torque was based on soil density, area of the helix, embedment depth and the pitch of helix. Absent from the newly developed capacity torque-correlation is the shaft diameter, which is generally known as the largest contributor factor affecting capacity-torque relationship, Perko (2009). Ghaly and Hanna's model was compared to test results from full scale field load tests and was found that the

developed model greatly overestimates pile capacity and was deemed not applicable for full scale field capacity as reported by Tappenden (2004).

2.4.2.3 Perko, 2009

Perko (2009) proposed a new capacity-torque correlation based on test results from 239 load tests as well as a theoretically derived capacity torque relationship based on energy model to further justify the relationship between torque and capacity. To determine the empirical relationship between torque and capacity, Perko plotted the measured K_t values obtained from the test results versus the effective shaft diameter, d_{eff}, as shown in Figure 2.12. Perko defined the effective shaft diameter as the diameter of the hole in the ground created by rotating the pile shaft 360 degrees during installation. Based on this definition, the effective diameter of a round shaft is basically its outside diameter. For square shafts, the effective diameter is the diagonal between opposite corners. Using an exponential regression analysis of the collected test data, Perko obtained the best-fit empirical equation relating K_t factor to the effective shaft diameter as shown in the relationship below:

$$K_t = \frac{\lambda_k}{d_{eff}^{0.92}} \tag{2.16}$$

Where:

λ_k is a fitting factor equal to 22 $in^{0.92}/ft$

d_{eff}: equals to outside diameter for round shafts and diagonal distance between opposite corners for square shaft.

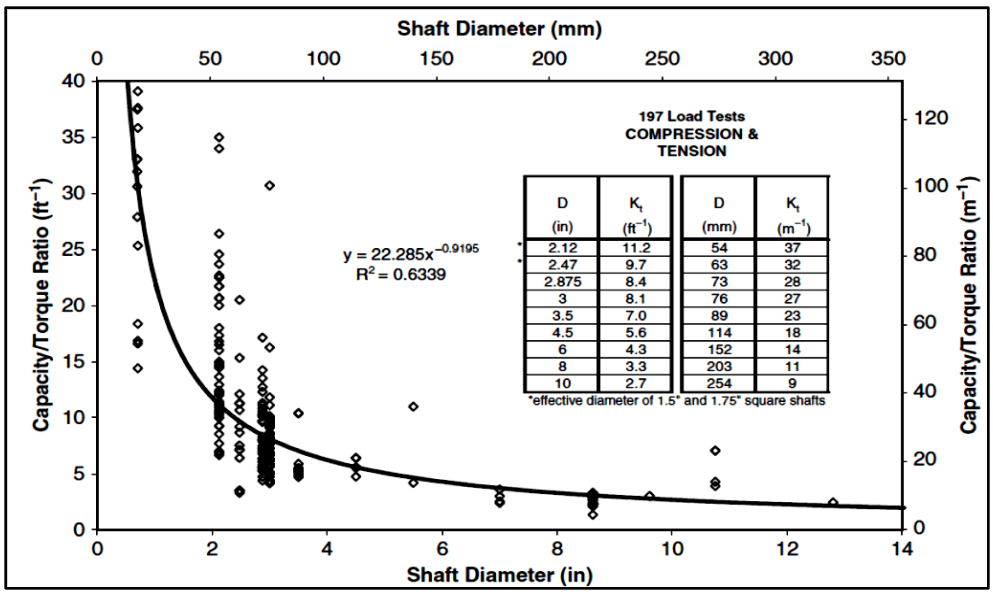

Figure 2.12 Empirical capacity-torque ratio (Perko, 2009)

The K_t values obtained from equation (2.16) were generally in good agreement with the previous work published by Hoyt and Clemence (1989). In addition, Perko examined the difference between tension and compression capacity correlation by separating the tension tests from the compression tests. Figures 2.13 and 2.14 show the plotted measured K_t as a function of the effective diameter for both tension and compression, respectively. The results from the regression analysis of both data sets indicate that the K_t values are higher in compression than tension, as reported from previous work. On the average, Perko suggested that K_t values are about 10% higher in compression than in tension. Other studies have reported that K_t values in compression could be 16 to 30 % higher than K_t values in tension. It is important to remember that in the test results that Perko used, the ultimate capacity was determined based on the modified Davisson (1972) method (10% net deflection), whereas Hoyt and Clemence

defined the plunging failure load as the load corresponding to a minimum strain rate of 4 inches per minute.

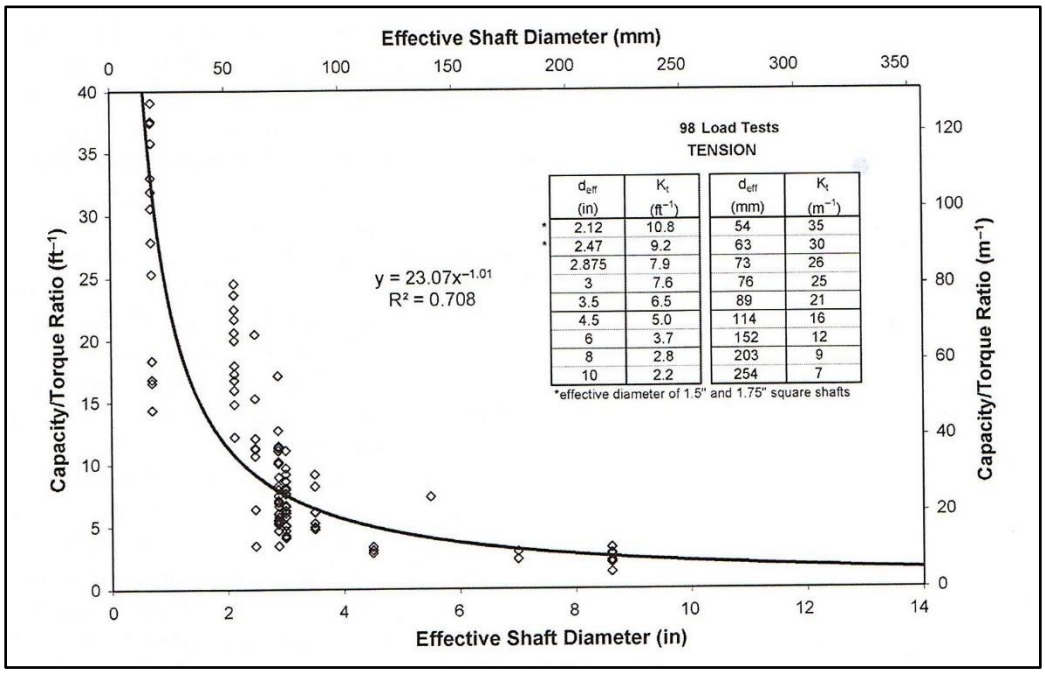

d_{eff} (in)	K_t (ft^{-1})	d_{eff} (mm)	K_t (m^{-1})
* 2.12	10.8	54	35
* 2.47	9.2	63	30
2.875	7.9	73	26
3	7.6	76	25
3.5	6.5	89	21
4.5	5.0	114	16
6	3.7	152	12
8	2.8	203	9
10	2.2	254	7

Figure 2.13 Empirical capacity-torque ratio, tension only. (Perko,2009)

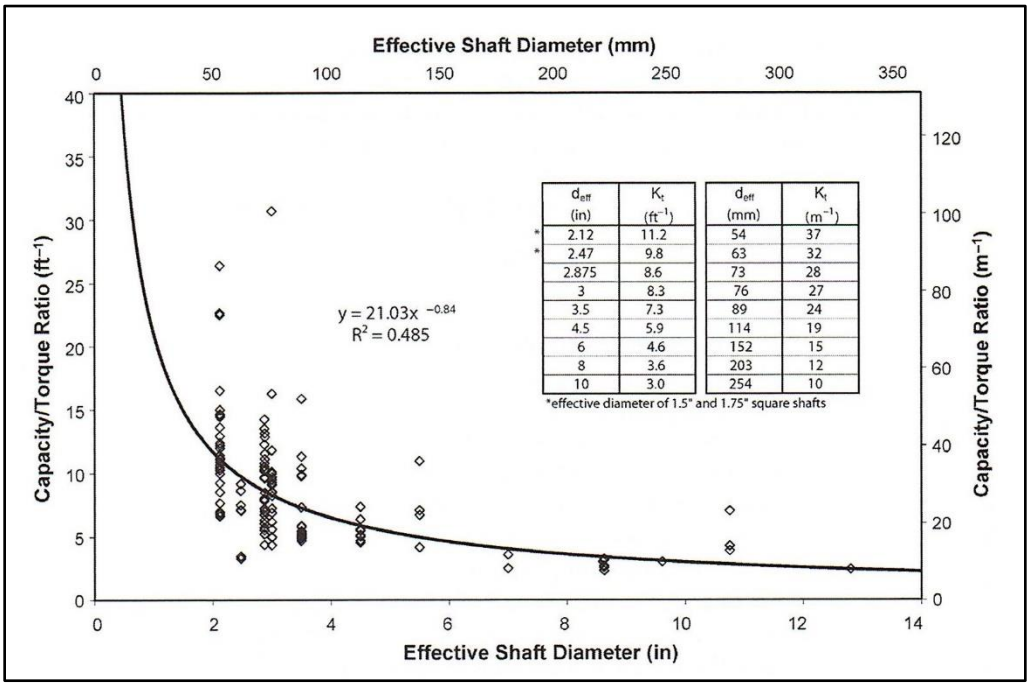

d_{eff} (in)	K_t (ft^{-1})	d_{eff} (mm)	K_t (m^{-1})
* 2.12	11.2	54	37
* 2.47	9.8	63	32
2.875	8.6	73	28
3	8.3	76	27
3.5	7.3	89	24
4.5	5.9	114	19
6	4.6	152	15
8	3.6	203	12
10	3.0	254	10

Figure 2.14 Empirical capacity-torque ratio, compression only. (Perko, 2009)

2.4.2.4 Filho, J.M.S.M.S, Morais, T.S.O, Tsuha, C.H.C, 2014

In this study, Filho, Morais, and Tsuha (2014) did not conclude with a specific or unique capacity-torque correlation that can be used for pile capacity prediction. However, they were able to identify and quantify variables affecting this relationship. They conducted tests to evaluate the fraction or percentage of the installation torque and the pullout capacity related to the shaft extensions and the lead section with helical plates, as well as its effect on the torque capacity ratio, K_t. The strain gages were used to determine the distribution of torque and load during installation and testing. In addition to the evaluation of the distribution of both torque and load within the shaft anchor, they also studied the effect of different lead section sizes on the capacity torque correlation, K_t. specifically, two test samples were composed of lead sections with a diameter of 73 mm and extensions with 101.6 mm. the other test sample was composed of a lead section with 101.6 mm in diameter and extensions that are the same size as the lead section.

For all test samples, the helix configuration consists of four plates with diameters of 254 mm, 305 mm, 356 mm and 356 mm. Two anchors were installed to a depth of 15 meters, the other one was installed to a depth of 12.5 meters. The ultimate anchor capacity obtained from the load test was based on a displacement equal to 10% of the average helix diameter. Based on the collected data from the installation torque and the load tests, Filho, Morais, and Tsuha concluded the following major points:

As the helical anchor penetrates deeper into the ground, the percentage of the total torque resisted by the shaft extensions increases, whereas the percentage of the total torque resisted by the lead section (with plates welded to it) decreases. This observation

shows the influence of the shaft length on the measured installation torque at the pile head.

The percentage of the shaft resistance (extensions) was found to be as high as 50% of the total uplift capacity of the anchor, especially when the anchor is installed deep into a firm suitable soil.

The capacity resisted by the top helix was about 20% of the total capacity resisted by the other three helices. This is due to the fact that the top helix is sitting on a soil that has been penetrated and disturbed more times than the other helices.

For the two identical anchors (same lead sections and extensions), the resulting capacity to torque ratios, K_t, are significantly different. This suggests that the K_t factor depend on other factors along with the shaft diameter, as found in the literature. The K_t factor is greater in the case in which the anchor shaft resistance is 50% of the total anchor pullout capacity compared to the case of the anchor shaft with low resistance.

2.4.2.5 Cherry and Souissi, 2010

Cherry and Souissi evaluated the test results of 93 full-scale compression and 109 full-scale tension load tests conducted at CTL|Thompson, Inc in Fort Collins, Colorado. The measured ultimate capacities (Q_m) were compared to the calculated ultimate capacities (Q_u) using AC358 capacity to torque ratios, individual bearing plates, and cylindrical shear methods. Statistical analysis of these results showed that helical piles in compression designed with the least Q_u determined from torque ratios (K_t), individual bearing plates, and cylindrical shear methods have a high reliability for all plate configurations. However, helical piles in tension based upon the least Q_u determined from torque ratios, individual bearing plates, and cylindrical shear

methods have varying reliability depending on plate configuration. They also concluded that compression piles perform better than tension piles. For compression tests, the average Q_m/Q_u was found to be 1.82 whereas for tension tests, the average Q_m/Q_u was found to be 1.56. This indicates that piles in compression have about 15% higher capacity than piles in tension. In addition, the compression tests resulted in a 99.99% reliability when using a FS = 2.0. In other words, there is a 99.99% chance that the pile deflection will not exceed 10% of the average helix diameter at calculated allowable load. In tension, results were found to be variable. Some results suggest a high reliability whereas some suggest a lower reliability.

2.4.2.6 Summary

In summary, and from the literature review presented above, it is clear that many research efforts were performed to study more accurately the nature of the capacity-torque relationship and its dependency on factors such as shaft geometry, helix configuration, final termination torque, axial load direction, helix pitch and soil type. From these studies, few theoretical models were developed for pile capacity prediction based on torque, Perko (2009) and Ghaly and Hanna (1991). Other capacity-torque factors, based on tests results, were reported. Yet, with the exception of Perko (2009), Hoyt & Clemence (1989), none of the other findings have translated into a practical simple formula (equation) that can be useful for the helical pile industry. Perko's power formula was based on test results and was incorporated into AC358 criteria in 2014 for predicting capacity of pile shafts as described in section 3.13.1.1 of the criteria. Hoyt and Clemence' capacity to torque ratio K_t, are also stated in the same section of the criteria for the specific pile shafts that were tested.

Both of the two published capacity-torque relationships predict the capacity of the pile based on K_t factor that is solely dependent on the shaft geometry (effective shaft diameter). None of these two relationships take into account the other discussed and suggested factors that are generally known to have an effect on the capacity-torque correlation. In this current study, a capacity-torque relationship is developed and takes into account the affecting factors axial load direction, helix configuration, shaft geometry and final termination torque.

3. CHAPTER 3: TESTING TYPES AND PROCEDURES

In the current testing program, two types of tests were performed: axial compression and tension tests. These are the only type of tests needed since the capacity-torque ratio, K_t, is used to predict the soil pile capacity in either axial compression or tension. These two types of tests and its procedures are described in detail below.

3.1 Compression test

The compression test used in this investigation is the static load test performed in general accordance with ASTM D1143, “Standard Test Methods for Deep Foundations Under Static Axial Compressive Load”. The collected data consists of measured applied load and pile head movement. The test was stopped when the pile cannot resist any more load (plunging), or when the net pile deflection (total deflection minus elastic shortening of the pile) exceeded 10% of the average diameter of the helix configuration. The test set up and procedure are described below.

3.1.1 Set up and Layout

This test method utilized an overhead test beam and load frame, with resistance to the applied load provided by four reaction piles, that were installed at a clear distance of 8 feet away from the test piles. The test beam spans across the test pile and was securely attached to the two load transfer beams (spreader beams) that are attached to the reaction piles via a suitable anchor system. A capacity jack (Hydraulic Ram) was placed between the test beam and the top of the test pile to apply the test load increments. A load cell (Omega LCHD-300K) and a readout (Display Omega DP41-S) were used for load increment measurements. Two stiff reference beams, supported independently of the loading system, were used for the two dial gauges measuring the total pile deflection

throughout the testing process. These reference beams were securely attached to supports at a clear distance of 8 feet from both the test pile and the reaction pile. Figure 3.1 below shows a typical set up for the compression test.

Figure 3.1 Compression set up (Courtesy of CTL|Thompson)

3.1.2 Test procedure

The pile load testing was conducted using the ASTM D1143 “Quick Test” procedure. The applied load was increased in increments of 5% of the anticipated failure load. For each test pile, the anticipated failure load was determined based on the final installation torque and the corresponding published K_t values for each pile diameter. Each load increment was added immediately following the completion of movement readings for the previous load interval. Readings were recorded at 0.5, 1, 2 and 4 minutes after completion of each load increment. For each load decrement, readings were taken at 1 and 4 minutes. At the end of the test, and after all load had been removed, readings were taken at 1, 4, 8 and 15 minutes.

All measuring equipment and devices used in the compression test were calibrated and compliant with the requirements of the testing standard.

3.2 Tension test

Like the compression test, the tension test used is the static load test performed in general accordance with ASTM 3689, “Standard Test Methods for Deep Foundations Under Static Axial Tension Load”. The collected data consists of measured applied load and pile head movement. The test was stopped when the pile cannot resist any more load (no increase in applied pressure with continuous large pile settlement), or when the net pile deflection (total deflection minus elastic lengthening of the pile) exceeded 10% of the average diameter of the helix configuration. The test set up and procedure are described below.

3.2.1 Set up and layout

The test set up consists of a test beam supported by cribbing at both ends. The distance between the cribbing and the test pile was 8 feet or more as required by the standard. The hydraulic jack was placed on the top of the test beam and anchored to the tension connection (Threaded bar) extending from the test pile. A load cell (Omega LCHD-300K) and a readout (Display Omega DP41-S) were used for load measurements. Two stiff reference beams, supported independently of the loading system, were used for the two dial gauges measuring the total pile movement throughout the testing process. These reference beams were securely attached to supports at a clear distance of 8 feet from both the test pile and the cribbing. Figure 3.2 below shows a typical set up for the tension test.

Figure 3.2 Tension set up (Courtesy of CTL|Thompson)

3.2.2 Test procedure

The pile load testing was conducted using the ASTM D3689 “Quick Test” procedure. The applied load was increased in increments of 5% of the anticipated failure load. For each test pile, the anticipated failure load was determined based on the final installation torque and the corresponding published K_t values for each pile diameter. Each load increment was added immediately following the completion of movement readings for the previous load interval. Readings were recorded at 0.5, 1, 2 and 4 minutes after completion of each load increment. For each load decrement, readings were taken at 1 and 4 minutes. At the end of the test, and after all load has been removed, readings were taken at 1, 4, 8 and 15 minutes.

All measuring equipment and devices used in tension testing were the same ones used in compression testing and therefore, were calibrated and compliant with the requirements of the testing standards.

3.2.3 Interpretation of axial load testing results

Axial compression and tension tests are probably the most common field tests performed. Despite numerous testing that has been carried out and the many papers that have reported on such tests, and the analysis thereof, there is still no agreement on one single method to determine the pile ultimate capacity from the collected test data. This has led to the use of different methods in analyzing the load-settlement curve obtained from the test data.

Generally, in pile testing, the ultimate failure load is defined as that load causing rapid settlement with no increase in pile resistance (plunging failure). However, this definition is purely strength based because it does not limit pile head movement, not to mention that equipment limitations associated with load testing often prevents reaching this failure load. There are many common analysis methods that were developed over the years, among which are the Davisson method (1972), Chin method (1970), Brinch Hansen method (1963), De Beer (1967), Butler & Hoy (1977), to name few.

There is one historic method that has been frequently used to determine ultimate pile capacity from test data. This method defines the ultimate capacity as the load that causes a pile movement equal to 10% of pile diameter. ICC-ES acceptance criteria for helical pile systems and devices, AC358 (2017) defines the ultimate soil capacity of a helical pile as that load that causes a net pile deflection equal to 10% of the average helix configuration diameter. Net deflection is defined as total measured deflection minus the elastic shortening or lengthening of the pile. This method is sometimes referenced to as the modified Davisson method.

To the author's knowledge, most of the research that have been conducted in regard to capacity torque-correlation verification of helical piles, have used the 10% method. In addition, AC358 (2017) requires that the ultimate soil capacity be determined using this method. Hence, all the tests result in this investigation were analyzed using the 10% method described in the criteria. The consistency of using the same analysis method is crucial in the sense that it allows comparison of test results obtained from different testing programs.

4. CHAPTER 4: TESTING PROGRAM

In this research, the testing program began around 2008, just after the first publication of the acceptance criteria AC358 (Acceptance criteria for helical Pile Systems and Devices) in 2007 by ICC-ES. The purpose of this criteria is to provide helical pile manufacturers with guidelines for demonstrating that the helical product is compliant with performing features of the applicable codes. In other words, it establishes requirements for helical pile systems to be recognized in an ICC-ES evaluation report (ESR).

For about the next 10 years, after the 2007 AC358 publication, many clients have used CTL|Thompson (Testing Agency) for testing their helical pile products to obtain an ICC-ES report. Among the AC358 testing requirements is torque correlation verification of the product. To obtain the capacity-torque ratio, K_t, 8 compression and 6 tension tests in total, are required for conforming systems, and twice these tests for non-conforming systems. The torque correlation conformance criteria is described in Table 3 of AC358. Over the next 10 years, numerous test data was collected from what we call ICC-ES testing for different helical pile manufacturers. Upon contacting these different manufacturers, I obtained authorization to use all the collected data for my research which is presented here.

For the first couple of years, from 2007 to 2009, I was the one conducting all the testing for helical pile manufacturers who chose CTL|Thompson for their testing needs for the purpose of obtaining an ICC-ES report for their product. Late in 2009, I became the technical manager of CTL|Thompson's accredited testing Laboratory. For the next several years, my duties were to continuously supervise all testing per AC358

procedures, analyze the collected test data and issue the final testing report for our clients.

4.1 Testing Agency and Accreditation

All the field tests used in this research, with the exception of the 17 tests provided by Perko, were conducted at CTL|Thompson, a civil engineering company located in Fort Collins, CO. CTLThompson has a testing laboratory that is accredited by International Accreditation Services ,IAS (1975). CTL|Thompson's accreditation was based on ISO/IEC 17025 (2008). Its scope of accreditation is testing Helical pile systems and devices per AC358 requirements. What does accreditation under ISO/IEC 17025 mean? (accurate test results)

ISO/IEC 17025 (2008) was developed as a special purpose standard for laboratories to specify the general requirements for their technical competence. While the standard is generic, it also recognizes that for accreditation purposes (i.e. for independent recognition of a laboratory's competence to perform specific tests, or calibrations) the standard may require development of guidelines to explain its use in specific areas of testing or measurement. ISO/IEC 17025 has two major components, namely management requirements and technical requirements.

The management requirements are written in language relevant to laboratory operations but were developed to meet the systems requirements similar to ISO 9001 (2015). For accreditation against ISO/IEC 17025, the emphasis is to establish the technical competence of a laboratory for a defined set of tests, measurements or calibrations. In doing so, however, compliance with the Standard's management

requirements is also assessed. However, accreditation against ISO/IEC 17025 should not be interpreted to be the same as certification against ISO 9001.

For the testing, or calibration laboratory to keep its accreditation up to date, the accreditation body (in CTL case, IAS (1975)) conducts yearly audits (assessment) on site to verify that the testing lab is compliant with all requirements of ISO/IEC 17025 (2008). Among these requirements, there are the technical competence and training of the staff involved as well as the calibration of all equipment's used. The equipment must be calibrated at least yearly and traceable to NIST standards.

To the author's best knowledge, CTL|Thompson is still the only accredited testing laboratory that has the capabilities to conduct all the tests required per AC358 for the purpose of obtaining an ICC-ES report for a helical pile product. CTL|Thompson is a third-party independent testing lab, which translates into more credibility for the obtained testing results.

4.2 Testing Standard

All the field tests used in this research were conducted according to the requirements of AC358. In this research, we are interested in the axial field compression and tension tests. These tests were conducted per ASTM D 1143 and ASTM D 3689 procedures, respectively.

4.3 Testing sample

All field tests (compression and tension) were conducted by CTL|Thompson testing laboratory, in Fort Collins, CO, with the exception of 7 compression and 11 tension tests provided by Dr. Perko for the 1.75" RCS (round corner square) shaft. With these 18 more tests, the total tests collected (compression and tension) over about 10 years were 799

in total. Among these tests, there are 441 axial compression tests and 358 axial tension tests. The shaft sizes range from 1-7/8” to 4.5” for round shafts and 1.5” to 1.75” for square shafts. The helix diameter ranges from 8” to 19”. The helix configuration in these tests comprises single, double and triple helices.

Before the test specimens are sent to the CTL|Thompson Lab, a CTL representative visits the manufacturing site, the warehouse or distribution center of the applicant for product sampling as required per section 3.0 of AC85 (Acceptance Criteria for Test Reports). The CTL Lab representative randomly selects the required test specimens and marks them with a permanent marker before shipment. The purpose of the visit is to ensure that the samples are truly representative of the standard manufactured product for which recognition is being sought as well as correlating the product material to the product specification through milcerts and other design specifications. Tables A.1 through A.8, in appendix A, show in detail all the testing samples with corresponding shaft size, helix configuration, axial load direction and soil type.

4.4 Test site location and soil investigation

The soil investigation of the test sites used for helical pile testing was conducted by CTL|Thomposn, Inc. The investigation involved field sampling and laboratory analysis, which culminated with a soil report for each site. The soil description and properties are summarized next. This summary is taken from the soil reports, curtesy of CTL|Thompson.

4.4.1 Clayey sites and soil properties

There were two clayey test sites used in this testing program. One test site is located at the Colorado State University campus in Fort Collins, Colorado. The other one

is located in Loveland, Colorado. The soil profiles of the two test sites are described below.

4.4.1.1 Colorado State University

Location and site description

The site is located in the “Bunker” area approximately a quarter mile south east of the Darrel Simmons Building on the Colorado State University campus at the Foothill Research Center at the west end of Laporte Avenue in Fort Collins, Colorado (see Figure F.1 in appendix F). The test site generally drains to the south with areas of higher elevation to the east and west. The area is primarily unimproved with dirt access roads. The area is used for research and equipment storage by Colorado State University. Landscaping in the area is native grasses, weeds, brush and cactus. The site is located in the western edge of the Denver Basin in the Colorado Piedmont Section of the Great Plains Physiographic Province in the State of Colorado. The bedrock at the site is believed to be Graneros shale. The overburden deposits that overlie the bedrock at the site consist of residual clay soils formed from weathering of the formation and transported colluvial soils that consist of a very similar material.

Subsurface Conditions

The site generally consists of approximately seventeen feet of sandy clay that sits on the top of claystone bedrock. Ground water was not encountered during the soil investigation. The soil and bedrock properties, as well as the site of the exploratory boring are shown in appendix F in Table F.1 and Figure F.2, respectively.

4.4.1.2 Loveland site 1

Location and site description

The site is located northwest of the intersection of Kincaid Drive and County Road 19 in Loveland, Colorado (see Figure F.3 in appendix F). A residential development is currently under construction to the west of the site, and further development is planned to the south. The site is on agricultural land and had been plowed at the time of our investigation. Portions of the property have been seeded. The site is located in the Colorado piedmont section of the great plains physiographic province. The surface soil is mapped as quaternary slocum alluvium, water deposited soil. The surficial soil is about 22 feet deep and consists of clay with sand and occasional small gravel mostly confined to thin layers or small buried rills or channels.

Subsurface conditions

The site generally consists of about 22 feet of slightly sandy to sandy clay over claystone bedrock. No ground water was encountered during the soil investigation. The soil and bedrock properties, as well as the site of the exploratory boring are shown in appendix F in Table F.2 and figure F.4, respectively.

4.4.2 Sandy sites and soil properties

There were three sandy sites used for the testing program. The sites are located at Platteville, CTL|Thompson in Fort Collins and Windsor. The soil profiles of the three sites are describe below.

4.4.2.1 Platteville site

Location and site description

The site is located at 17998 County Road 32, Platteville, Colorado (see Figure F.5 in appendix F). The area is primarily unimproved with dirt access roads. Ground cover at the site consists of native grasses, weeds, brush, and cactus. It is part of the Colorado

Piedmont Section of the great plains Physiographic province. The surface soil at the site is mapped as Quaternary age eolian (wind-blown) soil. The bedrock that underlies the eolian soils is interpolated from the map as Cretaceous Laramie Formation.

Subsurface Conditions

The site generally consists of about 20 to 21 feet of silty sand over weathered and unweathered claystone bedrock. No ground water was encountered during the investigation. The soil and bedrock properties, as well as the site of the exploratory boring are shown in appendix F in Table F.3 and Figure F.6, respectively.

4.4.2.2 CTL|Thompson site

Location and site description

The site is located at 351 Linden Street, south of the Cache La Poudre River. The test area is located in the unpaved parking area behind the existing building on the site. The test site generally drains to the north. Landscaping in the area is minimal and generally consists of weeds and small trees. The site is located near the western edge of the Colorado Piedmont Section of the Great Plains Physiographic Province in the State of Colorado.

Subsurface Conditions

The subsurface conditions were investigated by CTL | Thompson, Inc. in Fort Collins, Colorado. Two borings were performed in the vicinity of the field test area. The site generally consists of clayey to silty sands over sandstone bedrock. No ground water was encountered during the soil investigation. The available exploratory boring is shown in appendix F, Figure F.7.

4.4.2.3 Windsor site

Location and site description

The site consists of a vacant lot, on Technology Circle in Windsor, Colorado. The site surface is relatively flat and is a maintained grass covered lawn. The surrounding area is moderately developed with paved roadways, underground utilities, and commercial structures. The site lies in the Colorado Piedmont Section of the Great Plains Physiographic Province in the State of Colorado. Typically, in this area, Cretaceous aged claystone underlies the overburden deposits at depths between fifteen and fifty feet. The bedrock has a slight dip to the east.

Subsurface Conditions

The subsurface conditions were investigated by CTL | Thompson, Inc. in Fort Collins, Colorado. Two borings were performed at two opposite corners as shown on the attached map in appendix F. The site generally consists of approximately five to eight feet of sandy, clay fill. Sand with occasional gravels underlies the fill to a depth of about fourteen to seventeen feet. The sand lies above the top of sandy gravel with occasional cobbles to a depth of about twenty-seven feet where claystone bedrock was encountered. Ground water was encountered at about 25 feet during drilling. The available exploratory boring is shown in appendix F, Figure F.8.

4.5 Installation procedure and torque measurement

Throughout the testing program, the installation of the helical piles was performed in accordance with the requirements of AC358. The piles were generally installed at rates less than 25 revolution per minute. At the time of final torque measurement, the helical pile shaft advancement was about 85% or more of the helix pitch per revolution. Three

torque measurements devices were used throughout the testing process. In the early stages of the testing, an Eskridge torque motor with a torque output of 20,000 ft-lb was used. The torque measurement is taken from the differential pressure (psi) readings of two pressure gauges, which is then converted to torque (ft-lb) from a calibration chart. The calibration of the Eskridge motor was conducted at the site during testing.

The other two torque measurement devices used are an AWS-ITF-25K torque indicator manufactured by Advanced Witness Series, Inc located in California, and a Prodig-60K (INTELLITORK S400) manufactured by Prodig, LLC company located in Kansas. The Prodig-60K is a wireless screw pier monitoring system with a torque output of 60,000 ft-lbs. The AWS-ITF-25K is also a wireless digital torque indicator that has a torque output of 25,000 ft-lbs. These two torque devices are periodically calibrated in house using a Tinius-Olsen torque machine at CTL|Thompson. This machine has a torque capacity of 1 million lb-in and is calibrated annually by Tinus Olsen, an accredited calibration agency.

Before the pile installation, each lead section is marked at each foot starting from the bottom of the pile. The same was done for each extension used before it was connected for installation. The measured torque was recorded at each foot of advancement of the pile into the ground. The installation continues until the required embedment is achieved after which the final depth is measured and recorded with the final termination torque. Some manufacturers use the final termination torque as the average torque of the last three measurements over the last three feet. In this study, the torque used in the evaluation of ultimate capacity was the final reading torque.

5. CHAPTER 5: LOAD TEST DATA ANALYSIS

5.1 Determination of ultimate capacity

During compression and tension testing of the pile, both the total deflection and applied load were recorded according to the procedure described in section 8.2 of the quick load test method in ASTM D1143 and ASTM 3689 for compression and tension, respectively. The recorded data was then plotted with applied load on the x-axis and pile deflection on the y-axis (typical load-deflection curve). The total deflection, the net deflection and the maximum deflection described in AC358 were all plotted on the same graph for each test pile. Total deflection is the measured total movement of the pile during testing. Net deflection is the total measured movement minus the elastic shortening or elastic lengthening of the pile and was determined using the following simple formula:

$$\text{Net deflection} = \text{Total deflection} - (PL/AE)$$

Where P is the applied load (lb), L is the pile length (in), A is the area of the pile section (in^2) and E is the steel modulus of elasticity taken as 29,000 Ksi. The maximum allowable deflection per AC358 is equal to 10% of the average diameter (in) of the helix configuration.

Figure 5.1 shows a typical compression test results for a 10”/12” double helix pile. The average diameter is 11 inches (11”). Per AC358, the ultimate capacity is the load that causes a pile net deflection of 1.1” (10% Rule). From the plotted graph, the ultimate capacity is found to be 48,000 lbs.

Figure 5.2 shows a typical tension test results of 8”/10”/12” triple helix pile. The average diameter is 10”. Per AC358, the ultimate capacity is the load that causes a pile

net deflection of 1.0” (10% Rule). From the plotted graph, the ultimate capacity is found to be 42,500 lbs.

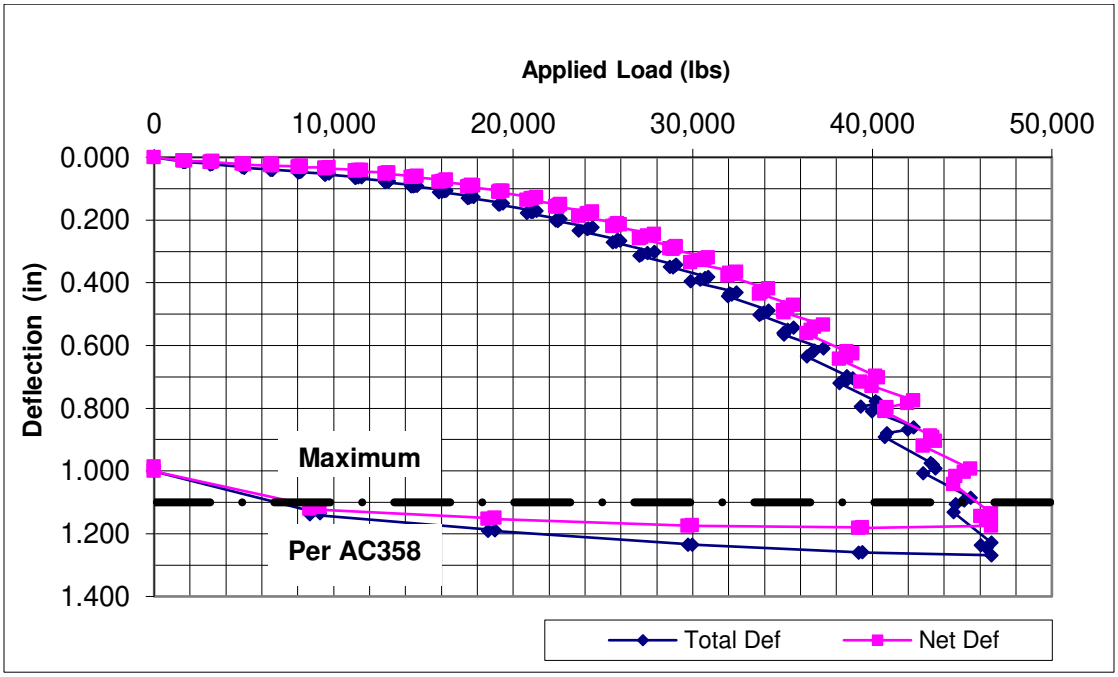

Figure 5.1 Compression load-deflection curve (Courtesy of CTL|Thompson)

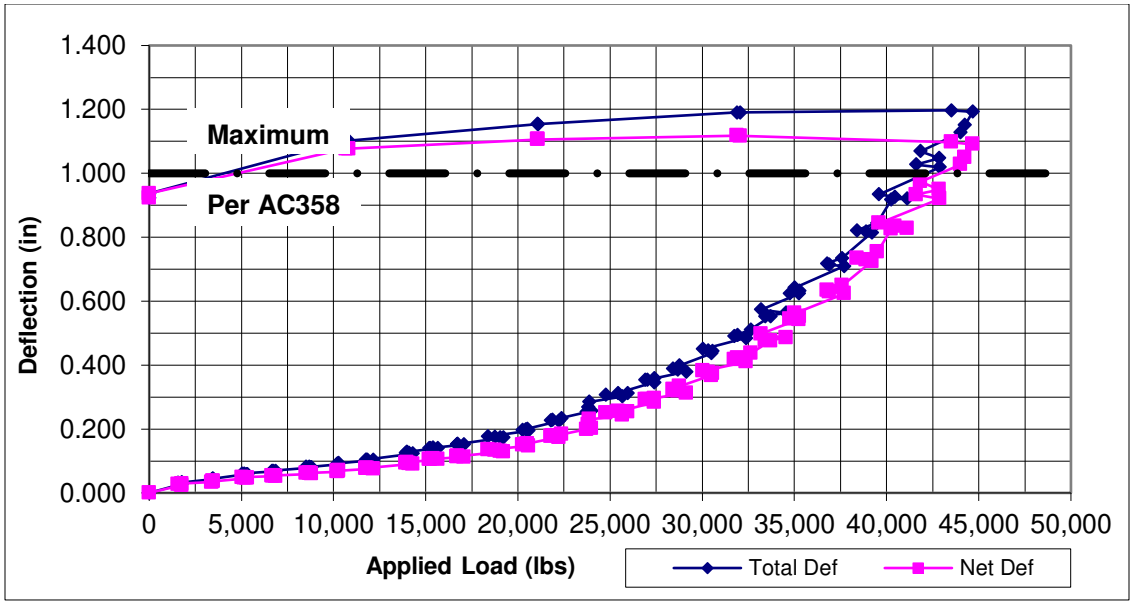

Figure 5.2 Tension load-deflection curve (Courtesy CTL|Thompson)

5.2 Organization of collected data

All collected data from the field tests (raw data) were organized in a spreadsheet with helical pile characteristics such as pile size (O.D for round shafts and shaft side length for square shaft), shaft thickness as applicable, final installation torque, helix configuration, soil type, test type (compression or tension) and measured ultimate capacity based on the modified Davisson method (10% rule). Given the large amount of data (many different shaft sizes) and the different variables used in the torque correlation regression analysis, most of the generated figures and tables are found in appendix A through E, since the analysis process is repetitive. Few figures (with comments) will be included in the core of the thesis as a guidance to the reader.

The same thing is repeated in regard to the reliability prediction approach. Most histograms will be found in appendix C. Few of them will be in the core of the thesis with explanation and justification.

5.3 Identified variables to be used in the analysis

It is common knowledge among the helical pile industry that there exists a relationship between final installation torque and ultimate pile capacity. Numerous papers were written about the various factors that could possibly affect the empirical capacity-torque ratio and ultimately the pile capacity. Pack (2000), Hawkins and Thorsten (2009) asserted that, among the factors affecting the torque-capacity relationship, are shaft size, helix configuration, pitch size, helix spacing and soil strength parameters. However, to this date, the torque-capacity ratio factor widely used around the world is still based on shaft pile diameter only, and consequently used to determine the ultimate pile capacity.

In this study, the following variables were used to determine its effects on the ultimate pile capacity, and ultimately the capacity-torque ratio, K_t. These factors are: axial load direction (compression, tension), helix configuration, final installation torque, shaft size and shaft shape (square or round). These factors are chosen because they are measurable or controllable. The effects of these variables are evaluated in Section 5.4.

5.4 Regression analysis of the test data

In almost all the numerous published studies, the K_t values, relating the final installation torque to ultimate pile capacity, were evaluated based on shaft diameter only. Based on the large amount of data, it is reasonable, as a starting point, to plot the measured K_t values versus the effective shaft diameter to determine how close the test data are to the fitted regression line. Figure 5.3 shows the plot of the measured K_t values versus the effective diameter for all shaft sizes and both test types (compression and tension). The measured K_t values were obtained from the ratio of the measured ultimate capacity (based on 10% rule) to the final installation torque for each test. The effective diameter is as defined previously.

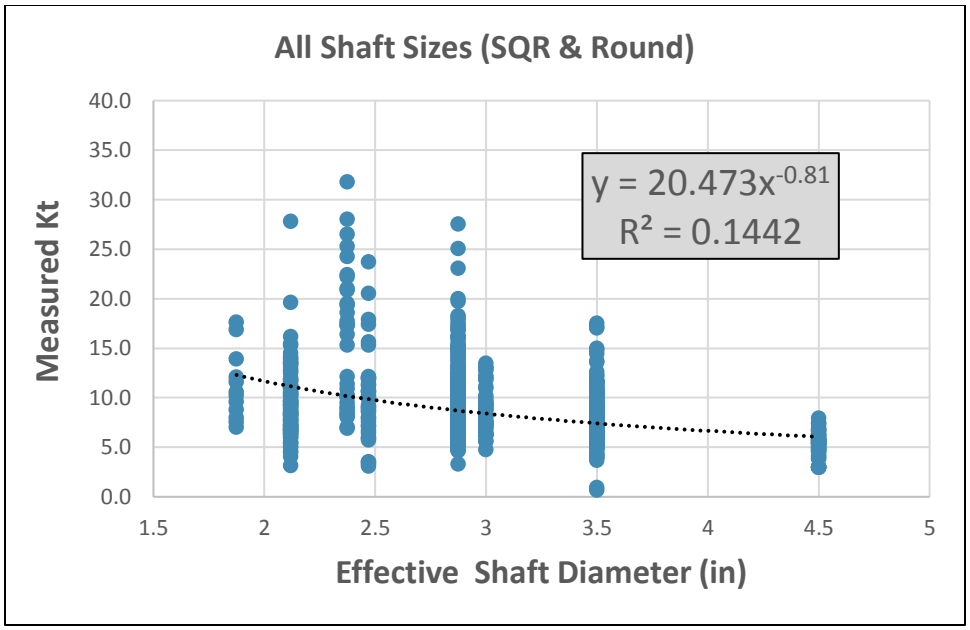

Figure 5.3 Measured K_t vs shaft effective diameter

From the figure above, we can conclude that the K_t value does indeed decrease with increasing shaft diameter and that the data are very scattered. The coefficient of determination R^2 is very low, which is an indication that the statistical correlation, based on shaft size only, is not strong. Other attempts were tried to find out the best correlation possible based on the shaft size, but with a slightly different approach. Among these attempts were plots of K_t values versus shaft polar moment of inertia and shaft section modulus. In both cases, the data points were very scattered with no clear statistical correlation improvement over the test points in Figure 5.3.

In this research, a new approach is taken to study the capacity-torque correlation. K_t has already been shown to depend on shaft diameter. From testing observation and published literature suggestions, K_t is also dependent on final installation torque and other variables. In this new approach, instead of using K_t value as the dependent variable, the

measured ultimate capacity (Q_u) is plotted against the ratio of the effective diameter to the final installation torque (D/T). The obtained formula, relating Q_u to D/T can then be arranged to determine K_t value, which itself will be dependent on shaft size and final installation torque.

Figures 5.4, 5.5 and 5.6 show the plots of the measured ultimate capacity (Q_u) versus the ratio of the effective shaft diameter to the final installation torque (D/T) for all shaft sizes (square and round), round shafts only, and square shafts only.

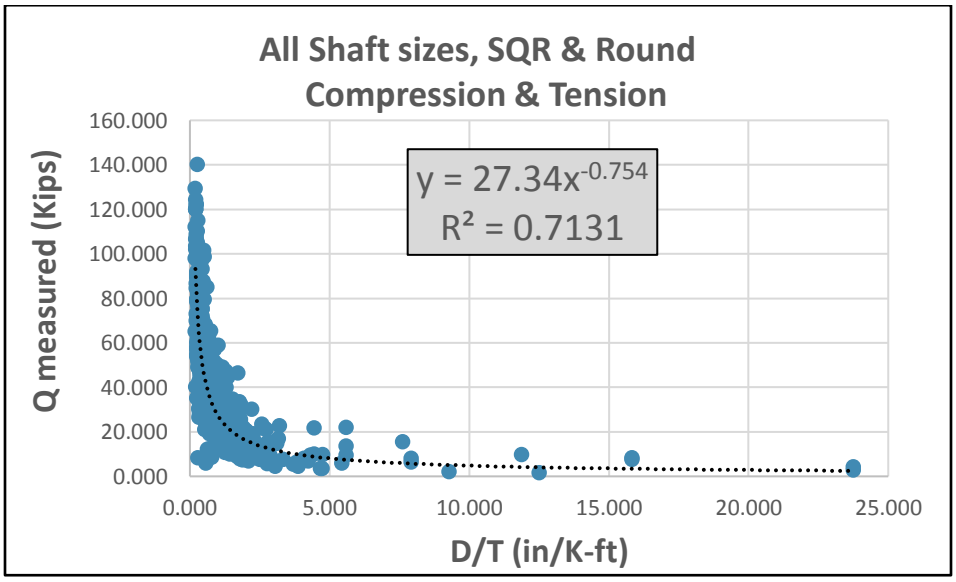

Figure 5.4 Measured Qu vs D/T

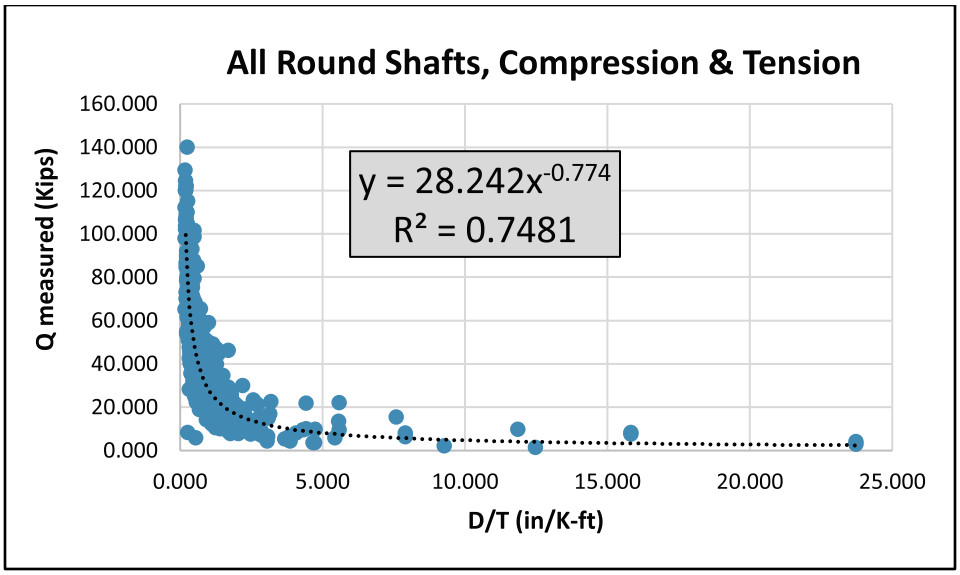

Figure 5.5 Measured Qu vs D/T

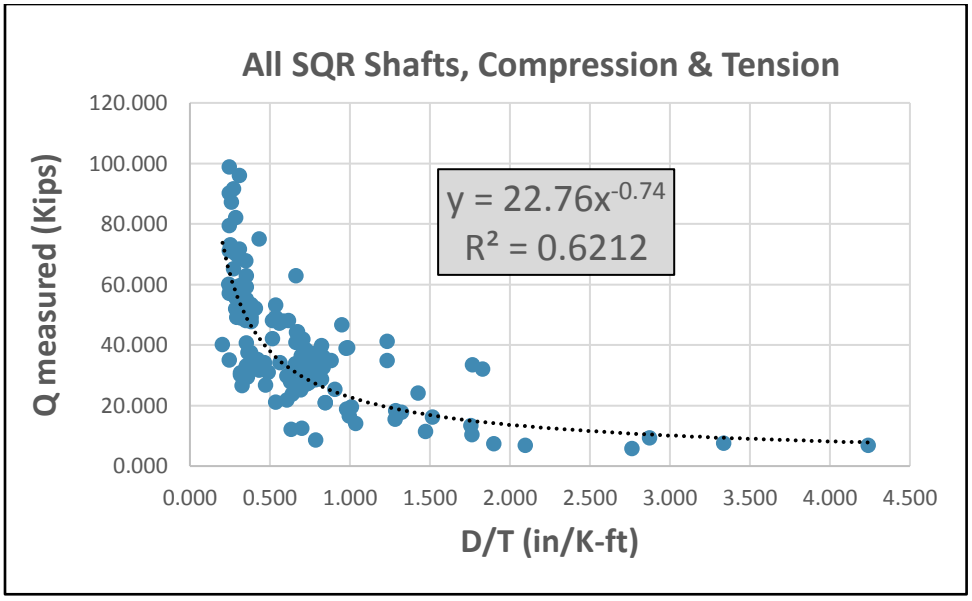

Figure 5.6 Measured Qu vs D/T

Looking at the 4 Figures above, one can conclude the following. Figures 5.4 through 5.6 show a common trend of how the measured pile capacity is changing with effective diameter to torque ratio. The plotted test points are not as scattered as the ones shown

in Figure 5.3, using measured K_t values vs effective diameter. In addition, the coefficient of determination R^2 is very reasonable for all graphs, indicating a good correlation.

From the regression analysis of the data, the best-fit equation obtained could be written in the form of:

$$Q_u = \alpha\,(D/T)^{\beta} \tag{5.1}$$

Where:

Q_u: Ultimate capacity of the pile (Kips)

D : Effective diameter (in)

T : Final installation torque (Kip-ft)

β : Fitting factor

α : Fitting factor (Kip*(Kip-ft/in)$^{\beta}$)

Equation 5.1 is written in general form. It can be rearranged to obtain the K_t factor as follows:

$$Qu = \alpha(D/T)^{\beta}\ T*T^{-1} = \alpha\ (D^{\beta}/T^{\beta+1})T \tag{5.2}$$

Which results in the following value of K_t:

$$K_t = \alpha(D^{\beta}/T^{\beta+1}) \tag{5.3}$$

Equation 5.1 is an empirical equation based on all collected test data. The fitting factor α is a positive number as shown in the graphs. The fitting factor β is found to be a negative number between -1 and zero ($-1<\beta<0$). The absolute value of the fitting factor β is higher than the absolute value of (β+1). This indicates that the effective shaft diameter has a larger effect on the capacity to torque ratio as stated by Perko (2009) and Hoyt and Clemence (1989). Figure 5.7 is a plot of measured K_t values for all shaft sizes versus final

installation torque. Both Figure 5.3 and Figure 5.7 are in general agreement with equation 5.3.

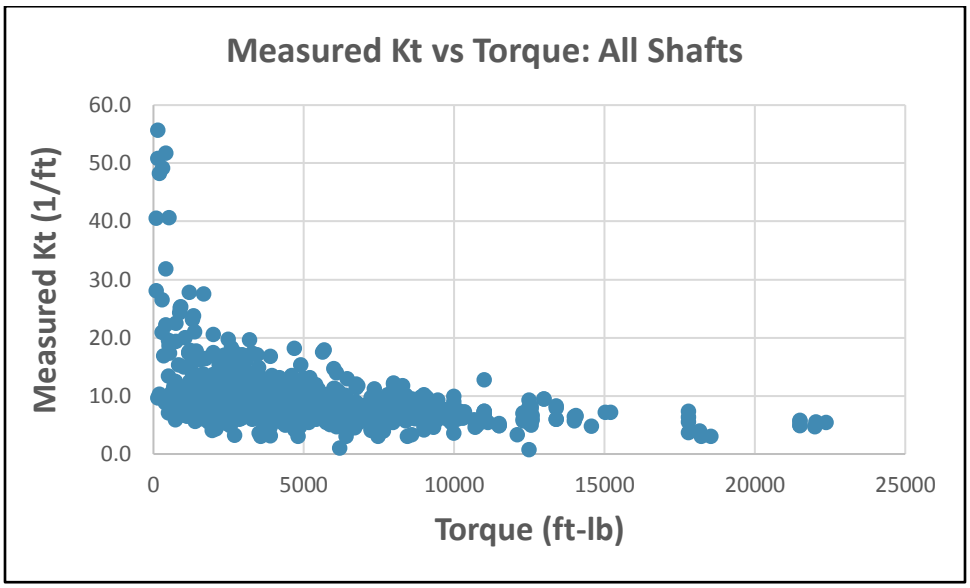

Figure 5.7 Measured K_t vs installation torque

5.5 Effect of each variable on pile capacity

A similar empirical formula to equation 5.1 is used to study the effect of the variables mentioned previously. In theory, when a dependent variable is a function of multiple independent variables, the effect of the independent variable is evaluated either by holding all the other independent variables constant, or by decoupling it from the others. In this case, the variables are part of an axial load test. The effect of each variable is evaluated by separating the round shaft from the square ones (shape), compression from tension (load direction), and single helix from multi-helix (helix configuration).

The test data is organized and analyzed as follows:

1. Round shafts:

- Round Multi-Helix Compression (RMHC)
- Round Single-Helix Compression (RSHC)

- Round Multi-Helix Tension (RMHT)
- Round Single-Helix Tension (RSHT)

2. Square shafts:

- Square Multi-Helix Compression (SMHC)
- Square Single-Helix Compression (SSHC)
- Square Multi-Helix Tension (SMHT)
- Square Single-Helix Tension (SSHT)

Both round and square shafts have 4 cases to be evaluated. In each case, the test data is plotted as ultimate capacity (Q_u) versus effective diameter to torque ratio (D/T). There are eight plots in total. Figures 5.8 and 5.9 are plots for round shafts, multi-helix compression (RMHC) and square shafts multi-helix compression (SMHC), respectively. The other six plots, Figures B.1 through B.6 are found in appendix B. In all cases, the best-fit empirical equation is similar to equation 5.1 with different α and β fitting factors, which is expected, since both fitting factors are a measure of the effect of the variables identified previously.

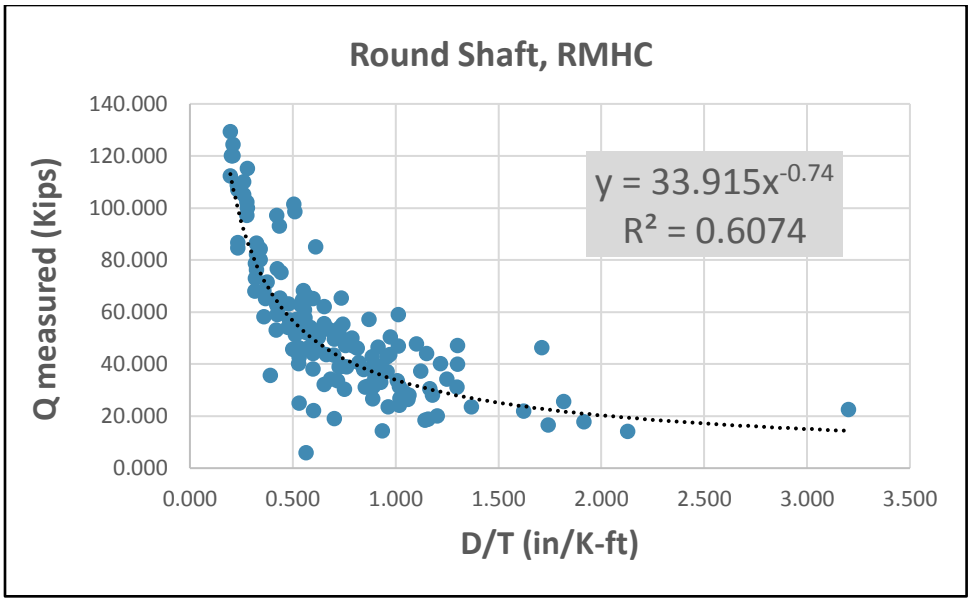

Figure 5.8 Qu vs D/T

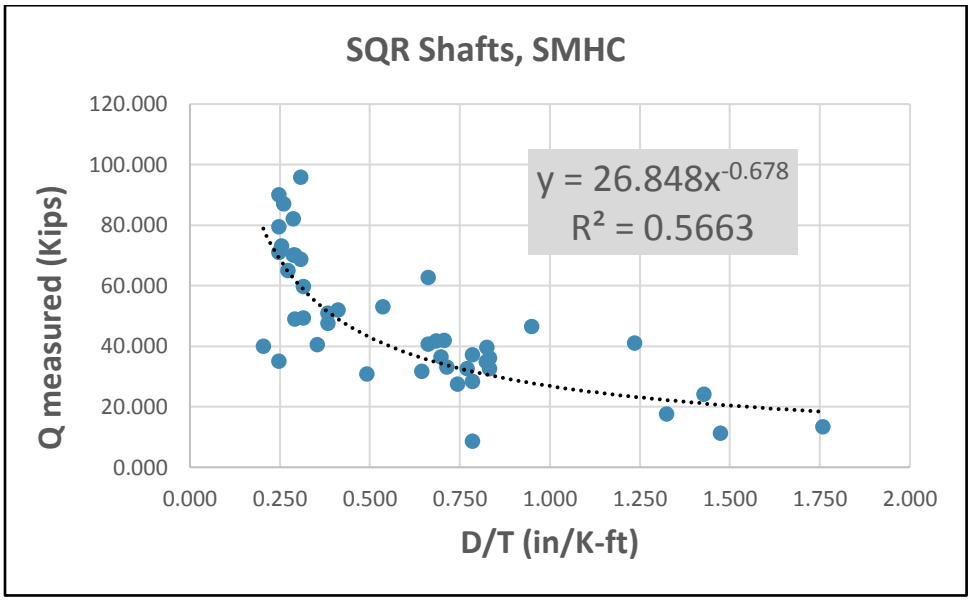

Figure 5.9 Qu vs D/T

5.6 Empirical relationship and its justification

In the previous section, there are eight cases evaluated for the different variables identified in section 5.3. This has resulted in eight different equations (see Figures in appendix B) with different α and β fitting factors. From the plots of Qu vs D/T, all the best-

fit empirical correlations take the general form of equation 5.1. From Figures 5.4, 5.5 and 5.6, the empirical correlation for round shafts is better that the other two as seen by the higher coefficient of determination R^2.

Since all the empirical equations are in the form of equation 5.1, it is reasonable and simpler to use one single equation that includes the effect of the variables identified in section 5.3. this new general formula is derived as follows. The basic equation used for this derivation is the one obtained from the analysis of all-round shafts, including both compression and tension. This equation is chosen because it has the highest coefficient of determination.

$$\text{Basic equation} = 28.242\ (D/T)^{-0.774} \tag{5.4}$$

The empirical equations obtained from Figures 5.14 through 5.21 are divided by the basic equation above. The average of the ratios obtained is called the λ factor, which reflects the effect of the variables identified in the previous section 5.3. In addition, and in each case, the standard deviation and coefficient of variance are determined to validate or invalidate the results. The standard deviation is used to measure the amount of variation or dispersion of the data set values from the average or the mean. A low standard deviation indicates that the data points tend to be close to the mean. The coefficient of variance is also another statistical measure of the dispersion of data points in a data series around the mean. Table 5.1 below shows the results used to determine the λ factor.

Table 5.1 Determination of λ factor

	Q_u RMHC Divided by Q Basic	Q_u RMHT Divided by Q Basic	Q_u RSHC Divided by Q Basic	Q_u RSHT Divided by Q Basic
		Round Shaft		
Average = λ	1.182	0.996	1.027	0.818
STDV	0.022	0.060	0.062	0.088
CV	0.019	0.060	0.060	0.108
		Square Shaft		
	Q_u SMHC Divided by Q Basic	Q_u SMHT Divided by Q Basic	Q_u SSHC Divided by Q Basic	Q_u SSHT Divided by Q Basic
Average = λ	0.894	0.798	0.763	0.601
STDV	0.051	0.009	0.038	0.025
CV	0.057	0.011	0.05	0.041

Where all the terms in the table are as previously defined in section 5.4.1.

From the obtained results in Table 5.1, one can clearly observe that the two statistical parameters (STDV, CV) are very small. This is an indication that all the data points are very closely scattered around the mean. Hence, taking the λ factor to be the average is statistically justified. Incorporating λ into the basic equation gives the general formula that takes into account the effect of all the variables discussed before. The ultimate soil capacity is then determined as:

$$Qu = \lambda * 28.242 * (D/T)^{-0.774} \qquad \text{Eq (5.5)}$$

Where:

Q_u : Pile ultimate capacity (Kips)

D : Effective pile diameter (in)

T : Final Installation torque (k-ft)

The determined λ factors are summarized in Table 5.2 below.

Table 5.2 λ factors

Round Shafts			
RMHC	RMHT	RSHC	RSHT
1.182	0.996	1.027	0.818
Square Shafts			
SMHC	SMHT	SSHC	SSHT
0.894	0.798	0.763	0.601

Equation 5.5 could be rearranged as follows:

$$Qu = \lambda*28.242*(D/T)^{-0.774} = \lambda*28.242*(D^{-0.774}/T^{0.226}) *T= K_m * T$$

Where K_m is the modified torque factor taking into account the effect of helix configuration, axial loading direction and shaft size and shape. K_m is given by:

$$K_m = \lambda*28.242*(D^{-0.774}/T^{0.226}) = \lambda*K_t \quad (5.6)$$

Where K_t is given by equation 5.3 and the unit of both K_m and K_t is ft^{-1}.

In helical pile design, the allowable or design load is given, and the ultimate capacity Q_u could be determined based on the recommended factor of safety. With the choice of the shaft size and the corresponding λ factor, the installation torque could be easily determined by solving equation 6.2 for the required minimum installation torque, which is given by:

$$T = D *[(0.0354 * Qu)/\lambda]^{1.292} \quad (5.7)$$

Another approach, that most are familiar with, is to generate a table that the design engineer and others can easily use to determine the required minimum torque and pile

capacity. Tables 5.3 and 5.4 are generated for a 2-7/8" O.D round shaft and a 1.5" RCS shaft. The tables for the other six shafts are found in appendix C. In generating a table for a particular shaft size, the torque must not exceed the rating torque of the specified shaft. The rating torque is the maximum installation torque that can be applied to the pile shaft without causing any damage that might affect the structural integrity of the pile. This rating torque is usually determined by lab testing in accordance with section 4.2.2 of AC358. Based on the collected test data, the 2-7/8" O.D shaft has a rating torque of about 9,000 ft-lb. The 1.5" RCS shaft has a rating torque of about 6,000 ft-lb. These two torque ratings are reflected in both tables.

By examining both tables below, one can clearly notice the following observations. First, the modified capacity to torque ratio, K_m, decreases as the installation torque increases, unlike the K_t value based on AC358, which remains constant for a given shaft size. In other words, the use of the traditional published K_t value underestimates the pile capacity (conservative estimate) at low torque and overestimates the pile capacity (unconservative) at high torque. Second, for any given torque, the predicted capacity based on AC358 for a given shaft is unchanged, whereas the predicted capacity based on modified K_m changes with respect to helix configuration and axial load direction. Third, it is common knowledge that the capacity to torque ratio is higher in compression than in tension, Perko (2009), Cherry and Souissi (2008). Looking at tables 5.3, 5.4 and the tables in appendix C, it clear that K_m is higher for compression than tension, whereas the K_t value based on AC358 is the same for both tension and compression.

Finally, for a given design load, the determined required minimum installation torque, based on AC358, is a unique value that does not take into account the axial load direction nor the helix configuration. On the other hand, the required minimum installation torque based on modified Km varies depending on helix configuration and axial load direction. These multi-choices of required minimum torque translate into more accurate and more economical pile design. It is essential to remember that the predicted capacities using equation (5.5) and shown in the tables below and in appendix C, are based on the 10% net deflection criteria, which states that the pile ultimate capacity is equal to the applied load that causes a net deflection equal to 10% of the average of the helix diameters of the pile. Using other criteria will for sure results in different pile capacities than the ones presented herein.

Notice: in the case of the 1-7/8" and 2-3/8" round shafts, all the tests performed were for single helix configuration only. Both shafts have very low rating torques, 1,300 and 2,500 ft-lb, respectively. For the 1-7/8" round shaft, the majority of the tests were conducted at torques ranging between 150 and 600 ft-lb. For the 2-3/8" round shaft, most of the tests were performed at torques less than 1,000 ft-lb. Therefore, caution should be taken when using the modified K_m for both of these shafts, especially for multi-helix configuration.

Table 5.3 Capacity-torque correlation based on K_m & AC358 K_t for 2-7/8" O.D shaft.

Torque (k-ft)	Predicted capacity Q based on modified Km								Predicted Q based on AC358 Kt	
	RMHC		RMHT		RSHC		RSHT			
	Km	Q(K)	Km	Q(K)	Km	Q(K)	Km	Q(K)	Kt	Q(Kips
0.5	17.2	8.6	14.5	7.3	15.0	7.5	11.9	6.0	9.0	4.5
1	14.7	14.7	12.4	12.4	12.8	12.8	10.2	10.2	9.0	9.0
1.5	13.5	20.2	11.3	17.0	11.7	17.5	9.3	14.0	9.0	13.5
2	12.6	25.2	10.6	21.2	11.0	21.9	8.7	17.4	9.0	18.0
2.5	12.0	30.0	10.1	25.2	10.4	26.0	8.3	20.7	9.0	22.5
3	11.5	34.5	9.7	29.1	10.0	30.0	8.0	23.9	9.0	27.0
3.5	11.1	38.9	9.4	32.8	9.6	33.8	7.7	26.9	9.0	31.5
4	10.8	43.1	9.1	36.3	9.4	37.5	7.5	29.8	9.0	36.0
4.5	10.5	47.2	8.8	39.8	9.1	41.0	7.3	32.7	9.0	40.5
5	10.2	51.2	8.6	43.2	8.9	44.5	7.1	35.5	9.0	45.0
5.5	10.0	55.2	8.4	46.5	8.7	47.9	6.9	38.2	9.0	49.5
6	9.8	59.0	8.3	49.7	8.5	51.3	6.8	40.8	9.0	54.0
6.5	9.7	62.8	8.1	52.9	8.4	54.5	6.7	43.4	9.0	58.5
7	9.5	66.5	8.0	56.0	8.3	57.8	6.6	46.0	9.0	63.0
7.5	9.3	70.1	7.9	59.1	8.1	60.9	6.5	48.5	9.0	67.5
8	9.2	73.7	7.8	62.1	8.0	64.0	6.4	51.0	9.0	72.0
8.5	9.1	77.2	7.7	65.1	7.9	67.1	6.3	53.5	9.0	76.5
9	9.0	80.7	7.6	68.0	7.8	70.2	6.2	55.9	9.0	81.0

Table 5.4 Capacity-torque correlation based on K_m & AC358 K_t for 1.5" RCS shaft

Torque (K-ft)	Predicted capacity Q, based on modified Km								Predicted Q based on AC358 Kt	
	SMHC		SMHT		SSHC		SSHT			
	Km	Q(K)	Km	Q(K)	Km	Q(K)	Km	Q(K)	Kt	Q(Kips)
0.5	16.5	8.3	14.7	7.4	14.1	7.0	11.1	5.5	10.0	5.0
1	14.1	14.1	12.6	12.6	12.0	12.0	9.5	9.5	10.0	10.0
1.5	12.9	19.3	11.5	17.2	11.0	16.5	8.7	13.0	10.0	15.0
2	12.1	24.1	10.8	21.5	10.3	20.6	8.1	16.2	10.0	20.0
2.5	11.5	28.7	10.2	25.6	9.8	24.5	7.7	19.3	10.0	25.0
3	11.0	33.0	9.8	29.5	9.4	28.2	7.4	22.2	10.0	30.0
3.5	10.6	37.2	9.5	33.2	9.1	31.8	7.1	25.0	10.0	35.0
4	10.3	41.3	9.2	36.8	8.8	35.2	6.9	27.7	10.0	40.0
4.5	10.0	45.2	9.0	40.4	8.6	38.6	6.8	30.4	10.0	45.0
5	9.8	49.1	8.8	43.8	8.4	41.9	6.6	33.0	10.0	50.0
5.5	9.6	52.8	8.6	47.1	8.2	45.1	6.5	35.5	10.0	55.0
6	9.4	56.5	8.4	50.4	8.0	48.2	6.3	38.0	10.0	60.0

6. CHAPTER 6: RELIABILTY OF CAPACITY PREDICTION APPROACH

Reliability is defined as the probability that a product performs its intended purpose satisfactory over the long term. Hence, probability theory and statistics are important tools for reliability in engineering. In helical pile design, a factor of safety of 2 is usually used. To evaluate the reliability of the predicted capacity, based on equation 5.5, a similar approach to that taken by Hoyts and Clemence (1989) is used. In this approach, the measured capacity is basically compared to the predicted capacity divided by a factor of safety of 2. This same approach is also used in AC358 to evaluate the K_t value of helical pile products.

The λ factor in the prediction formula represents 8 different cases, which are dependent on the shaft geometry, helix configuration and axial load direction. In each case, the probability is evaluated twice. One is based on AC358 predicted capacity using the published K_t values. The other one is based on predicted capacity using equation 5.5. In each case, a histogram of measured capacity divided by the predicted capacity is plotted. The histogram gives a first indication of the nature of the data distribution, which will lead to the use of the proper density function for probability determination. Figure 6.1 shows the histograms plot of raw data for the round multi-helix configuration in compression (RMHC). The other plots, Figures D.1 through D.15 are found in appendix D.

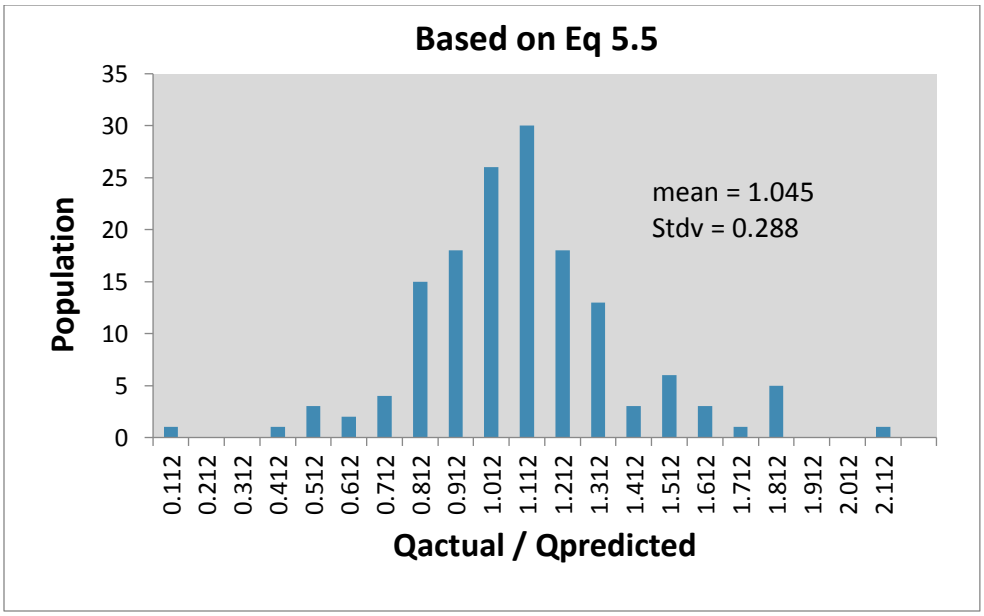

Figure 6.1 Histogram of (Q actual / Q predicted). RMHC

From the 16 plots of the histograms, it is apparent that the data is not normally distributed. In addition to the fact that the data represents random variables that are product of other variables, it is clear that the distribution is skewed to the right from the mean and that all data is positive (zero is the minimum). This suggests that the data follows a lognormal distribution, which is discussed and validated next in detail.

By definition, a random variable is log-normally distributed if the logarithm of the variable is normally distributed. To validate that the raw data is long normally distributed, the logarithm of the raw data was computed and analyzed. Figure 6.2 shows the histogram for RMHC based on the logarithm of the raw data values.

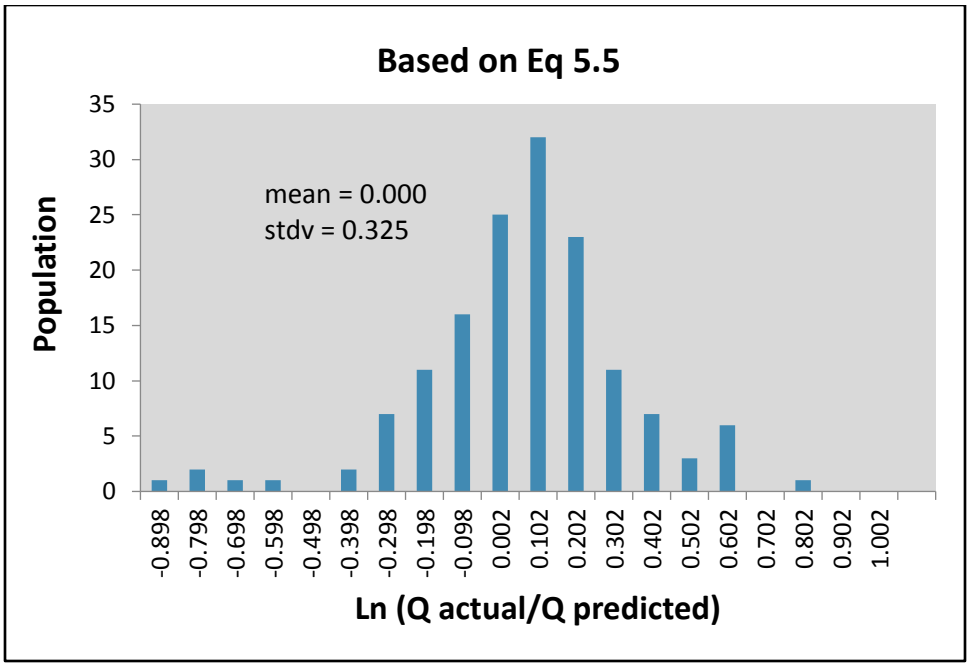

Figure 6.2 Histogram of Ln (Q actual / Q predicted). RMHC

From figure 6.2, the data seems to be normally distributed around the mean with the exception of couple of outliers on the left side. This is an indication that the raw data is log-normally distributed. However, this is still a visual test. A better, more widely accepted and suitable test for normality of the logarithmic data, called Q-Q test, is used and described next.

In statistics, a Q–Q (quantile-quantile) plot is a probability plot that compares two probability distributions by plotting their quantiles against each other. In other words, the Z score of the standard normal distribution (theoretical) is plotted against the actual Z score of the logarithm of the raw data. If the distributions are similar, then the points on the Q-Q plot should approximately lie around the line representing the function y = x. Figure 6.3 shows the Q-Q plot for RMHC. The other 15 plots for the other cases are found in appendix E.

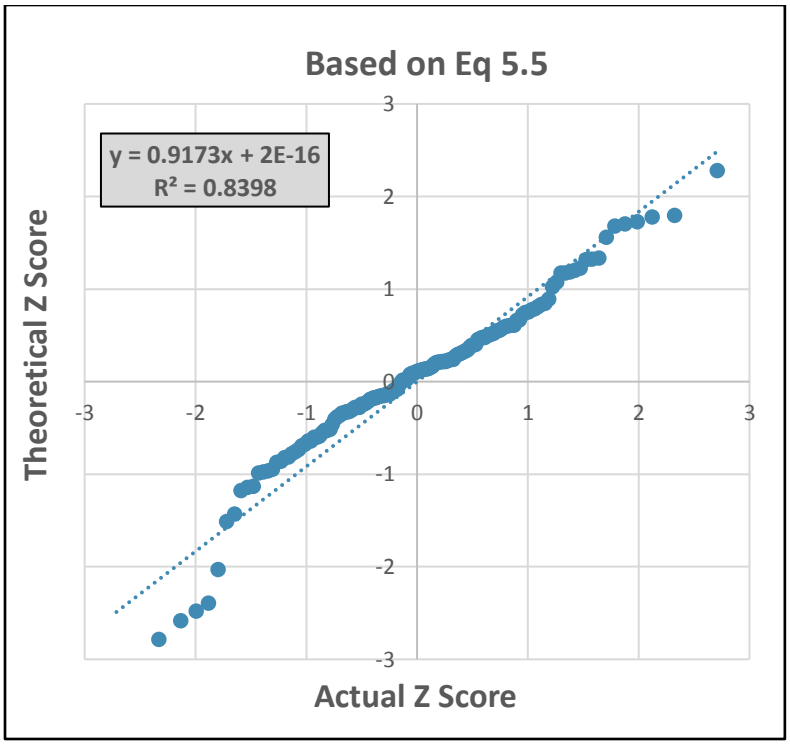

Figure 6.3 Q-Q Plot.RMHC

From figure 6.3 and the rest of the figures in appendix E, it seems that the plotted data tends to follow a straight line of the form y = x. This indicates that the data is normally distributed. For the cases of RMHC and RSHC, the Q-Q plots based on AC358 K_t seem to follow a straight 45-degree line with some outliers. Still, the best fit lines have an R^2 of 0.94 and 0.93 respectively, which are considered high coefficient of determination, indicating an acceptable correlation. The Q-Q plots for the square single helix configuration in tension (SSHT) based on modified K_m and AC358 K_t have an R^2 of 0.82 and 0.84, which are considered very reasonable. The plotted data above is actually the logarithm of the raw data collected and analyzed from testing. Since the logarithm of the collected data is normally distributed, then the actual raw data must have a log-normal distribution. This type of distribution is used to compute the probability of the measured

capacity with respect to the allowable predicted capacity using a factor of safety of 2. This analysis is performed for the 8 different values of λ, presented in the previous section. The predicted allowable capacity is determined using equation 5.5 and the published K_t values in AC358. Since the distribution of the analyzed collected data has been shown to follow a lognormal distribution, the most accurate way to compute the probability that the measured capacity is greater than half of the predicted capacity, is to use the cumulative lognormal distribution function. The probability was determined for both predicted capacities based on AC358 K_t values and the newly developed modified K_m.

The reliability function using the log-normal distribution is defined as:

$$R(x) = 1 - \Phi[(\ln(x) - \mu)/\sigma] \quad (6.1)$$

Where:

Φ : Standard normal cumulative distribution function

μ : Mean of the logarithm of the data

σ : Standard deviation of the logarithm of the data

x : Ratio of Q measured to Q predicted

To compute the probability that the measured capacity is higher than half of the predicted capacity (x=0.5), one can use either equation (6.1) or the lognormal cumulative distribution function in excel. To use the cumulative lognormal distribution function in excel, the following arguments are needed:

- x is a required argument. It is the value at which we like to evaluate the function. In this case, x is equal to 0.5 since we are using a factor of safety of 2, and we are looking to determine the probability that the actual measured capacity is higher than half of the predicted capacity.

- Mean is a required argument which is equal to the mean of the natural log of the ratio of measured capacity to predicted capacity.
- Standard deviation is a required argument which is equal to the standard deviation of the natural log of the ratio of the measured capacity to the predicted capacity.

The excel lognormal distribution function is given by:

LOGNORMALDIST (x, mean, standard-dev)

In equation (6.1), the term $[(\ln(x)-\mu)/\sigma]$ is basically the normal distribution Z score of the logarithmically transformed data. $\Phi[(\ln(x)-\mu)/\sigma]$ is the probability of measured capacity that is less than half of the predicted capacity. The excel function above also gives the probability of measured capacity over half the predicted capacity that is less than 0.5. to obtain the probability that measured capacity is higher than half of the predicted capacity, the results must be subtracted from unity. Both methods were used and resulted exactly in the same probability numbers. The probabilities computed for the eight different cases (different λ) are shown in Table 6.1.

From the results in Table 6.1, and in the case of round multi-helix compression (RMHC), the probability that the measured capacity is higher than half of the predicted capacity is about the same using either modified K_m or AC358 K_t, with the one based on AC358 slightly higher. For all other cases, the probability based on modified K_m is higher than the one based on AC358 K_t, especially in the case of square shafts. This clearly indicates that the newly developed formula is an improvement over the traditional used K_t value as depicted both by its accuracy (smaller standard deviation) and reliability (higher probability).

Table 6.1 Probability of Q measured higher than 0.5 Q predicted

Method	Mean	Standard Deviation	Max	Min	Probabaility of Qmeas is greater or equal to 0.5 Qpredicted (%)
Round Shafts Multi-Helix Compression (RMHC)					
Modified Km	1.045	0.288	2.099	0.112	98.30
AC358 Kt	1.262	0.419	3.058	0.134	99.30
Round Shafts Multi-Helix Tension (RMHT)					
Modified Km	1.032	0.246	1.948	0.110	99.30
AC358 Kt	1.029	0.294	2.188	0.095	98.30
Round Shafts Single Helix Compression (RSHC)					
Modified Km	1.059	0.385	2.866	0.351	97.80
AC358 Kt	1.286	0.801	5.553	0.516	96.90
Round Shafts Single Helix Tension (RSHT)					
Modified Km	1.029	0.268	1.982	0.441	99.50
AC358 Kt	0.908	0.241	2.222	0.366	98.60
SQR Shafts Multi-Helix Compression (SMHC)					
Modified Km	1.054	0.328	1.912	0.279	97.40
AC358 Kt	1.055	0.387	2.050	0.315	94.90
SQR Shafts Multi-Helix Tension (SMHT)					
Modified Km	1.036	0.267	1.714	0.374	99.30
AC358 Kt	0.916	0.239	1.560	0.308	97.40
SQR Shafts Single-Helix Compression (SSHC)					
Modified Km	1.059	0.398	2.404	0.515	98.00
AC358 Kt	0.950	0.428	2.779	0.407	93.30
SQR Shafts Single Helix Tension (SSHT)					
Modified Km	1.087	0.567	3.009	0.697	96.50
AC358 Kt	0.793	0.461	2.370	0.447	80.70

7. CHAPTER 7: CONCLUSION AND RECOMMENDATIONS

7.1 Summary and conclusion

The objective of this research was to determine a new capacity-torque correlation that takes into account the effects of shaft size, shaft geometry, axial load direction, helix configuration and installation torque. The analysis of the collected data resulted in a new empirical capacity-torque relationship expressed by the formula in equation (5.5) and presented below:

$$Q_u = \lambda * 28.242 * (D/T)^{-0.774}$$

Where all the terms in the above equation are as defined before. In helical pile design, the allowable or design load is given, and the ultimate capacity Q_u could be determined based on the recommended factor of safety. With the choice of the shaft size and the corresponding λ factor, the installation torque could be easily determined by solving equation 5.5 for the required minimum installation torque, which is given by:

$$T = D * [(0.0354 * Q_u)/\lambda]^{1.292}$$

Another simple approach is to generate a table similar to the one presented in chapter 6. The required elements are shaft size, corresponding λ factors and the installation torque in increments. The maximum installation torque in the table must not exceed the rating torque (obtained from testing or by other acceptable means) of the shaft in consideration. The generated table is a tool that can be used by the design engineer or others to select the appropriate shaft size and minimum required installation torque. It also clearly shows the difference between using the published AC358 K_t values and the modified capacity-torque ration K_m. For a given shaft size, the published AC358 Kt value

is a constant number, which results in one unique selection of required minimum installation torque and corresponding pile capacity, regardless of load direction and helix configuration. As stated before, this selection will result in underestimating pile capacity at low torque and overestimating it at high torque. On the other hand, and for the same given shaft size, the modified capacity-torque ratio K_m, is not a constant but varies with λ factors, giving the design engineer more choices for selecting pile size and minimum required torque.

Finally, and as stated previously in the abstract, the reliability of the new developed empirical capacity-torque relationship was determined and compared to the reliability based on AC358 historical K_t values. The probability results in Table 6.1 show that the capacity-torque correlation based on the modified capacity-torque ratio K_m, assures a higher degree of success than the one based on published AC358 K_t values. Figures 7.1 and 7.2 below represents plots of the actual measured capacity versus the predicted capacity based on AC358 K_t values and the modified K_m values, respectively. The plots reiterate that the predicted capacity based on K_m factor is more reliable than the predicted capacity based on the historical AC358 K_t values, as indicated by the higher coefficient of determination R^2.

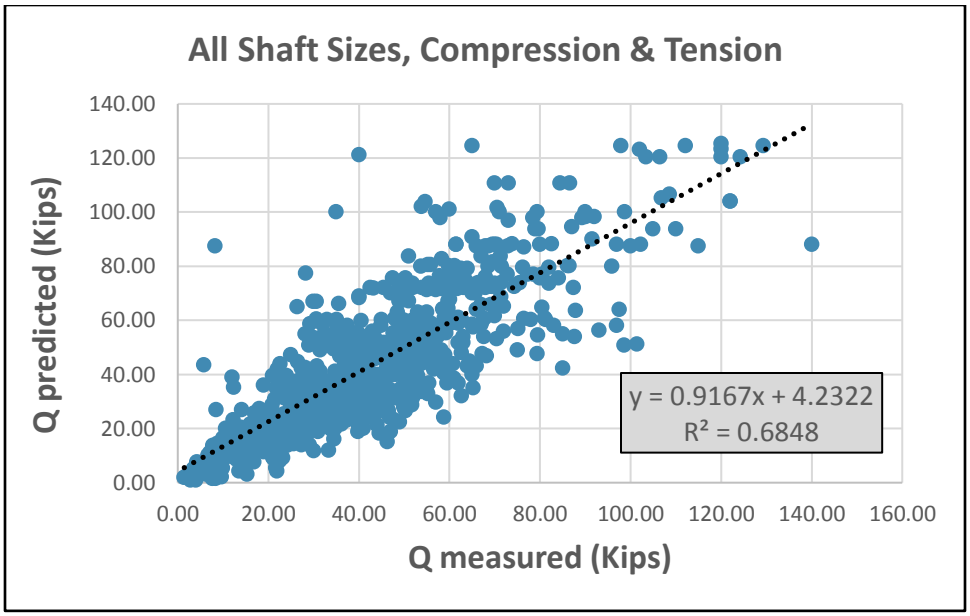

Figure 7.1 Measured capacity vs predicted capacity. Based on AC358 K_t

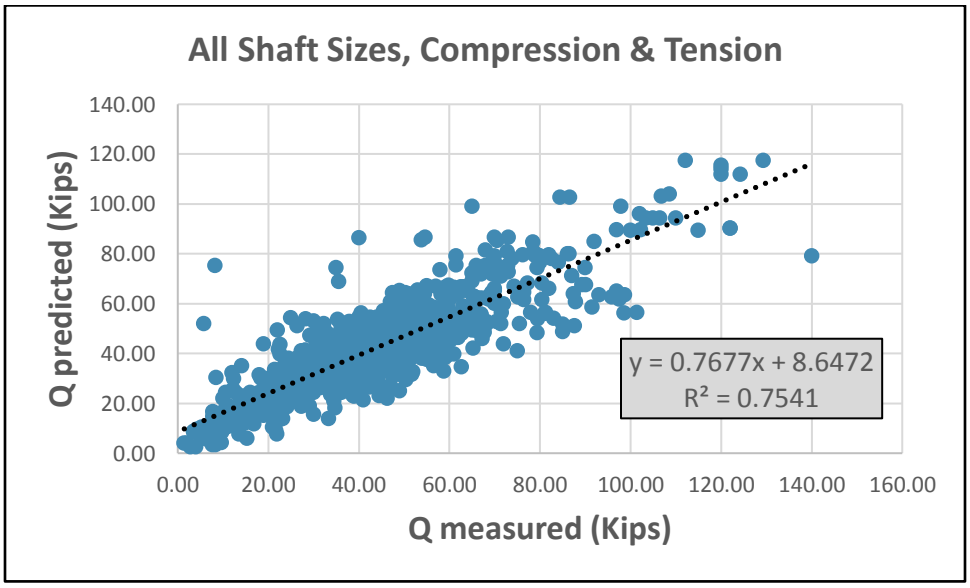

Figure 7.2 Measured capacity vs predicted capacity. Based on K_m

7.2 Limitation and future recommendations

The current investigation of capacity-torque correlation was based on tests conducted on what is called small diameter helical piles. Specifically, the shaft sizes used in this research are 1.5” and 1.75” round corner square shafts and 1-7/8”, 2-3/8”,2-7/8”,

3.0”, 3.5”, 4.5” round shafts. Caution and engineering judgment should be used when applying this torque correlation to large diameter helical piles or other shaft sizes outside the range of shaft sizes used in this research. In addition, all the tests were conducted at the same five sites (three sandy sites and 2 clayey sites) with particular and specific soil properties, upon which the new developed torque-capacity relationship was based. To further investigate the effect of soil properties, future testing could be performed at different soil sites (different sandy and clayey sites) with wide range of shear strength properties. Furthermore, this will help better study the effect of soil type (sand, clay) on the λ factor.

Finally, all these tests were conducted for various helical pile manufacturers as part of the application for an ICC-ES reports for their products. The tests were conducted per the requirements of ICC-ES acceptance criteria AC358. Among these requirements, two compressions and two tensions tests must be conducted on piles installed to the maximum rating torque of the product. Most of the tests were installed to a final torque that is between 30% and 70% of the product rating torque, which could possibly result in an empirical relationship that is more skewed toward this data range. This is reflected on all plots of the ultimate capacity versus the ratio of effective diameter to installation torque. This new developed method was found to be inherently more accurate at low torque than at higher torque. To better study more accurately the effect of the installation torque, future investigation should consider investigating the magnitude of the installation torque equally over a wider range of the pile rating torque. One recommendation is to conduct tests installed at torques ranging from 10% to 100% of the product rating torque at an increment of 10%.

REFERENCES

AC358, 2017.” Acceptance Criteria for Helical Pile Systems and Devices”. www.icc-es.org

ASTM D 1143/D 1143M-07. “Standard Test Methods for Deep Foundations Under Static Axial Compressive Load.” Annual Book of Standards. West Conshohocken, PA: ASTM International.

ASTM D1586 / D1586M-18: “Standard Test Method for Standard Penetration Test (SPT) and Split-Barrel Sampling of Soils.” Annual Book of Standards. West Conshohocken, PA: ASTM International.

ASTM D3689/D3689M- 07. “Standard Test Methods for Deep Foundations Under Static Axial Tensile Load.” Annual Book of Standards. West Conshohocken, PA: ASTM International.

Bowles. J.E 1968. “Foundation Analysis and Design.” First Edition, McGraw-Hill, Inc, New York City, NY.

Bowles. J.E 1988. “Foundation Analysis and Design.” Fourth Edition, McGraw-Hill, Inc, New York City, NY.

Butler, H.D and Hoy, H.E, 1977. “Users Manual for the Texas Quick-Load Method for Foundation Load Testing.” Report No. FHWA-IP-77-8. Federal Highway Administration, Washington, DC, 59 pp.

Cherry, J.A. and Souissi, M. 2010 "Helical Pile Capacity to Torque Ratios, Current Practice, and Reliability", GeoTrends: Proceedings of the 2010 Biennial Geotechnical Seminar, C.M. Gross, et al., Eds., ASCE, Denver, CO

Chin, F.K. 1970. “Estimation of the Ultimate Load of Piles not carried to Failure.” Proceedings 2nd Southeast Asian Conference on Soil Engineering, pp. 81-90.

Cole, W.H. 1978. “An innovative Use for Multi-Helix Anchors.” Presented at the EEI T&D Subcommittee, Key Biscayne, FL.

CTL|Thompson, Inc. 1971 west 12th avenue, Denver, Colorado, 80204. www.ctlthompson.com

Das, B.M. 2011. “Geotechnical Engineering Handbook.” J. Ross Publishing, Inc. Fort Lauderdale, Florida.

Davisson, M.T. 1972. High Capacity Piles. Proceedings, Lecture Series, Innovations in Foundation Construction, ASCE, Illinois Section, Chicago, March 22, pp. 81-112.

DeBeer, E.E. 1967. “ Proefondervindelijke Bijdrage tot de studie van zand onder funderingem op staal”, Tjdshrift der Openbar Werken van het grensdraag vermogen van Beigie Nos 6-67 and 1-, 4-, 5-, 6-68.

DFI 2012. “Helical Foundation and Tie-Backs Specialty Seminar”, Deep Foundation Institute, Denver, Colorado.

DFI 2015. “Helical Foundation and Tie-Backs Specialty Seminar”, Deep Foundation Institute, Saint Louis, Missouri.

Filho, J.M.S.M.S, Morais, T.S.O, Tsuha, C.H.C. 2014. “A new Experimental Procedure to Investigate the Torque Correlation Factor of Helical Anchors.” Electronic Journal of Geotechnical Engineering, Vol 19. Bundle P.

Fleming, K., Waltman, A., Randolph, M. F., and Elson, K. (2009). *Piling Engineering, 3rd ed.* Taylor & Francis, London and New York.

Ghaly, A.M and A.M Hanna, A. 1991. “Experimental and Theoretical Studies on Installation Torque of Screw Anchors.” Canadian Geotechnical Journal, 28, No.3, pp. 353-364.

Gill, H.S and J.J Udwari.1980. “Pullout Tests: Multi-Helix Screw Anchors.” Report prepared for the Virginia Electric and Power Company, Richmond, VA.

Hansen, J.B. 1963.” Discussion: Hyperbolic stress-strain response: cohesive soil.” Journal of Soil Mechanics, Foundation Division, 89(4), 241-242.

Hawkins, K. and Thorsten, R. 2009. “Load Test Results - Large Diameter Helical Pipe Piles.” Contemporary Topics in Deep Foundations: pp. 488-495.

Hendrickson, R.1984. The Ocean Almanac. New York: Doubleday.

Hoyt, R. M., and Clemence, S. P.1989. “Uplift Capacity of Helical Anchors in Soil.” Proceedings of the 12th International Conference on Soil Mechanics and Foundation Engineering, Rio de Janeiro, Brazil Vol. 2, pp. 1019-1022.

Hu, Y and Randolph, M.F. 2002.” Bearing Capacity of Caisson Foundations on Normally Consolidated Clay.” Soil and Foundations, 42(5), 71-77.

ICC-Evaluation Services. 2003.“AC358 Acceptance Criteria for Helical Pile Systems and Devices.” www.icc-es.org

International Accreditation Services (IAS, 1975), Brea, California. www.iasonline.org.

International Association of Plumbing and Mechanical Officials (IAPMO, 1926), Ontario, California. www.iapmo.org.

International Code Council.2009. “*International Building Code (IBC).”* Washington, DC: International Code Council.

ISO 9001: 2015: “Quality Management Systems-Requirements.” International Organization for Standardization, Geneva, Switzerland. www.iso.org.

ISO/IEC 17025: 2015: “General Requirements for the Competence of Testing and

Calibration Laboratories.” International Organization for Standardization, Geneva, Switzerland. www.iso.org.

Livneh, B., and El Naggar, M. H.2008. "Axial testing and numerical modelling of square shaft. helical piles under compressive and tensile loading." *Can. Geotech. J.,* 45, 1142-1155.

Lutenegger, A. J. 2009. "Cylindrical shear or plate bearing? – uplift behavior of multi-helix screw anchors in clay." 2009 International Foundation Congress and Equipment Expo, Contemporary Topics in Deep Foundations. *ASCE, 456-463.*

Lutenegger, A. J. 2011. "Historical development of iron screw-pile foundations: 1836-1900." *Int. J. for the History of Eng. & Tech.,* 81(1), 108-128.

Lutenegger, A. J. 2015. “Quick Design Guide for Screw-Piles and Helical Anchors in Soils, V1.0.” International Society for Helical Foundations (ISHF).

Meyerhof, G. G. 1976. “Bearing Capacity and Settlement of Foundations.” Journal of Geotechnical and Geo-environmental Engineering, Vol. 102, No 3, pp 195-228.

Pack, J.S. 2000. “Design of Helical Piles for Heavily Loaded Structures.” New Technological and Design Development in Deep Foundations, Reston, VA: ASCE Press, pp. 335-367

Perko, H. A. 2009. “Helical Piles: A Practical Guide to Design and Installation.” New Jersey. John Wiley and Sons.

Ruberti. N.M. 2015. “Investigation of Installation Torque and Torque-to-Capacity Relationship of Screw Piles and Helical Anchors.” Master’s Thesis. University of Massachusetts Amherst, MA.

Sakr, M. 2009. “Performance of helical piles in oil sand.” Canadian Geotechnical Journal.

46 (9), 1046-1061.

Tappenden, K.M. 2004. “Predicting the Axial Capacity of Screw Piles Installed in Western Canadian Soils.” Master’s thesis, University of Alberta, Edmonton, Alberta.

Terzaghi, K. 1943. “Theoretical Soil Mechanics.” New York: John Wiley and Sons.

US NAVY DESIGN MANUAL DM-7, NAVFAC, 1986, “Foundation and earth Structures.” overnment Printing Office, Washington, DC.

Wilson. Guthlac. 1950. “*The Bearing capacity of Screw Piles and Screw Crete Cylinders*” in the journal of the ICE, Volume 34 issue 5, March 1950, pp.4-73.

APPENDIX A: TESTING TEST SAMPLES

Table A.1 Test samples for 1.5" RCS shaft

Helix configuration	Soil Type	No of Compression tests	No of Tension tests
Single	Clay	28	6
	Sand	5	6
	Bed Rock	4	0
Double	Clay	7	4
	Sand	5	4
	Bed Rock	0	0
Triple	Clay	13	10
	Sand	5	4
	Bed Rock	4	4
	Total	**71**	**38**

Table A.2 Test samples for 1.75" RCS shaft

Helix configuration	Soil Type	No of Compression tests	No of Tension tests
Single	Clay	3	2
	Sand	1	3
	Bed Rock	2	0
Double	Clay	2	1
	Sand	1	1
	Bed Rock	0	0
Triple	Clay	1	1
	Sand	1	1
	Bed Rock	2	2
	Total	**13**	**11**

Table A.3 Test samples for 1-7/8" O.D shaft

Helix configuration	Soil Type	No of Compression tests	No of Tension tests
Single	Clay	1	0
	Sand	5	6
	Bed Rock	0	0
	Total	6	6

Table A.4 Test samples for 2-3/8" O.D shaft

Helix configuration	Soil Type	No of Compression tests	No of Tension tests
Single	Clay	3	3
	Sand	26	3
	Bed Rock	2	0
	Total	31	6

Table A.5 Test samples for 2-7/8" O.D shaft

Helix configuration	Soil Type	No of Compression tests	No of Tension tests
Single	Clay	45	34
	Sand	29	27
	Bed Rock	12	0
Double	Clay	15	19
	Sand	15	17
	Bed Rock	0	0
Triple	Clay	18	14
	Sand	17	16
	Bed Rock	12	12
	Total	**163**	**139**

Table A.6 Test samples for 3.0" O.D shaft

Helix configuration	Soil Type	No of Compression tests	No of Tension tests
Single	Clay	7	9
	Sand	7	4
	Bed Rock	2	0
Double	Clay	3	2
	Sand	1	1
	Bed Rock	0	0
Triple	Clay	4	3
	Sand	1	1
	Bed Rock	2	2
	Total	**27**	**22**

Table A.7 Test samples for 3.5" O.D shaft

Helix configuration	Soil Type	No of Compression tests	No of Tension tests
Single	Clay	36	22
	Sand	19	24
	Bed Rock	2	0
Double	Clay	10	11
	Sand	10	10
	Bed Rock	0	0
Triple	Clay	18	21
	Sand	10	11
	Bed Rock	4	4
	Total	**109**	**103**

Table A.8 Tests samples for 4.5" O.D shaft

Helix configuration	Soil Type	No of Compression tests	No of Tension tests
Single	Clay	9	4
	Sand	3	3
	Bed Rock	2	0
Double	Clay	3	3
	Sand	3	3
	Bed Rock	0	0
Triple	Clay	6	5
	Sand	3	3
	Bed Rock	2	2
	Total	**31**	**23**

APPENDIX B: CAPACITY VS DIAMETER TO TORQUE RATIO CORRELATION PLOTS

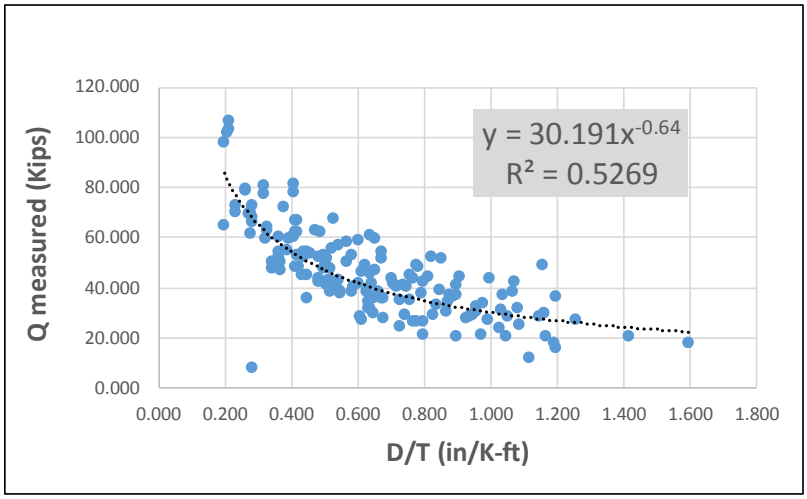

Figure B.1 Measured Q vs D/T. RMHT

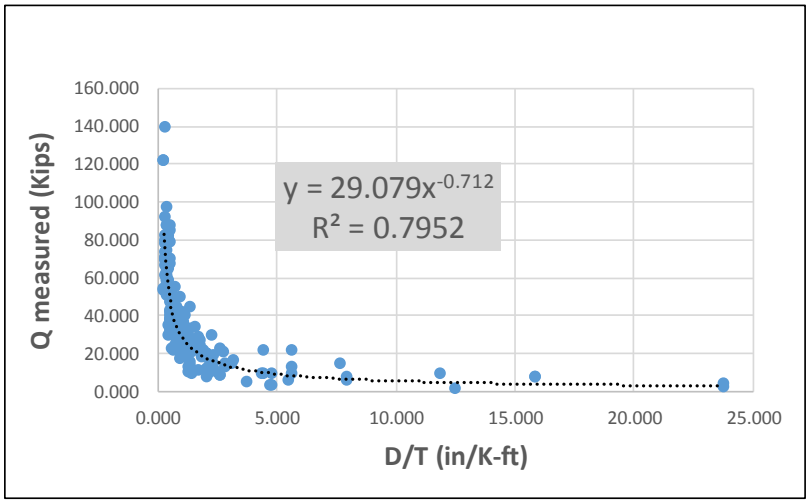

Figure B.2 Measured Q vs D/T.RSHC

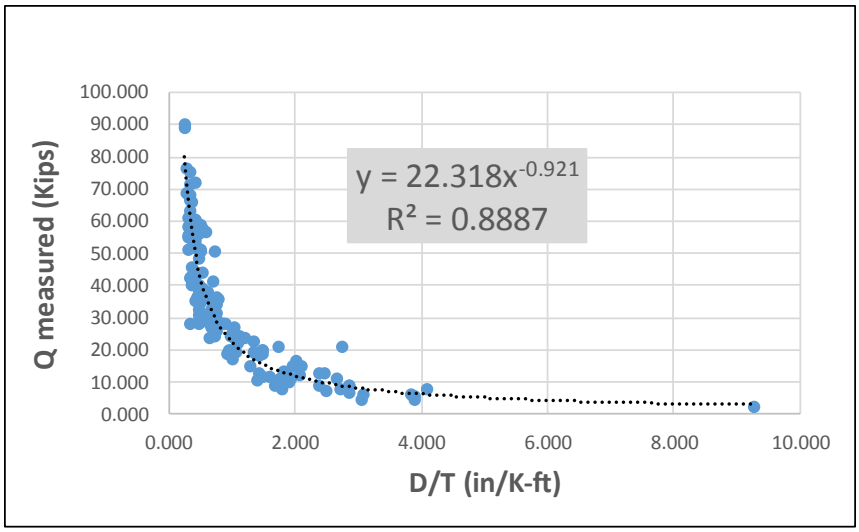

Figure B.3 Measured Q vs D/T.RSHT

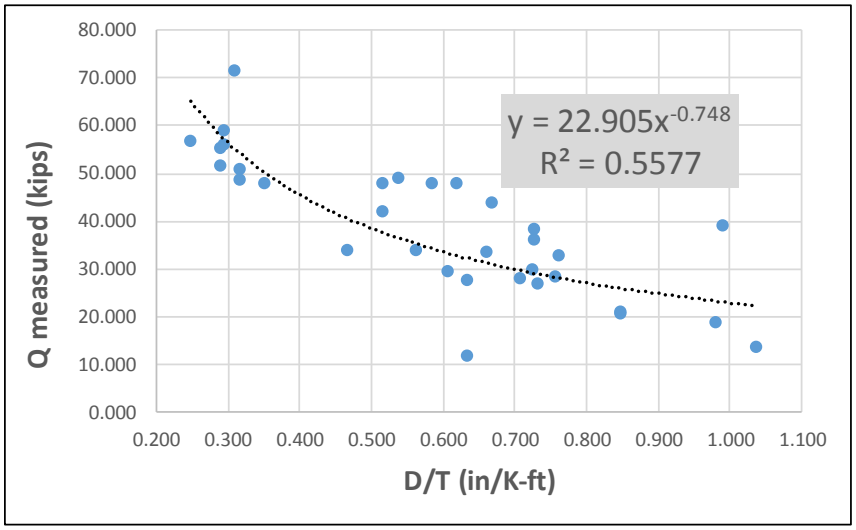

Figure B.4 Measured Q vs T/D.SMHT

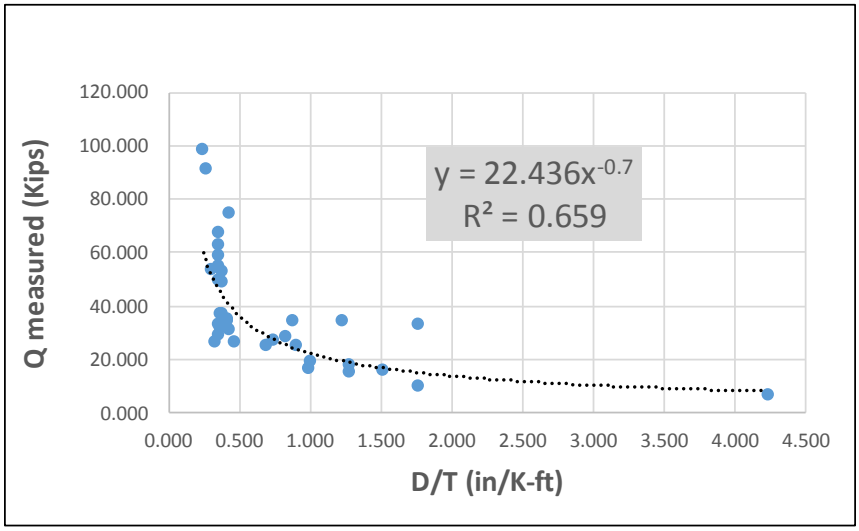

Figure B.5 Measured Q vs D/T.SSHC

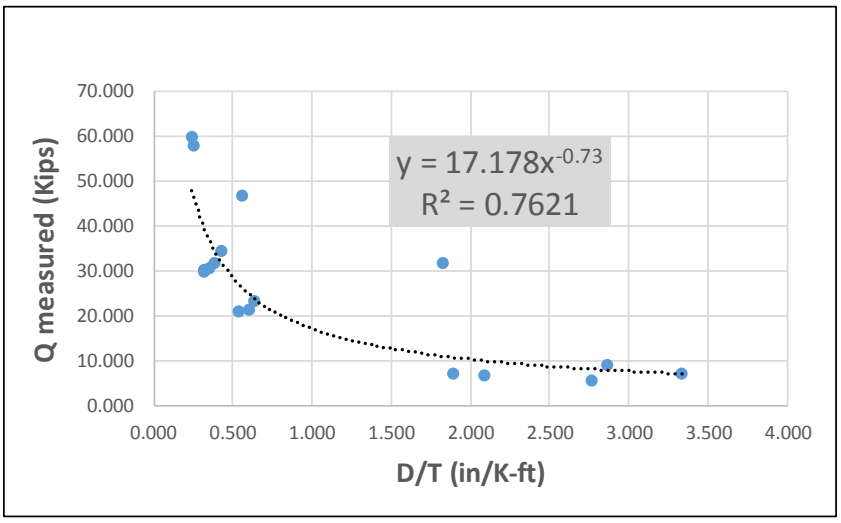

Figure B.6 Measured Q vs D/T.SSHT

APPENDIX C: TABLES OF CAPACITY TORQUE CORRELATION

Table C.1 Capacity-torque correlation based on Km & AC358 Kt for 1-7/8" O.D shaft

Torque (k-ft)	Predicted capacity Q based on modified Km								Predicted Q based on AC358 Kt	
	RMHC		RMHT		RSHC		RSHT			
	Km	Q(K)	Km	Q(K)	Km	Q(K)	Km	Q(K)	Kt	Q(Kips
0.5	24.0	12.0	20.2	10.1	20.9	10.4	16.6	8.3	12.5	6.3
0.75	21.9	16.4	18.5	13.8	19.0	14.3	15.2	11.4	12.5	9.4
1	20.5	20.5	17.3	17.3	17.8	17.8	14.2	14.2	12.5	12.5
1.25	19.5	24.4	16.4	20.6	17.0	21.2	13.5	16.9	12.5	15.6
1.5	18.7	28.1	15.8	23.7	16.3	24.4	13.0	19.4	12.5	18.8

Table C.2 Capacity-torque correlation based on Km & AC358 Kt for 2-3/8" O.D shaft

Torque (k-ft)	Predicted capacity Q based on modified Km								Predicted Q based on AC358 Kt	
	RMHC		RMHT		RSHC		RSHT			
	Km	Q(K)	Km	Q(K)	Km	Q(K)	Km	Q(K)	Kt	Q(Kips
0.5	20.0	10.0	16.8	8.4	17.4	8.7	13.8	6.9	10.1	5.1
0.75	18.2	13.7	15.4	11.5	15.8	11.9	12.6	9.5	10.1	7.6
1	17.1	17.1	14.4	14.4	14.8	14.8	11.8	11.8	10.1	10.1
1.25	16.2	20.3	13.7	17.1	14.1	17.6	11.2	14.1	10.1	12.6
1.5	15.6	23.4	13.1	19.7	13.5	20.3	10.8	16.2	10.1	15.2
1.75	15.1	26.4	12.7	22.2	13.1	22.9	10.4	18.2	10.1	17.7
2	14.6	29.2	12.3	24.6	12.7	25.4	10.1	20.2	10.1	20.2
2.25	14.2	32.0	12.0	27.0	12.4	27.8	9.8	22.2	10.1	22.7
2.5	13.9	34.7	11.7	29.3	12.1	30.2	9.6	24.0	10.1	25.3

Table C.3 Capacity-torque correlation based on Km & AC358 Kt for 3.0" O.D shaft

Torque (k-ft)	Predicted capacity Q based on modified Km								Predicted Q based on AC358 Kt	
	RMHC		RMHT		RSHC		RSHT			
	Km	Q(K)	Km	Q(K)	Km	Q(K)	Km	Q(K)	Kt	Q(Kips
0.5	16.7	8.3	14.1	7.0	14.5	7.2	11.5	5.8	8.0	4.0
1	14.3	14.3	12.0	12.0	12.4	12.4	9.9	9.9	8.0	8.0
1.5	13.0	19.5	11.0	16.4	11.3	17.0	9.0	13.5	8.0	12.0
2	12.2	24.4	10.3	20.6	10.6	21.2	8.4	16.9	8.0	16.0
2.5	11.6	29.0	9.8	24.4	10.1	25.2	8.0	20.1	8.0	20.0
3	11.1	33.4	9.4	28.1	9.7	29.0	7.7	23.1	8.0	24.0
3.5	10.7	37.6	9.1	31.7	9.3	32.7	7.4	26.0	8.0	28.0
4	10.4	41.7	8.8	35.1	9.1	36.2	7.2	28.9	8.0	32.0
4.5	10.2	45.7	8.6	38.5	8.8	39.7	7.0	31.6	8.0	36.0
5	9.9	49.6	8.4	41.8	8.6	43.1	6.9	34.3	8.0	40.0
5.5	9.7	53.4	8.2	45.0	8.4	46.4	6.7	36.9	8.0	44.0
6	9.5	57.1	8.0	48.1	8.3	49.6	6.6	39.5	8.0	48.0
6.5	9.3	60.7	7.9	51.2	8.1	52.8	6.5	42.0	8.0	52.0
7	9.2	64.3	7.7	54.2	8.0	55.9	6.4	44.5	8.0	56.0
7.5	9.0	67.8	7.6	57.2	7.9	58.9	6.3	47.0	8.0	60.0
8	8.9	71.3	7.5	60.1	7.7	62.0	6.2	49.4	8.0	64.0
8.5	8.8	74.7	7.4	63.0	7.6	64.9	6.1	51.7	8.0	68.0
9	8.7	78.1	7.3	65.8	7.5	67.9	6.0	54.1	8.0	72.0
9.5	8.6	81.5	7.2	68.6	7.5	70.8	5.9	56.4	8.0	76.0
10	8.5	84.8	7.1	71.4	7.4	73.7	5.9	58.7	8.0	80.0
10.5	8.4	88.0	7.1	74.2	7.3	76.5	5.8	60.9	8.0	84.0
11	8.3	91.3	7.0	76.9	7.2	79.3	5.7	63.2	8.0	88.0
11.5	8.2	94.4	6.9	79.6	7.1	82.1	5.7	65.4	8.0	92.0
12	8.1	97.6	6.9	82.3	7.1	84.8	5.6	67.6	8.0	96.0
12.5	8.1	100.7	6.8	84.9	7.0	87.5	5.6	69.7	8.0	100.0

Table C.4. Capacity-Torque correlation based on Km & AC358 Kt for 3.5" O.D shaft

Torque (k-ft)	Predicted capacity Q based on modified Km								Predicted Q based on AC358 Kt	
	RMHC		RMHT		RSHC		RSHT			
	Km	Q(K)	Km	Q(K)	Km	Q(K)	Km	Q(K)	Kt	Q(Kips
0.5	14.8	7.4	12.5	6.2	12.9	6.4	10.2	5.1	7.0	3.5
1	12.7	12.7	10.7	10.7	11.0	11.0	8.8	8.8	7.0	7.0
1.5	11.6	17.3	9.7	14.6	10.0	15.1	8.0	12.0	7.0	10.5
2	10.8	21.6	9.1	18.2	9.4	18.8	7.5	15.0	7.0	14.0
2.5	10.3	25.7	8.7	21.7	8.9	22.4	7.1	17.8	7.0	17.5
3	9.9	29.6	8.3	25.0	8.6	25.7	6.8	20.5	7.0	21.0
3.5	9.5	33.4	8.0	28.1	8.3	29.0	6.6	23.1	7.0	24.5
4	9.3	37.0	7.8	31.2	8.0	32.2	6.4	25.6	7.0	28.0
4.5	9.0	40.5	7.6	34.2	7.8	35.2	6.2	28.1	7.0	31.5
5	8.8	44.0	7.4	37.1	7.6	38.2	6.1	30.4	7.0	35.0
5.5	8.6	47.4	7.3	39.9	7.5	41.2	6.0	32.8	7.0	38.5
6	8.4	50.7	7.1	42.7	7.3	44.0	5.8	35.1	7.0	42.0
6.5	8.3	53.9	7.0	45.4	7.2	46.8	5.7	37.3	7.0	45.5
7	8.2	57.1	6.9	48.1	7.1	49.6	5.6	39.5	7.0	49.0
7.5	8.0	60.2	6.8	50.7	7.0	52.3	5.6	41.7	7.0	52.5
8	7.9	63.3	6.7	53.3	6.9	55.0	5.5	43.8	7.0	56.0
8.5	7.8	66.3	6.6	55.9	6.8	57.6	5.4	45.9	7.0	59.5
9	7.7	69.3	6.5	58.4	6.7	60.2	5.3	48.0	7.0	63.0
9.5	7.6	72.3	6.4	60.9	6.6	62.8	5.3	50.0	7.0	66.5
10	7.5	75.2	6.3	63.4	6.5	65.4	5.2	52.1	7.0	70.0
10.5	7.4	78.1	6.3	65.8	6.5	67.9	5.1	54.1	7.0	73.5
11	7.4	81.0	6.2	68.2	6.4	70.4	5.1	56.1	7.0	77.0
11.5	7.3	83.8	6.1	70.6	6.3	72.8	5.0	58.0	7.0	80.5
12	7.2	86.6	6.1	73.0	6.3	75.3	5.0	60.0	7.0	84.0
12.5	7.2	89.4	6.0	75.3	6.2	77.7	5.0	61.9	7.0	87.5
13	7.1	92.2	6.0	77.7	6.2	80.1	4.9	63.8	7.0	91.0
13.5	7.0	94.9	5.9	80.0	6.1	82.5	4.9	65.7	7.0	94.5
14	7.0	97.6	5.9	82.3	6.1	84.8	4.8	67.6	7.0	98.0
14.5	6.9	100.3	5.8	84.5	6.0	87.1	4.8	69.4	7.0	101.5
15	6.9	103.0	5.8	86.8	6.0	89.5	4.8	71.3	7.0	105.0
15.5	6.8	105.6	5.7	89.0	5.9	91.8	4.7	73.1	7.0	108.5
16	6.8	108.2	5.7	91.2	5.9	94.0	4.7	74.9	7.0	112.0
16.5	6.7	110.9	5.7	93.4	5.8	96.3	4.6	76.7	7.0	115.5
17	6.7	113.4	5.6	95.6	5.8	98.6	4.6	78.5	7.0	119.0

Table C.5 Capacity-torque correlation based on Km & AC358 for 4.5" O.D shaft

Torque (k-ft)	Predicted capacity Q based on modified Km								Predicted Q based on AC358 Kt	
	RMHC		RMHT		RSHC		RSHT			
	Km	Q(K)	Km	Q(K)	Km	Q(K)	Km	Q(K)	Kt	Q(Kips
1	10.4	10.4	8.8	8.8	9.1	9.1	7.2	7.2	5.6	5.6
2	8.9	17.8	7.5	15.0	7.7	15.5	6.2	12.3	5.6	11.2
3	8.1	24.4	6.9	20.6	7.1	21.2	5.6	16.9	5.6	16.8
4	7.6	30.5	6.4	25.7	6.6	26.5	5.3	21.1	5.6	22.4
5	7.2	36.2	6.1	30.5	6.3	31.5	5.0	25.1	5.6	28.0
6	7.0	41.7	5.9	35.1	6.0	36.2	4.8	28.9	5.6	33.6
7	6.7	47.0	5.7	39.6	5.8	40.8	4.6	32.5	5.6	39.2
8	6.5	52.1	5.5	43.9	5.7	45.3	4.5	36.1	5.6	44.8
9	6.3	57.1	5.3	48.1	5.5	49.6	4.4	39.5	5.6	50.4
10	6.2	61.9	5.2	52.2	5.4	53.8	4.3	42.9	5.6	56.0
11	6.1	66.7	5.1	56.2	5.3	57.9	4.2	46.1	5.6	61.6
12	5.9	71.3	5.0	60.1	5.2	62.0	4.1	49.4	5.6	67.2
13	5.8	75.9	4.9	63.9	5.1	65.9	4.0	52.5	5.6	72.8
14	5.7	80.4	4.8	67.7	5.0	69.8	4.0	55.6	5.6	78.4
15	5.7	84.8	4.8	71.4	4.9	73.7	3.9	58.7	5.6	84.0
16	5.6	89.1	4.7	75.1	4.8	77.4	3.9	61.7	5.6	89.6
17	5.5	93.4	4.6	78.7	4.8	81.1	3.8	64.6	5.6	95.2
18	5.4	97.6	4.6	82.3	4.7	84.8	3.8	67.6	5.6	100.8
19	5.4	101.8	4.5	85.8	4.7	88.4	3.7	70.4	5.6	106.4
20	5.3	105.9	4.5	89.2	4.6	92.0	3.7	73.3	5.6	112.0
21	5.2	110.0	4.4	92.7	4.6	95.6	3.6	76.1	5.6	117.6
22	5.2	114.0	4.4	96.1	4.5	99.1	3.6	78.9	5.6	123.2
23	5.1	118.0	4.3	99.4	4.5	102.5	3.6	81.7	5.6	128.8
24	5.1	122.0	4.3	102.8	4.4	106.0	3.5	84.4	5.6	134.4
25	5.0	125.9	4.2	106.1	4.4	109.4	3.5	87.1	5.6	140.0

Table C.6 Capacity-torque correlation based on Km & AC358 Kt for 1.75" RCS shaft

Torque (K-ft)	Predicted capacity Q, based on modified Km								Predicted Q based on AC358 Kt	
	SMHC		SMHT		SSHC		SSHT			
	Km	Q(K)	Km	Q(K)	Km	Q(K)	Km	Q(K)	Kt	Q(Kips)
0.5	14.7	7.3	13.1	6.5	12.5	6.3	9.9	4.9	10.0	5.0
1	12.5	12.5	11.2	11.2	10.7	10.7	8.4	8.4	10.0	10.0
1.5	11.4	17.2	10.2	15.3	9.8	14.6	7.7	11.5	10.0	15.0
2	10.7	21.4	9.6	19.1	9.2	18.3	7.2	14.4	10.0	20.0
2.5	10.2	25.5	9.1	22.7	8.7	21.8	6.9	17.1	10.0	25.0
3	9.8	29.3	8.7	26.2	8.3	25.0	6.6	19.7	10.0	30.0
3.5	9.4	33.1	8.4	29.5	8.1	28.2	6.4	22.2	10.0	35.0
4	9.2	36.7	8.2	32.7	7.8	31.3	6.2	24.6	10.0	40.0
4.5	8.9	40.2	8.0	35.9	7.6	34.3	6.0	27.0	10.0	45.0
5	8.7	43.6	7.8	38.9	7.4	37.2	5.9	29.3	10.0	50.0
5.5	8.5	46.9	7.6	41.9	7.3	40.0	5.7	31.5	10.0	55.0
6	8.4	50.2	7.5	44.8	7.1	42.8	5.6	33.7	10.0	60.0
6.5	8.2	53.4	7.3	47.7	7.0	45.6	5.5	35.9	10.0	65.0
7	8.1	56.5	7.2	50.5	6.9	48.3	5.4	38.0	10.0	70.0
7.5	8.0	59.6	7.1	53.2	6.8	50.9	5.3	40.1	10.0	75.0
8	7.8	62.7	7.0	56.0	6.7	53.5	5.3	42.2	10.0	80.0
8.5	7.7	65.7	6.9	58.7	6.6	56.1	5.2	44.2	10.0	85.0
9	7.6	68.7	6.8	61.3	6.5	58.6	5.1	46.2	10.0	90.0
9.5	7.5	71.6	6.7	63.9	6.4	61.1	5.1	48.1	10.0	95.0
10	7.5	74.5	6.7	66.5	6.4	63.6	5.0	50.1	10.0	100.0

APPENDIX D: HISTOGRAM OF MEASURED CAPACITY OVER PREDICTED CAPACITY

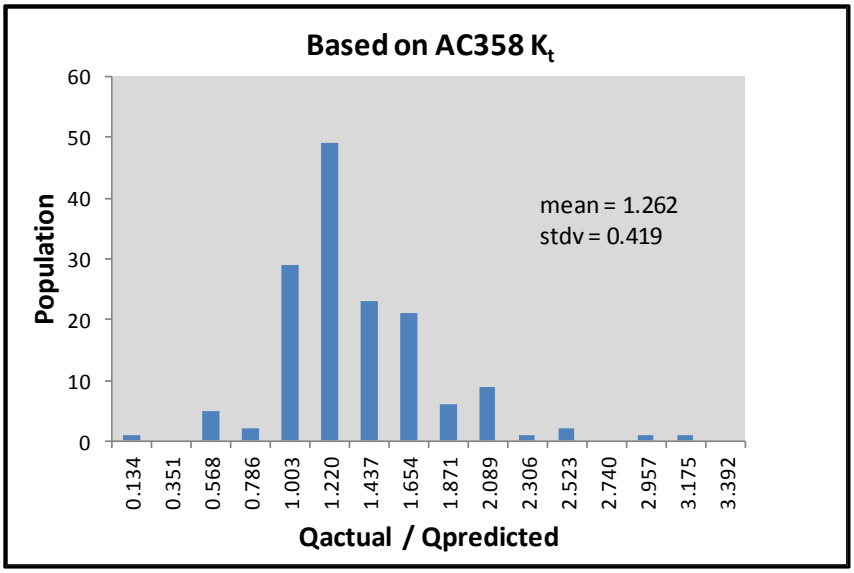

Figure D.1 Histogram of (Q actual/ Q predicted). RMHC

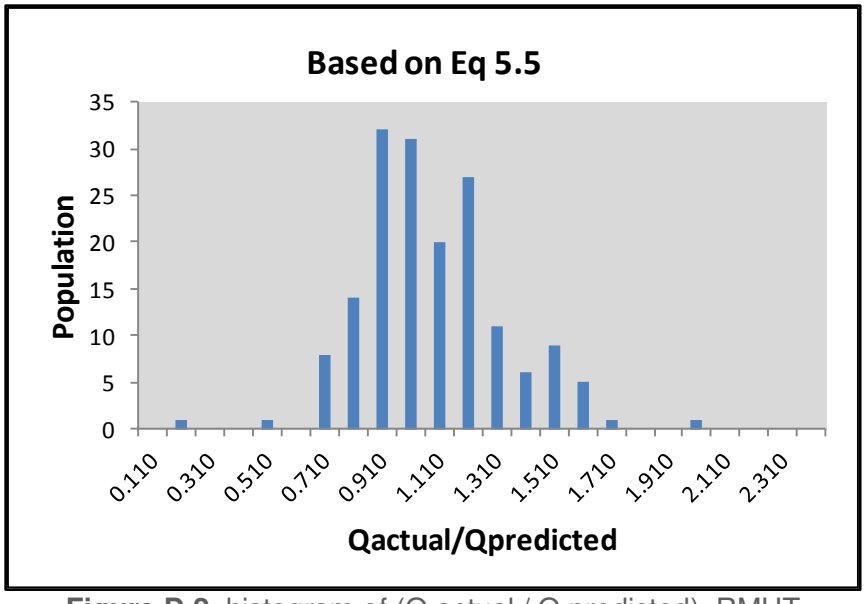

Figure D.2. histogram of (Q actual / Q predicted). RMHT

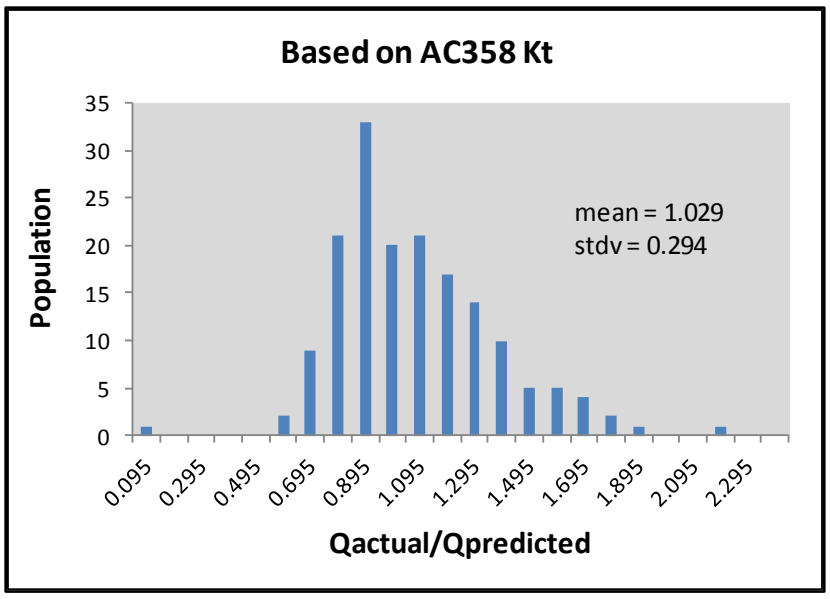

Figure D.3 Histogram of (Q actual / Q predicted). RMHT

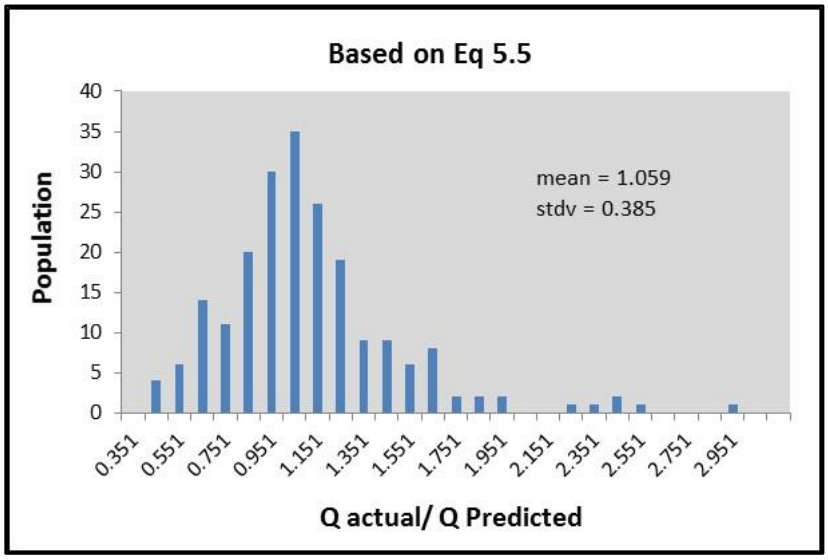

Figure D.4 Histogram of (Q actual / Q predicted). RSHC

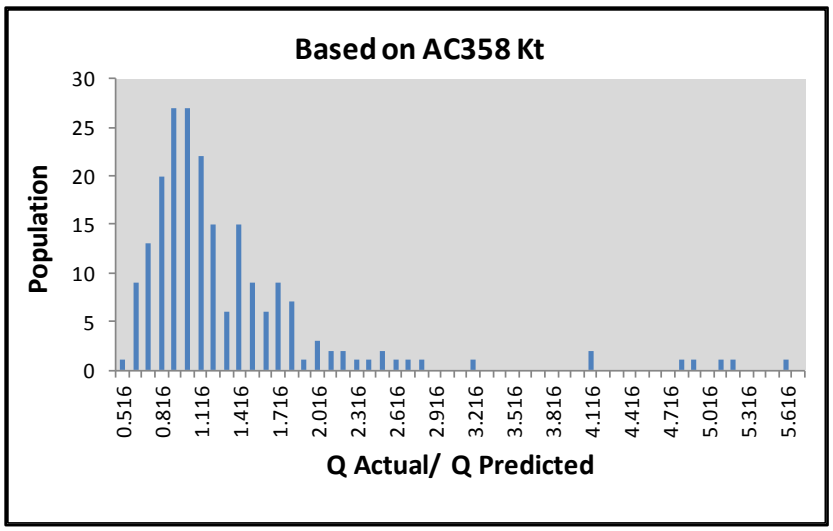

Figure D.5 Histogram of (Q actual / Q predicted). RSHC

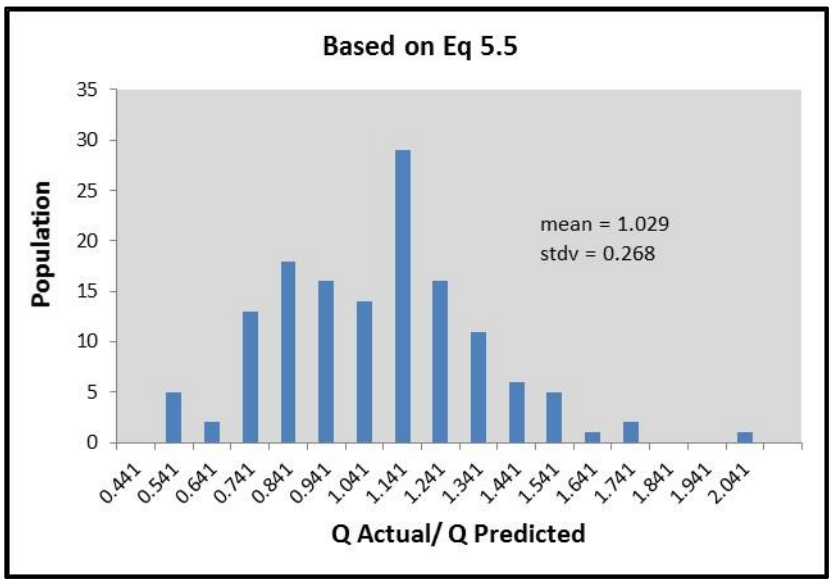

Figure D.6 Histogram of (Q actual/ Q predicted). RSHT

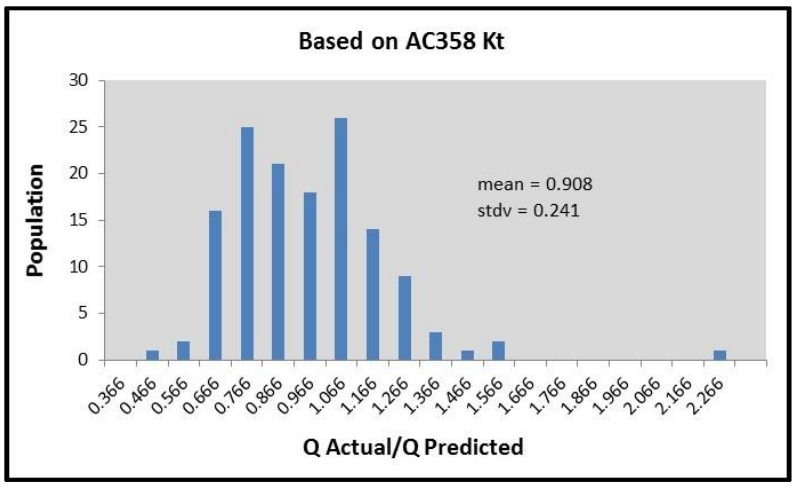

Figure D.7 Histogram of (Q actual / Q predicted). RSHT

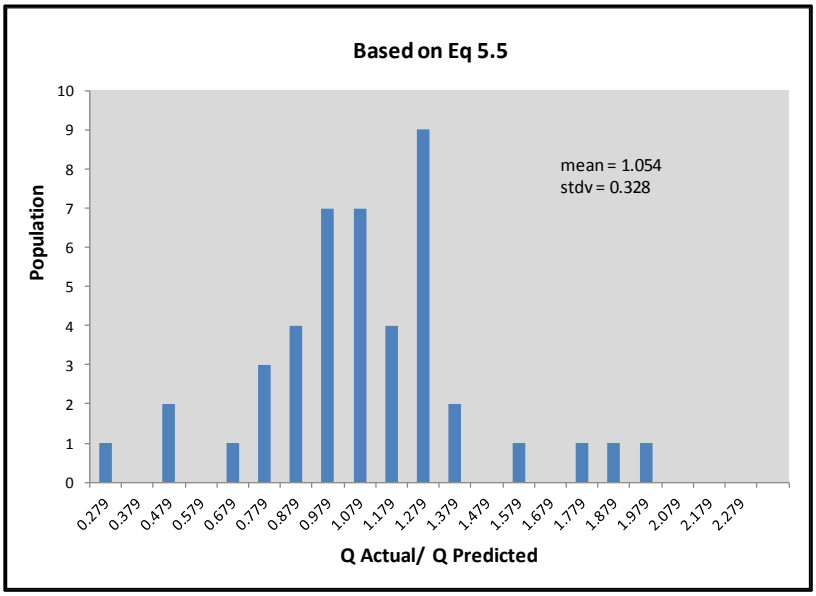

Figure D.8 Histogram of (Q actual/ Q predicted). SMHC

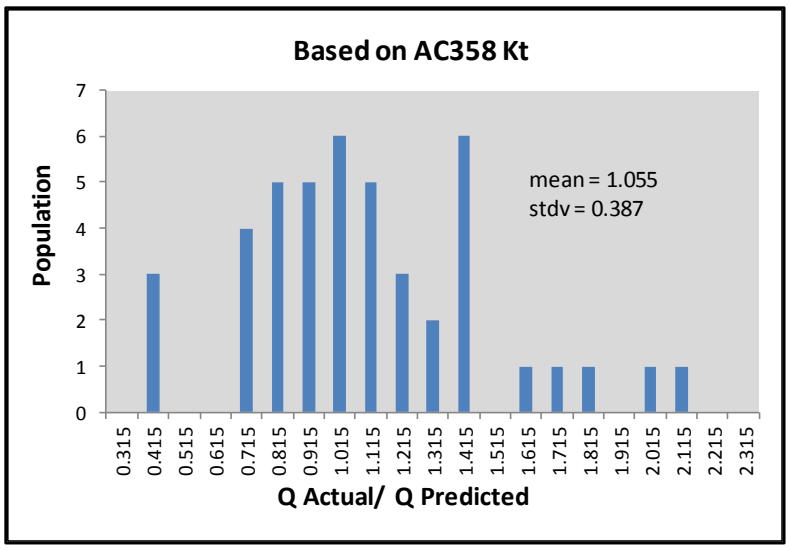

Figure D.9 Histogram of (Q actual / Q predicted). SMHC

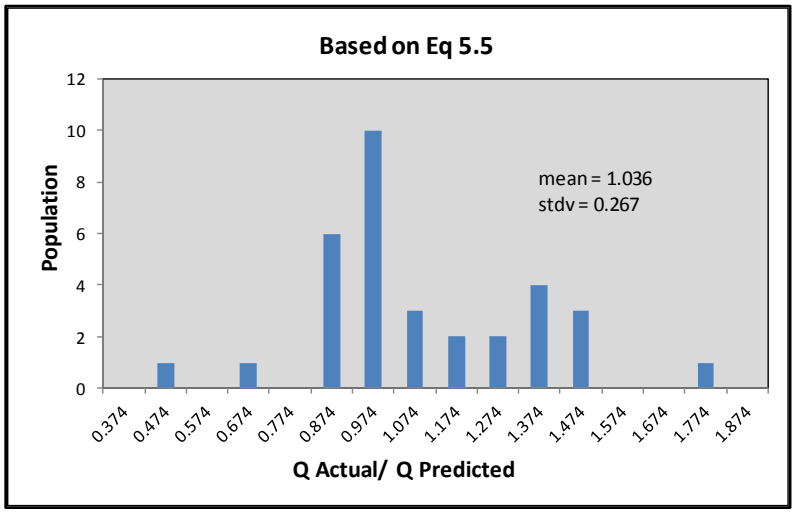

Figure D.10 Histogram of (Q actual / Q predicted). SMHT

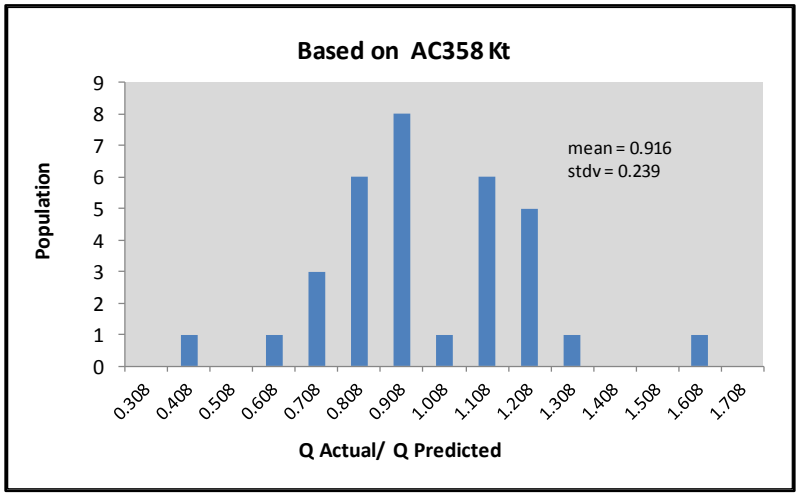

Figure D.11 Histogram of (Q actual / Q predicted). SMHT

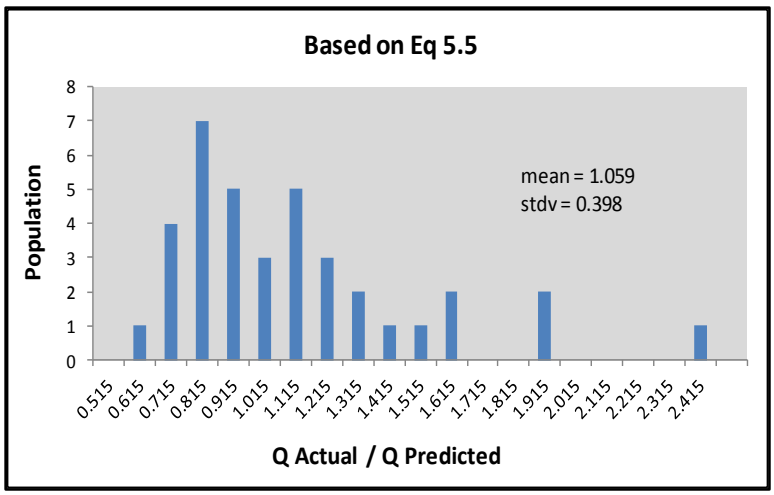

Figure D.12 Histogram of (Q actual / Q predicted). SSHC

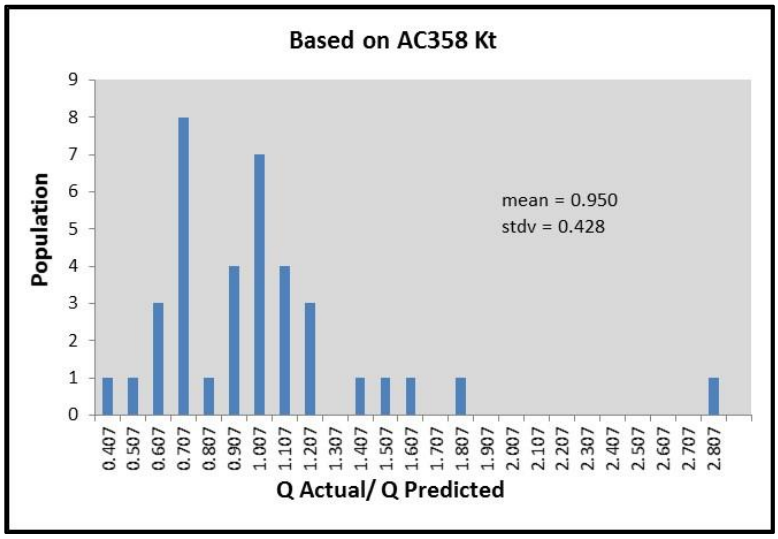

Figure D.13 Histogram of (Q actual / Q predicted). SSHC

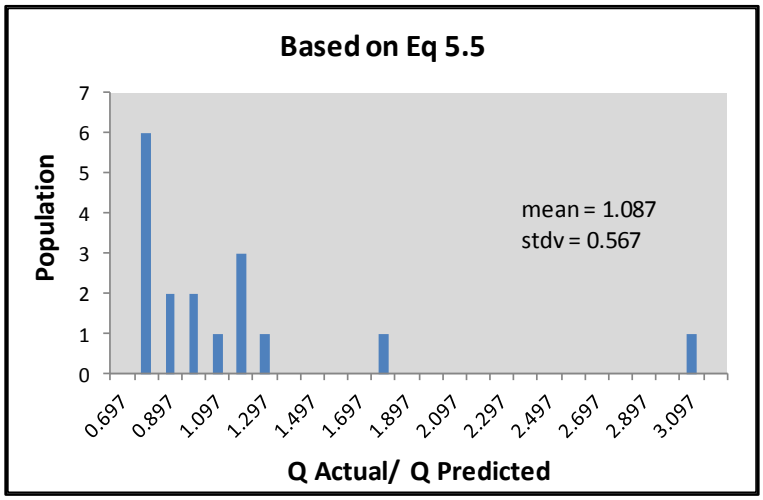

Figure D.14 Histogram of (Q actual / Q predicted). SSHT

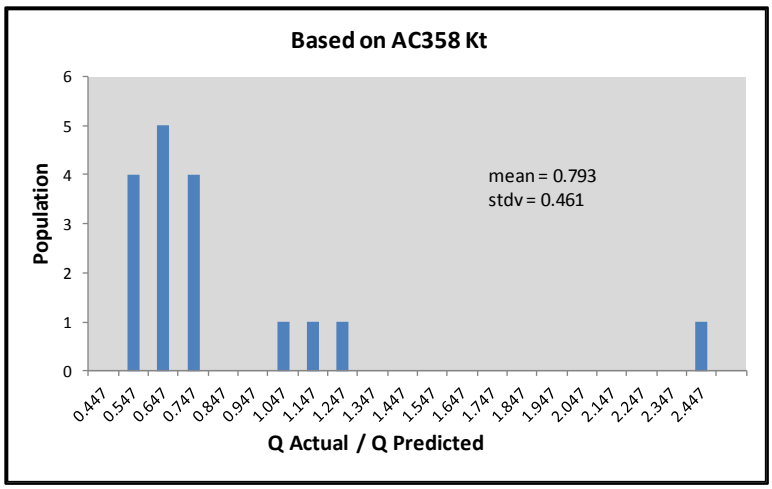

Figure D.15 Histogram of (Q actual / Q predicted). SSHT

APPENDIX E: Q-Q (QUANTILE-QUANTILE) PLOTS

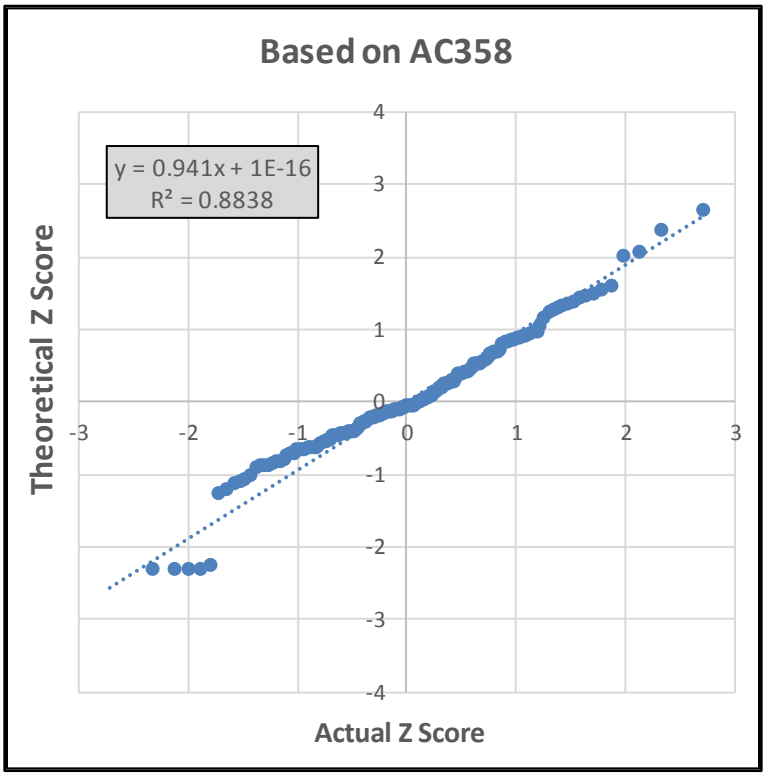

Figure E.1 Q-Q Plot. RMHC

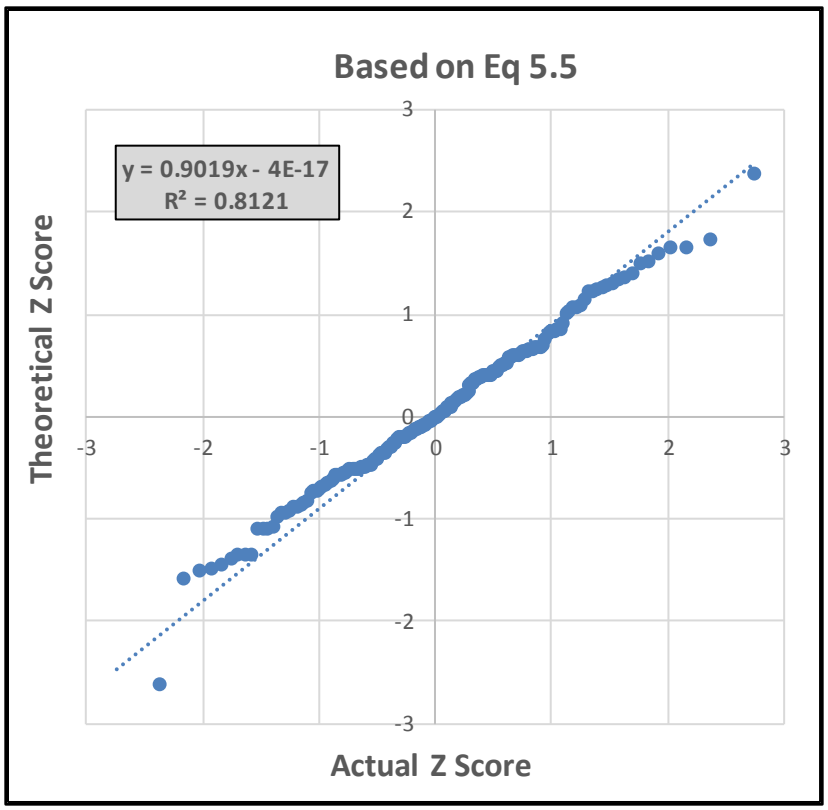

Figure E.2 Q-Q Plot. RMHT

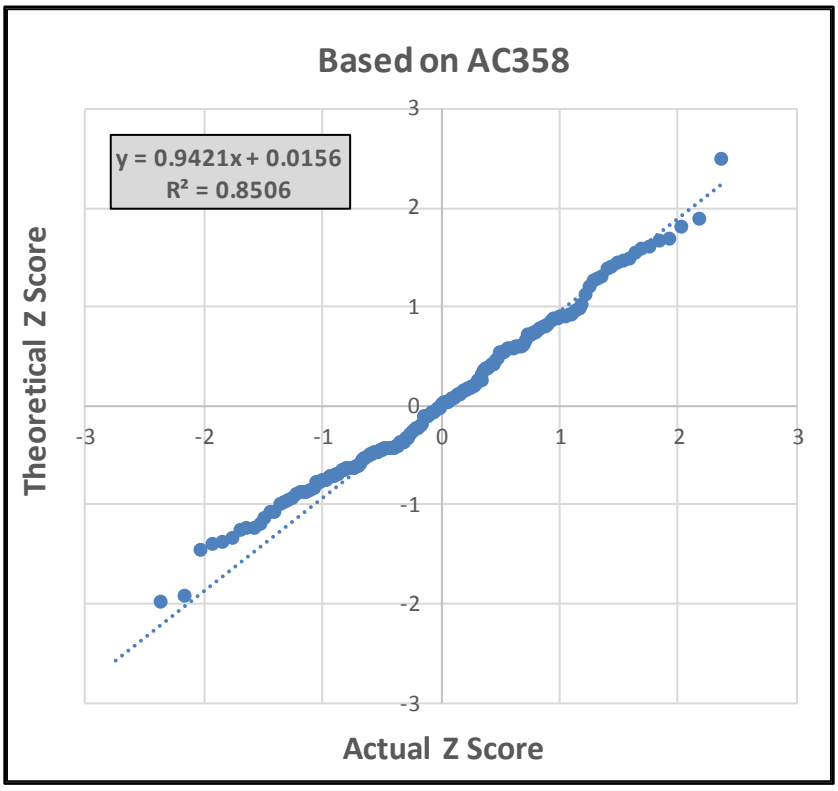

Figure E.3 Q-Q Plot. RMHT

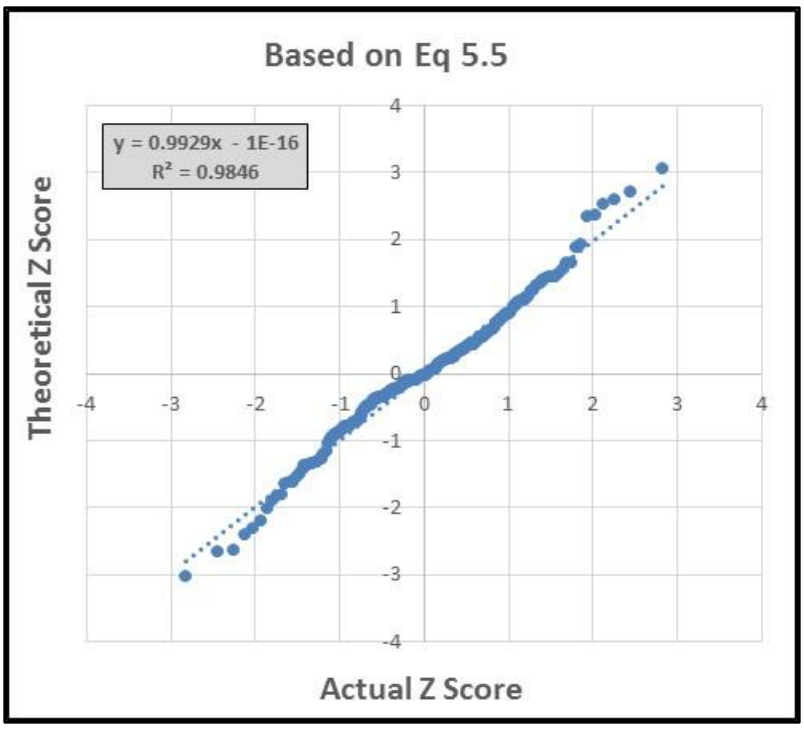

Figure E.4 Q-Q Plot. RSHC

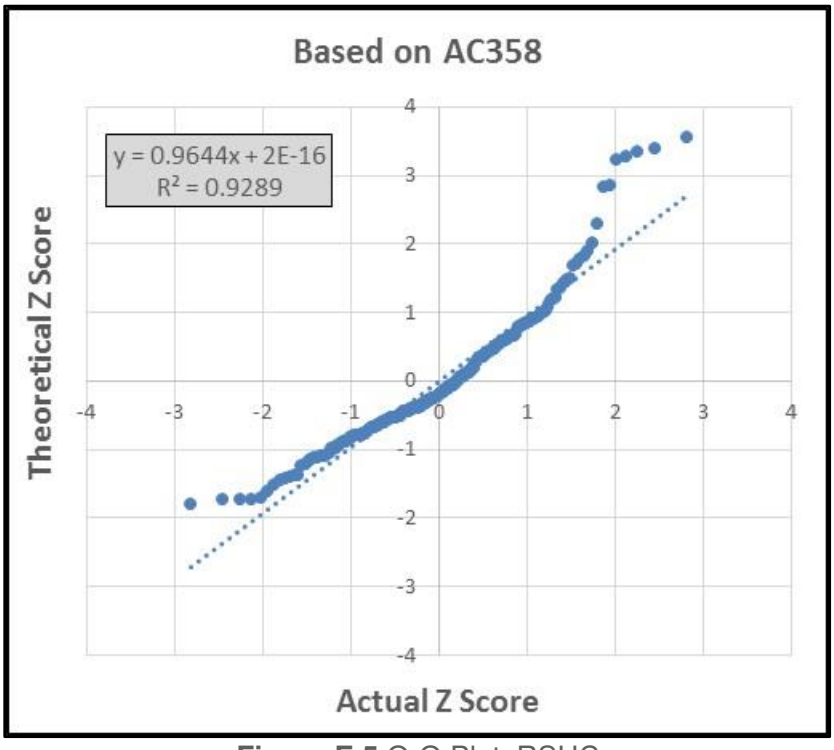

Figure E.5 Q-Q Plot. RSHC

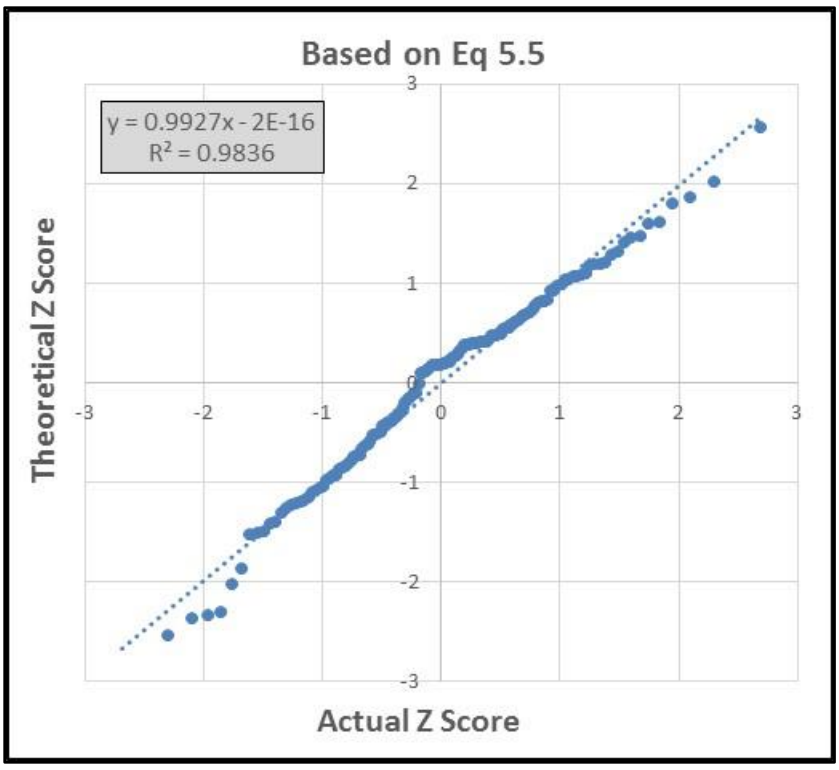

Figure E.6 Q-Q Plot.RSHT

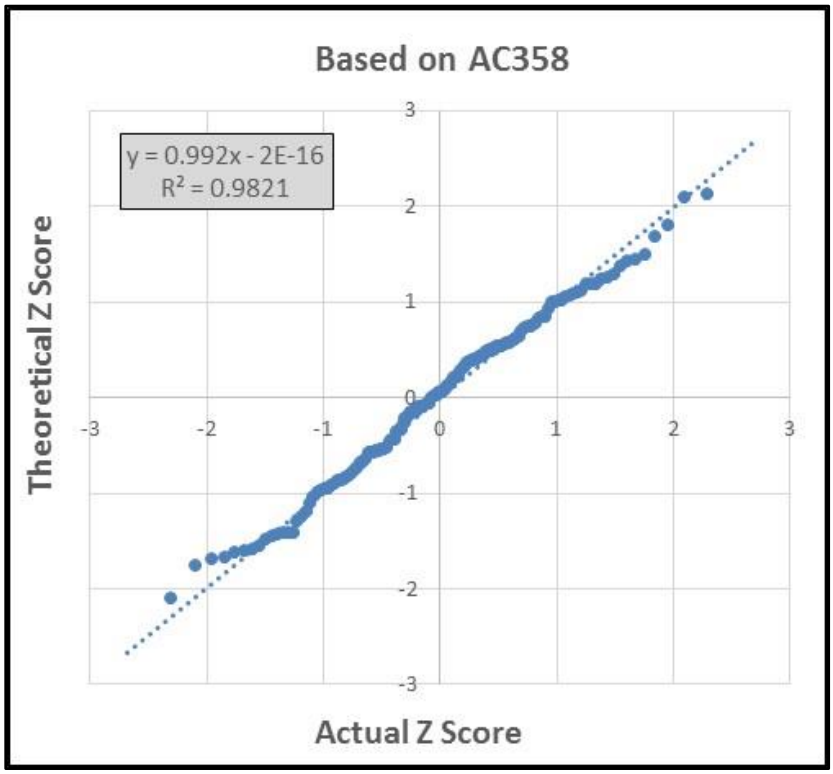

Figure E.7 Q-Q Plot. RSHT

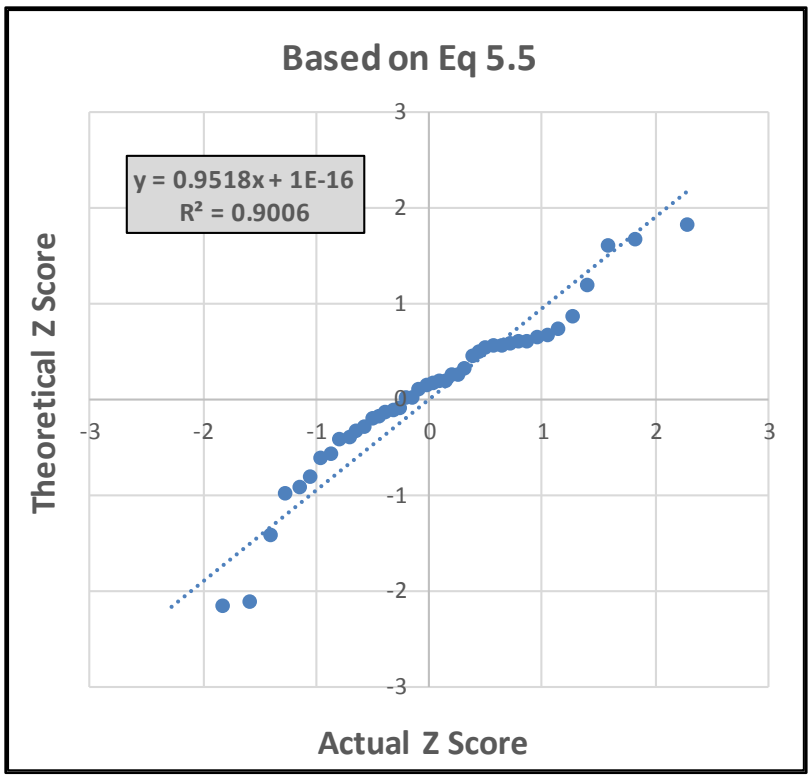

Figure E.8 Q-Q Plot. SMHC

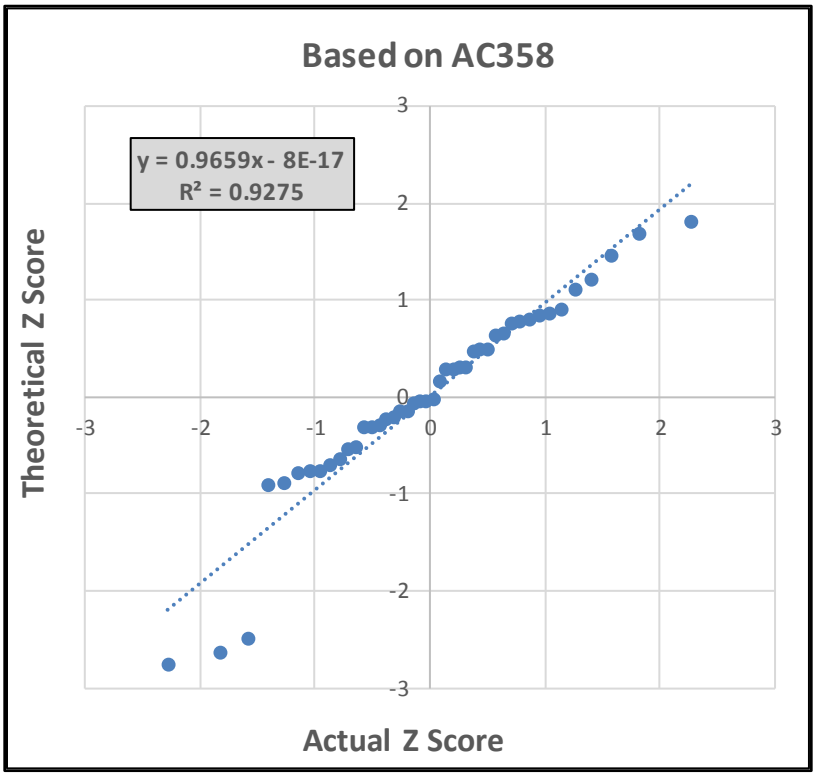

Figure E.9 Q-Q Plot.SMHC

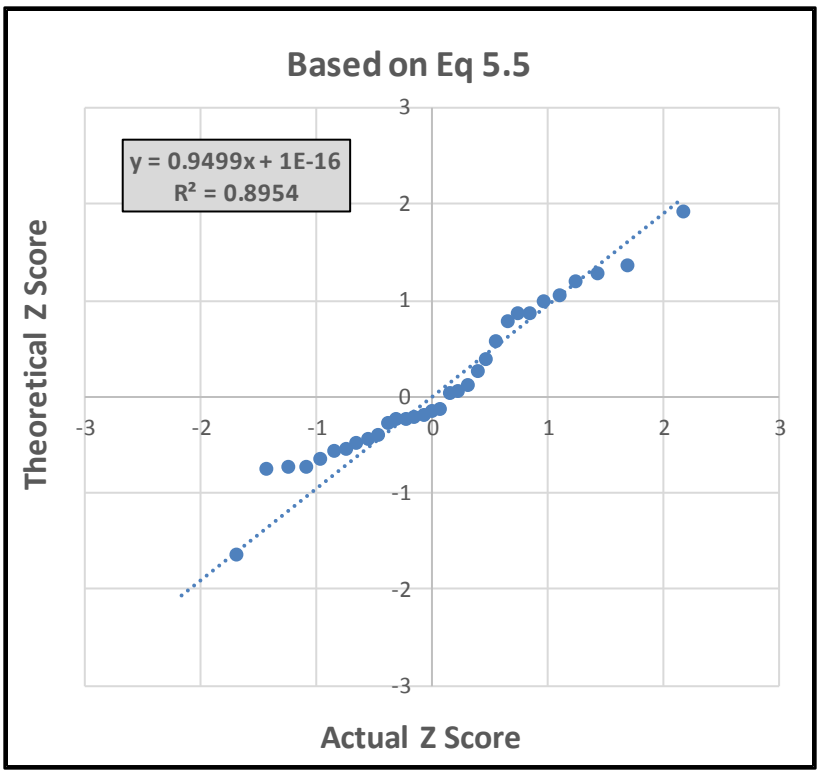

Figure E.10 Q-Q Plot.SMHT

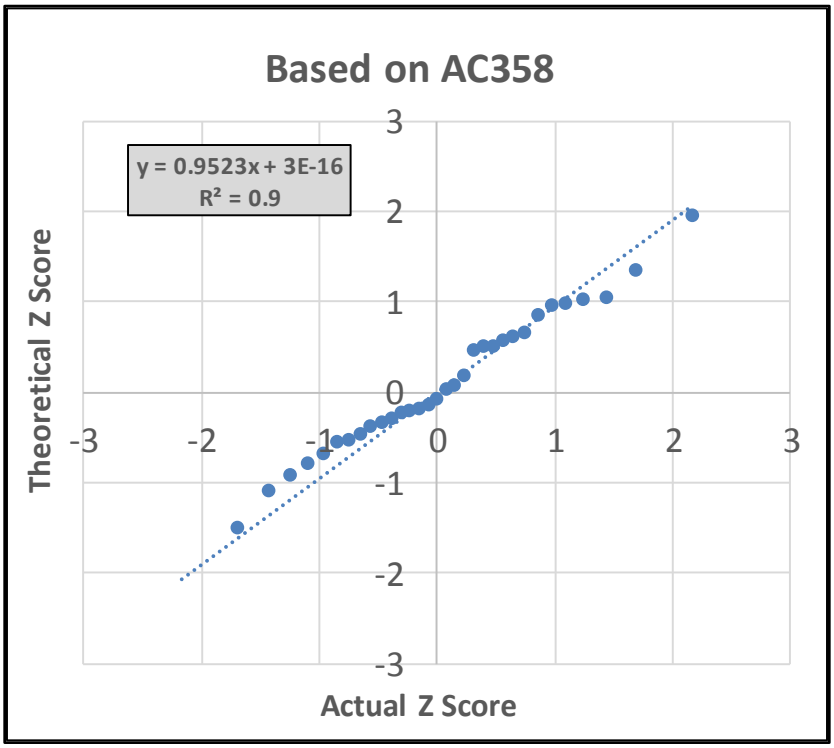

Figure E.11 Q-Q Plot.SMHT

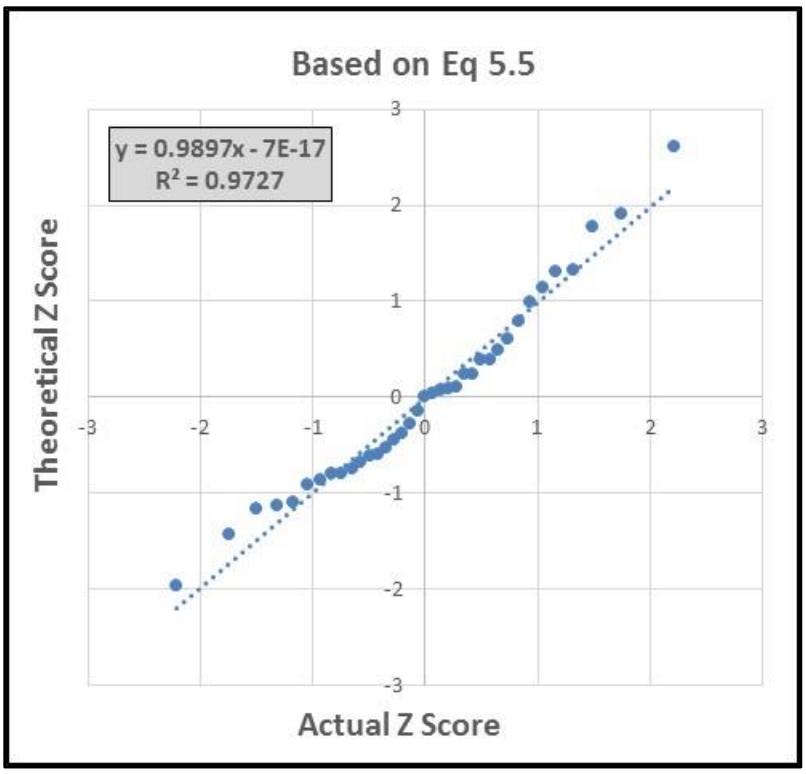

Figure E.12 Q-Q Plot.SSHC

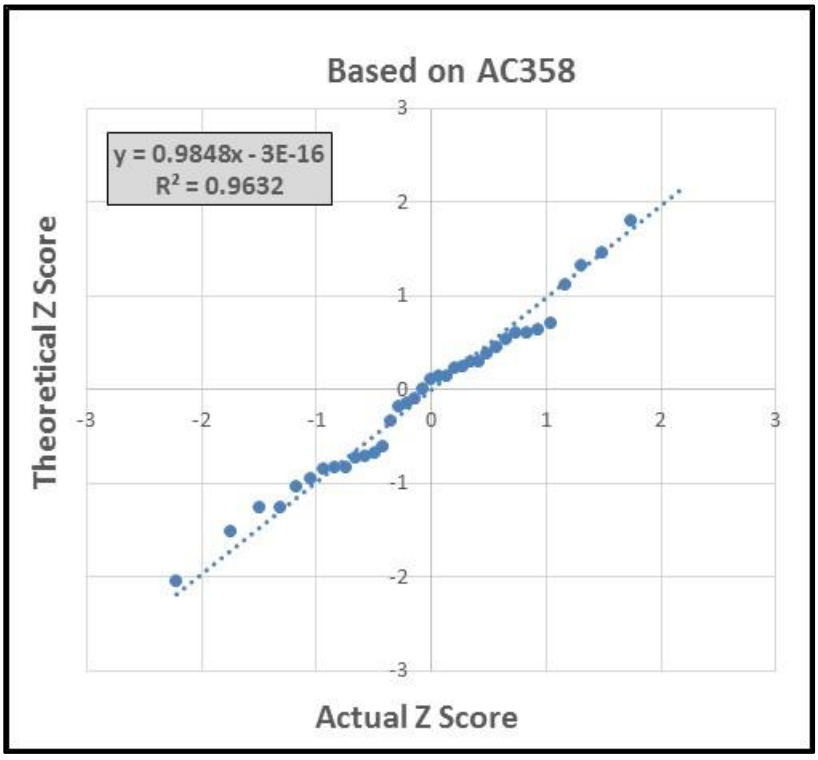

Figure E.13 Q-Q Plot.SSHC

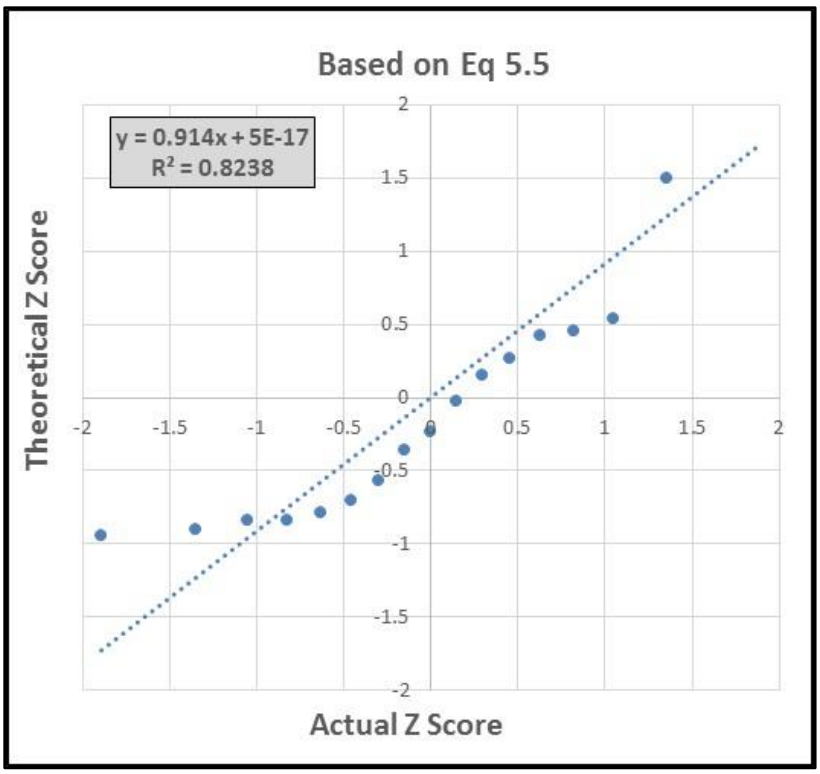

Figure E.14 Q-Q Plot.SSHT

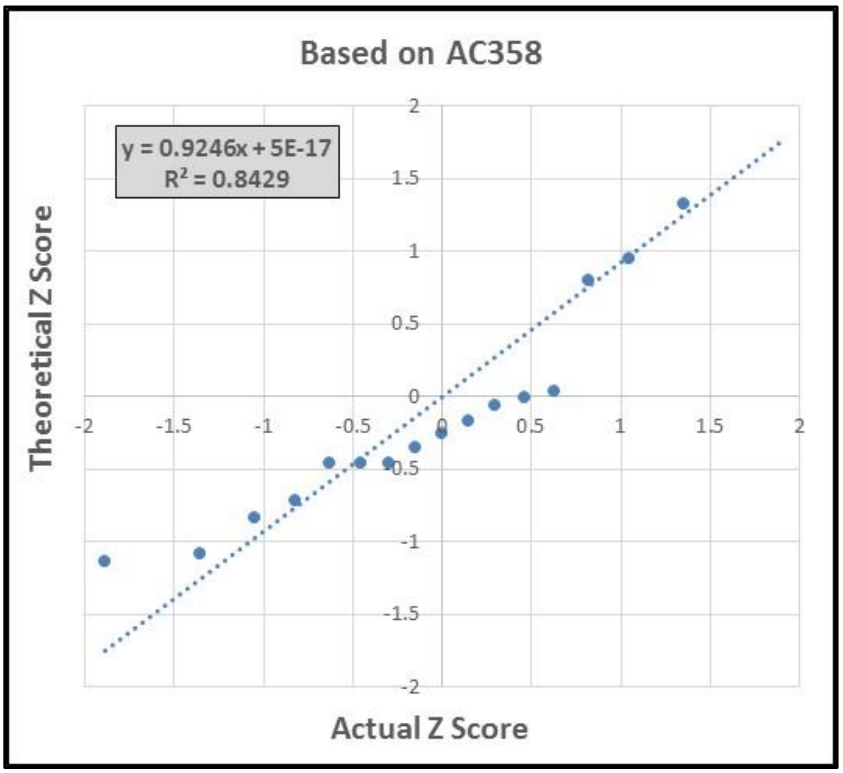

Figure E.15 Q-Q Plot.SSHT

APPENDIX F: TEST SITE LOCATIONS AND SOIL PROPERTIES

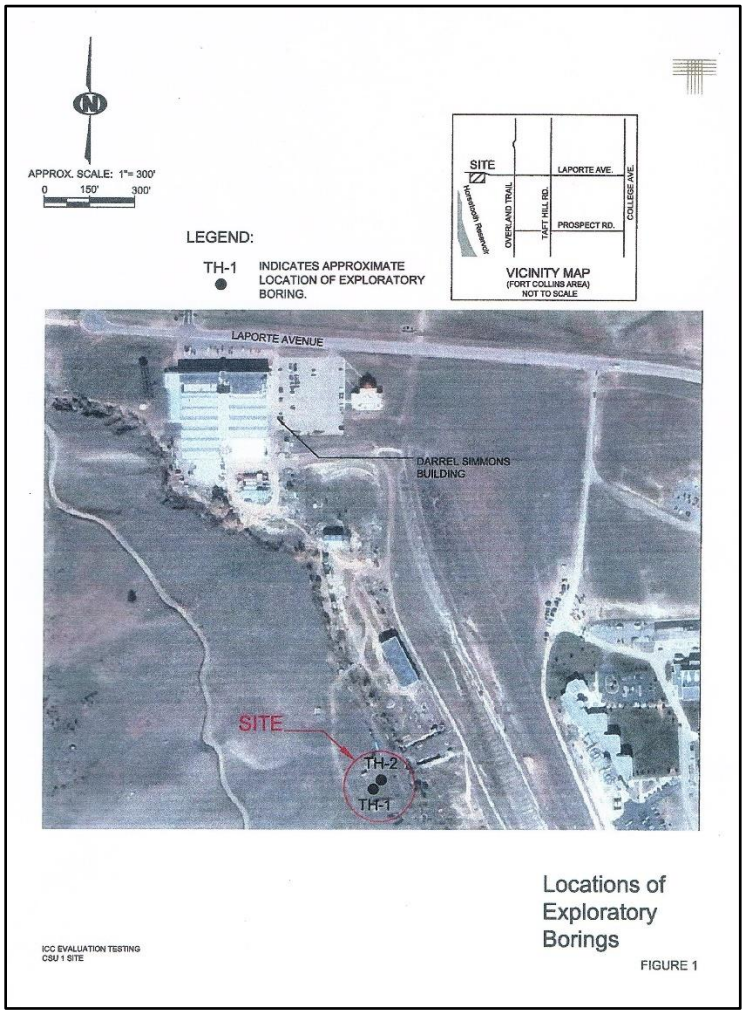

Figure F.1 CSU test site location (Courtesy of CTL|Thompson)

Table F.1 Soil & Bedrock properties at CSU site (Courtesy of CTL|Thompson)

Material	Friction Angle, Φ (deg)	Cohesion, c (psf)	Total Unit Weight (pcf)
Sandy to Slightly Sandy Clay	0	3,000 to 3,500	118 to 125
Weathered Claystone Bedrock	0	3,500 to 4,000	120 to 125
Claystone Bedrock	0	4,000 to 6,000	120 to 130

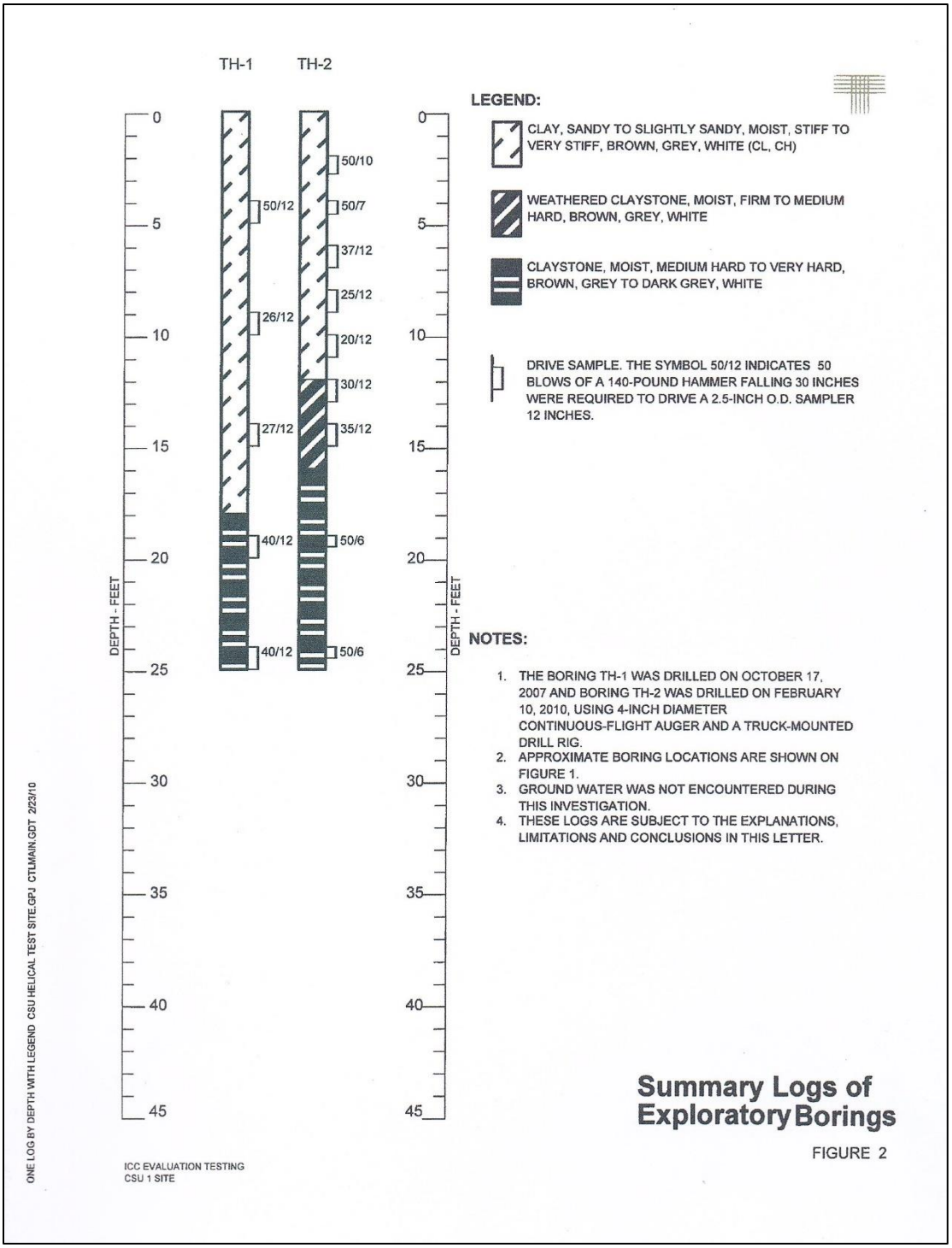

Figure F.2 CSU soil boring Log (Courtesy of CTL|Thompson)

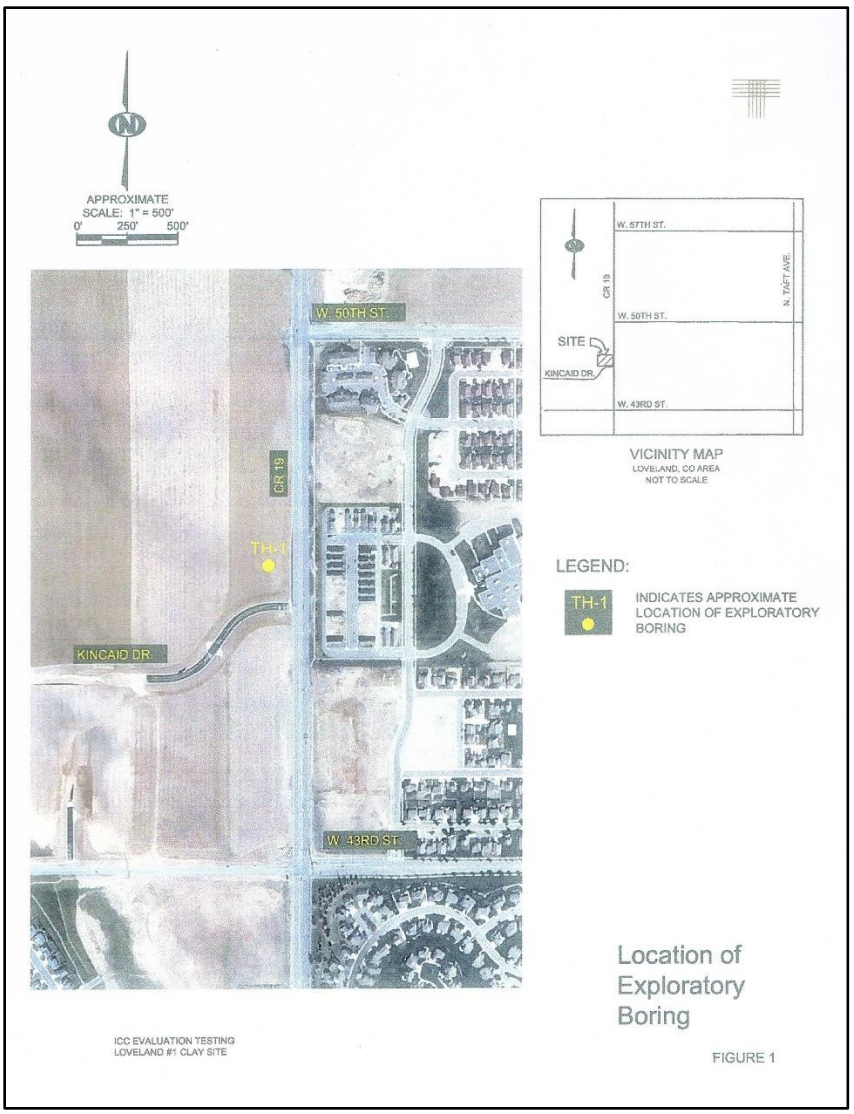

Figure F.3 Loveland test site location (Courtesy of CTL|Thompson)

Table F.2 Soil & Bedrock properties at Loveland site (Courtesy of CTL|Thompson)

Material	Friction Angle, Φ (deg)	Cohesion, c (psi)	Total Unit Weight (pcf)
Sandy Clay	0	3,000 – 5,000	120 - 130
Claystone Bedrock	0	4,000 – 6,000	130 - 140

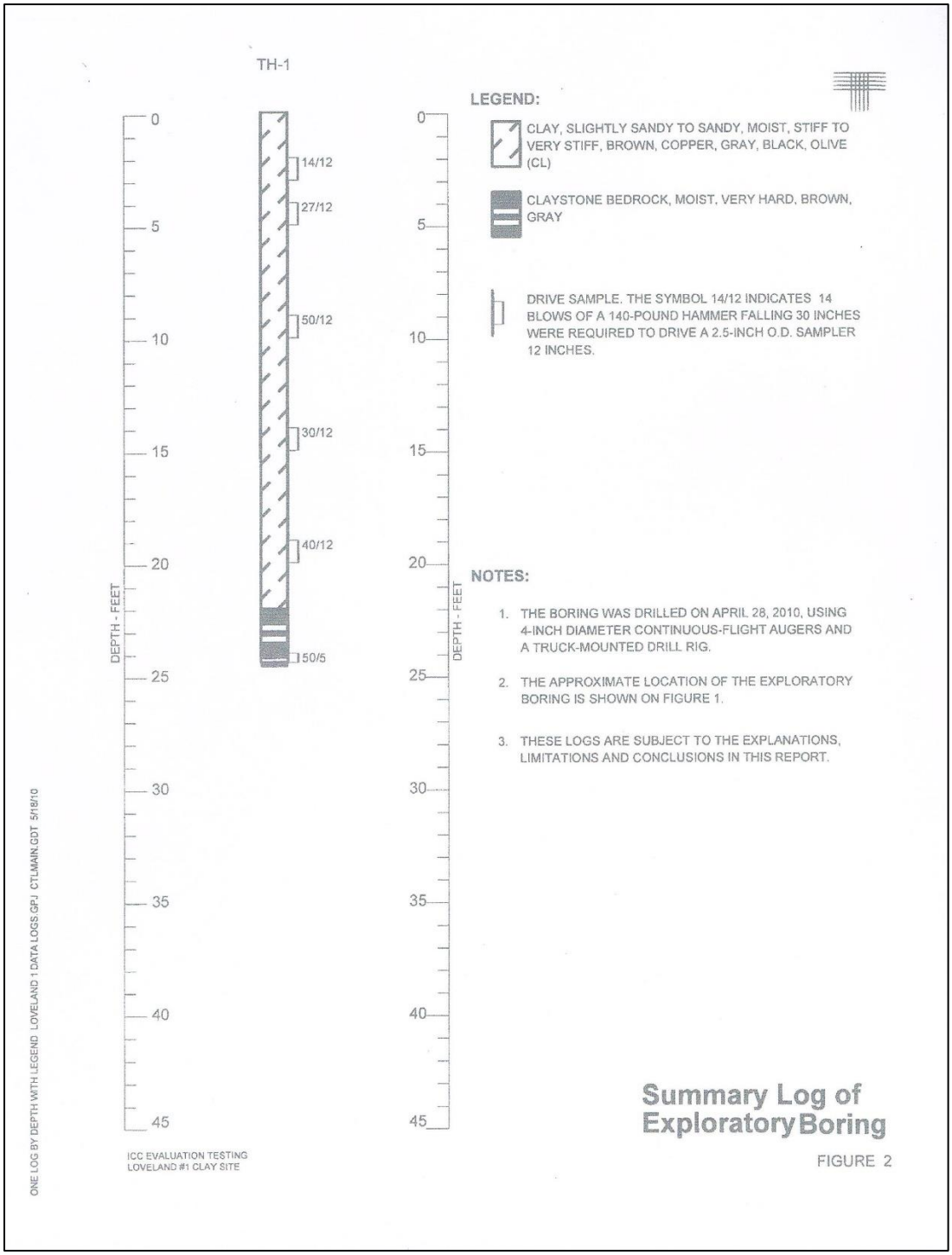

Figure F.4 Loveland soil boring (courtesy of CTL|Thompson)

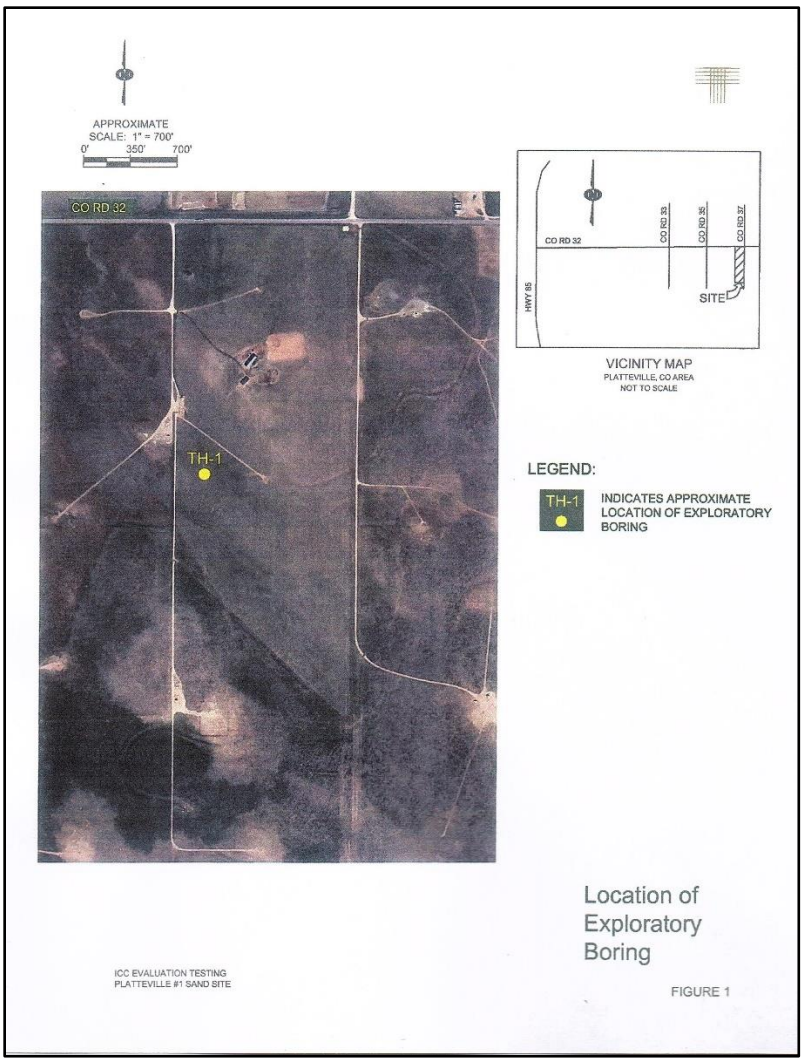

Figure F.5 Platteville test site location (courtesy of CTL|Thompson)

Table F.3 Soil & Bedrock properties at Platteville site (courtesy of CTL|Thompson)

Material	Friction Angle, Φ (deg)	Cohesion, c (psi)	Total Unit Weight (pcf)
Silty Sand	28 - 32	0	120 - 130
Weathered Claystone Bedrock	0	3,000 - 4,000	120 -125
Claystone Bedrock	0	4,000 – 6,000	125 - 135

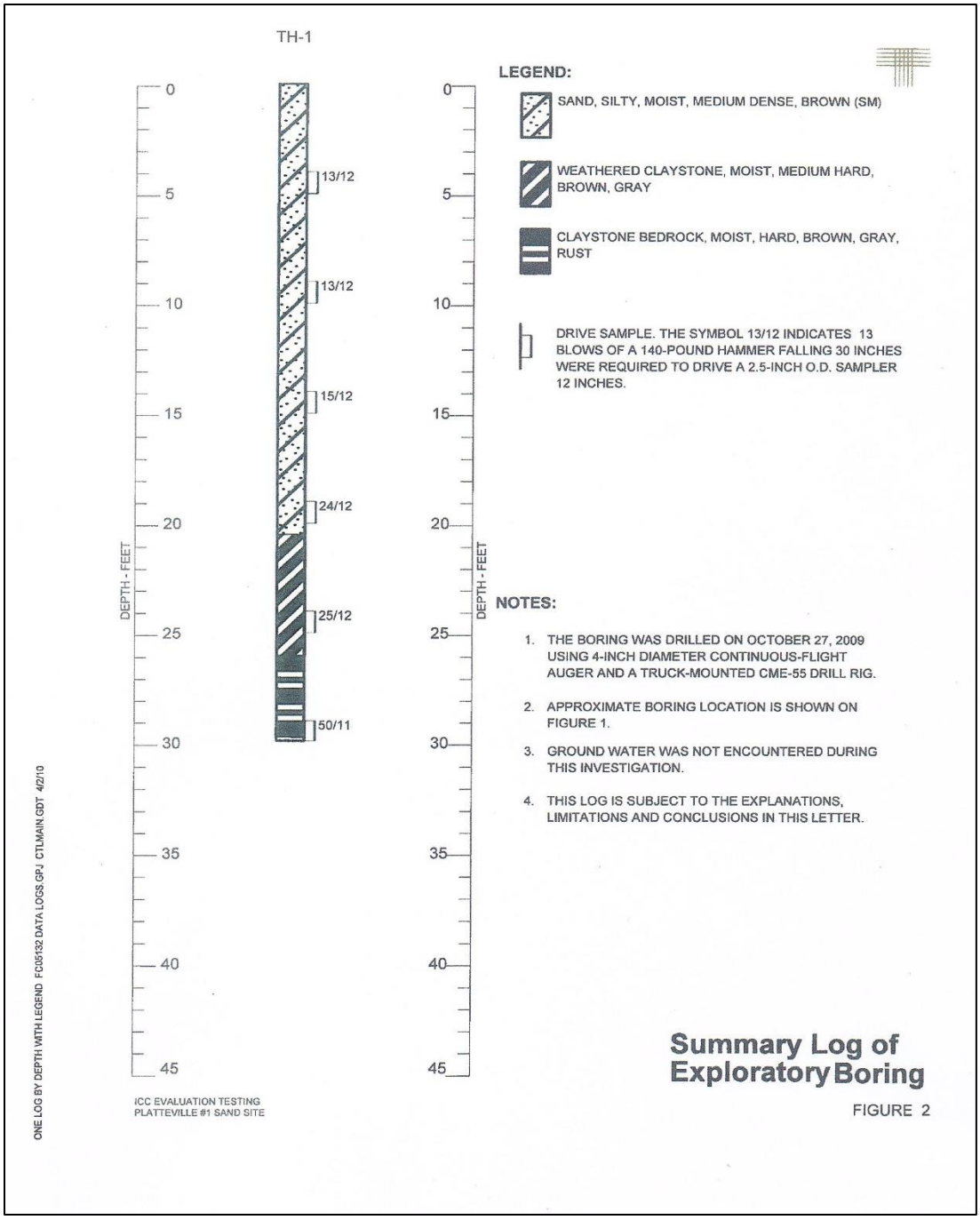

Figure F.6 Platteville soil boring (Courtesy of CTL|Thompson)

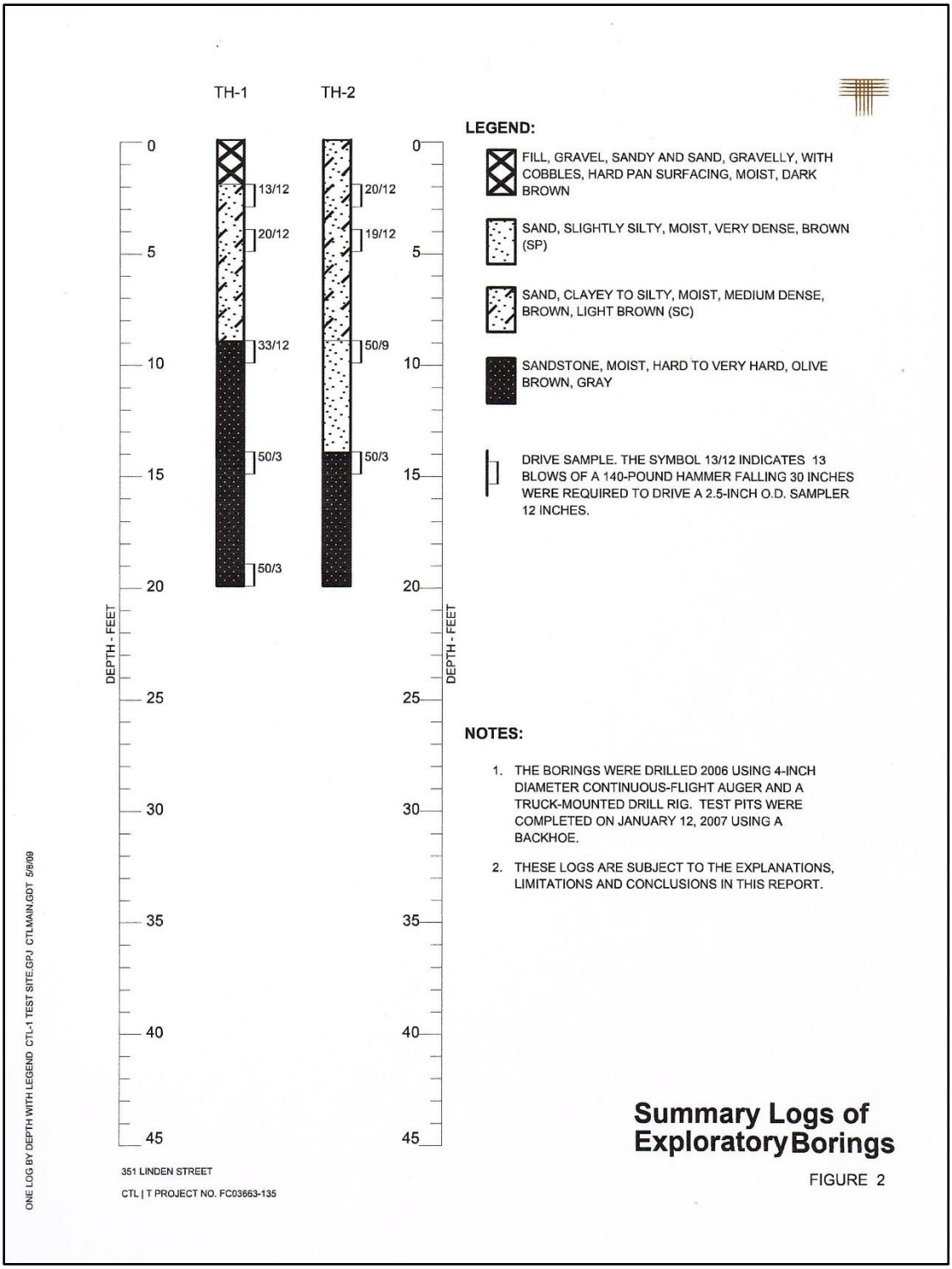

Figure F.7 351 Linden Street soil boring (Courtesy of CTL|Thompson)

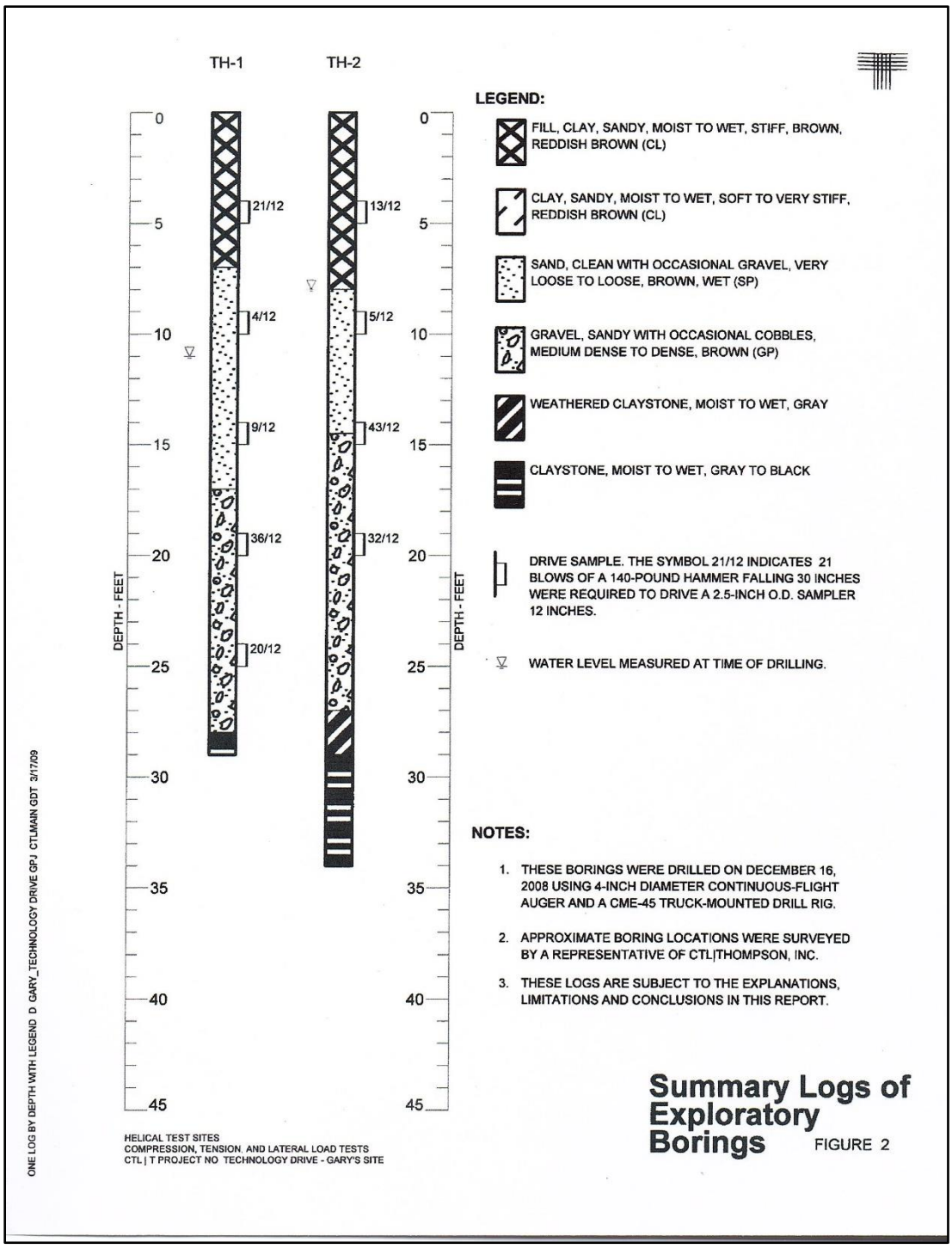

Figure F.8 Windsor soil boring (Courtesy of CTL|Thompson)